University of Ioannina, School of Health Sciences, Department of Medicine
Inter-institutional Interdepartmental Program of Postgraduate Studies "Molecular and Cellular Biology and Biotechnology"

MSc thesis

Role of the ubiquitin-like protein SUMO in spindle organization

Role of SUMO protein in the regulation of the yeast chromosome passenger complex

Laboratory of Biology, Faculty of Medicine, University of Ioannina
Lab of spindle positioning and organization, Centre de Recherche en Biologie cellulaire de Montpellier (CRBM) – CNRS

Semertsidis Georgios
Registration Number 118
Ioannina, September 2024

Evaluation Committee

Stathis Frillingos	Master's program Director, Professor of Biological Chemistry, Dept. of Medicine, UoI
Dimitris Liakopoulos	Supervisor Group Leader (Research Director DR2), CRBM, Assist. Professor of Biology, Dept. of Medicine, UoI
Dimitris Beis	Associate Professor of Biological Chemistry, Dept. of Medicine, UoI
Paschalis Thomas Doulias	Assist. Professor of Biochemistry, Dept. of Chemistry, UoI
Thomais Papamarcaki	Professor, Department of Medicine, UoI

Table of contents

Acknowledgements

This research thesis was conducted at the Biology Laboratory of the Medical Department at the University of Ioannina, and part of the work took place at the Centre de Recherche en Biologie Cellulaire de Montpellier (CRBM). The supervising professor was Dimitris Liakopoulos, an assistant professor at the University of Ioannina and a Group Leader (Research Director DR2) at CRBM.

I would like to express my gratitude to Mr. Liakopoulos for his support and patience throughout this thesis. I also deeply appreciate the opportunity to participate in his research and the chance to work and study abroad. This experience allowed me to learn new techniques, work diligently, and encounter diverse work cultures and people.

I extend my acknowledgements to all members of the Biology Laboratory, to Mr. Eustathios Friligos, my classmates at the Medical School, my teachers and my colleagues at CRBM: Ariane Abrieu, Florence Gaven, Paul Lambey, Simos Nadalis, Didier Portran, and Dimitra Lani.

Lastly, I want to thank my family and friends for their unwavering support.

Abstract

Progression of cells into anaphase occurs only when microtubules are correctly attached to chromosome kinetochores, a process that is frequently error-prone in eukaryotic cells. In yeast, where kinetochores interact with a single microtubule, attachment errors may result from mechanical or molecular disruptions.

The spindle assembly checkpoint (SAC) monitors and resolves these errors by halting anaphase onset until all chromosomes are properly attached and bioriented. Misattachments can lead to aneuploidy, characterised by deviations in chromosome number, which is associated with tumorigenesis and cancer. The kinase Ipl1/Aurora B, a pivotal component of the Chromosomal Passenger Complex (CPC) is essential for correcting these attachment errors, cooperating with SAC.

During metaphase to anaphase progression, the CPC translocates from centromeres to the spindle midzone, fulfilling critical roles in maintaining chromosomal stability, ensuring accurate segregation.

It has been suggested that the localization and activity of Ipl1 are influenced by CPC sumoylation. Sumoylation is a post-translational modification involving the attachment of the ubiquitin-like protein SUMO to specific protein targets. This study investigates the role of CPC sumoylation in the localization and activation of its components, as well as its impact on cell growth and spindle dynamics in *Saccharomyces cerevisiae* cells.

The results indicate that while the sumoylation of other CPC components does not significantly affect *S. cerevisiae* growth, Ipl1 sumoylation appears to be essential, as cells lacking this modification were non-viable. Additionally, there is strong evidence that SUMO does not influence the localization of the CPC in *S. cerevisiae*, as localization

experiments in loss-of-sumoylation mutants showed no significant difference compared to wild-type cells.

However, SUMO may affect Ipl1 activity, as an increase in final spindle length was observed in *S. cerevisiae* mutants lacking CPC sumoylation. Equivalent differences in spindle size were observed in previous studies, suggesting that loss of Ipl1 function results in spindle elongation. However, these particular findings observed that the loss of Ipl1 function leads to an extension in spindle elongation time, something that was not observed in our findings. This suggests that sumoylation may influence phosphorylation of specific substrates by Ipl1 that are involved in spindle size, rather than its overall activity.

Περίληψη

Η είσοδος των κυττάρων στην ανάφαση πραγματοποιείται μόνο όταν οι μικροσωληνίσκοι είναι σωστά συνδεδεμένοι με τους κινητοχώρους των χρωμοσωμάτων, μία διαδικασία που συχνά παρουσιάζει σφάλματα στα ευκαρυωτικά κύτταρα. Στο ζυμομύκητα, όπου οι κινητοχώροι συνδέονται με μόνο ένα μικροσωληνίσκο, τα σφάλματα μπορεί να προκύψουν από μηχανικές ή μοριακές διαταραχές.

Το Σημείο Ελέγχου της Ατράκτου -Spindle Assembly Checkpoint (SAC)- παρακολουθεί και επιλύει αυτά τα σφάλματα, σταματώντας την έναρξη της ανάφασης μέχρι όλα τα χρωμοσώματα να είναι σωστά συνδεδεμένα με τους μικροσωληνίσκους και σωστά προσανατολισμένα. Λάθη σύνδεσης μπορούν να οδηγήσουν σε ανευπλοειδία, μία κατάσταση που χαρακτηρίζεται από διαφορές και αποκλίσεις στον αριθμό των χρωμοσωμάτων και συνδέεται με την καρκινογένεση. Η κινάση Ipl1/Aurora B, η οποία είναι βασικό μέλος του συμπλόκου Chromosome Passenger Complex (CPC), είναι απαραίτητη για την διόρθωση αυτών των σφαλμάτων, συνεργαζόμενη με το SAC.

Κατά την διάρκεια της μετάβασης από την μετάφαση στην ανάφαση, το CPC μετατοπίζεται από τα κεντρομερή στην μέση ζώνη (midzone) της ατράκτου, πραγματοποιώντας σημαντικές λειτουργίες στην σταθερότητα των χρωμοσωμάτων και στην εξασφάλιση του σωστού διαχωρισμού τους.

Έχει προταθεί ότι ο εντοπισμός και η δραστικότητα της Ipl1 επηρεάζονται από την σουμοϋλίωση του συμπλόκου CPC. Η σουμοϋλίωση είναι μια μετα-μεταφραστική τροποποίηση που περιλαμβάνει την δέσμευση της πρωτεΐνης SUMO σε συγκεκριμένα σημεία στις πρωτεΐνες. Η παρούσα μελέτη ερευνά τον ρόλο της SUMO στον εντοπισμό και στην ενεργοποίηση των μελών του CPC, καθώς και την επίδρασή της στην ανάπτυξη των κυττάρων και στην δυναμική της ατράκτου σε κύτταρα ζύμης *Saccharomyces cerevisiae*.

Τα αποτελέσματα δείχνουν ότι ενώ η σουμοϋλίωση των άλλων συστατικών του CPC δεν επηρεάζει σημαντικά την ανάπτυξη του *S. cerevisiae*, φαίνεται ότι για την Ipl1 είναι απαραίτητη, καθώς κύτταρα στα οποία η Ipl1 δεν τροποποιείται από την SUMO δεν ήταν βιώσιμα. Επίσης υπάρχουν ισχυρές ενδείξεις ότι η SUMO δεν επηρεάζει τον εντοπισμό του CPC στο *S. cerevisiae*, καθώς δεν παρατηρήθηκε διαφορά στον εντοπισμό του εν λόγω συμπλόκου σε μεταλλαγμένα κύτταρα που δεν είχαν αυτή τη σουμοϋλίωση συγκριτικά με κύτταρα φυσικού τύπου.

Ωστόσο, η SUMO ίσως επηρεάζει την δραστικότητα της Ipl1, καθώς παρατηρήθηκε αύξηση στο τελικό μήκος της ατράκτου σε μεταλλαγμένα κύτταρα *S. cerevisiae* που δεν φέρουν σουμοϋλίωση στο CPC. Αντίστοιχες διαφορές στο μέγεθος της ατράκτου παρατηρήθηκαν και σε προηγούμενες μελέτες, που υποδηλώνουν ότι η απώλεια λειτουργίας της Ipl1 οδηγεί σε επιμήκυνση της ατράκτου. Ωστόσο, στις μελέτες αυτές παρατηρήθηκε επίσης ότι η απώλεια λειτουργίας της Ipl1 οδηγεί και σε παράταση του χρόνου επιμήκυνσης της ατράκτου, κάτι το οποίο δεν παρατηρήθηκε στα ευρήματά μας. Αυτό υποδηλώνει πως ίσως η σουμοϋλίωση επηρεάζει την φωσφορυλίωση από την Ipl1 μόνο συγκεκριμένων υποστρωμάτων που εμπλέκονται στο μέγεθος της ατράκτου, και όχι την ενεργότητά της γενικότερα.

List of abbreviations

Abbreviation	Expansion
APC/C	Anaphase-Promoting Complex/Cyclosome
BIR	Baculovirus IAP Repeat
CPC	Chromosome Passenger Complex
DIC	Differential Interference Contrast microscopy
HR	Homologous Recombination
HU	Hydroxyurea
IAP	Inhibitor of Apoptosis Protein
KMN	First letters of Knl1, Mis12, and Ndc80
MATa	Mating Type a ("a")
MATalpha	Mating Type alpha ("α")
n.d.	Not determined - Unknown published date
pLDDT	Per-residue Local Distance Difference Test

1. Introduction

1.1 Cell Cycle

1.1.1 Phases of the Cell Cycle

The year 1879, Walther Flemming, in his book *"Zellsubstanz, Kern und Zelltheilung"* (Cell Substance, Nucleus and Cell Division) is referring to eukaryotic chromosome activity during cell division. This was the first ever detailed analysis of how cells multiply and how chromosomes are segregated, and the first time that concepts such as "prophase", "metaphase" and "anaphase" were mentioned. Initially cell division as a concept was introduced by Carl Nageli, but his findings were insufficient to interpret the process of mitosis (1879: Mitosis Observed, n.d.).

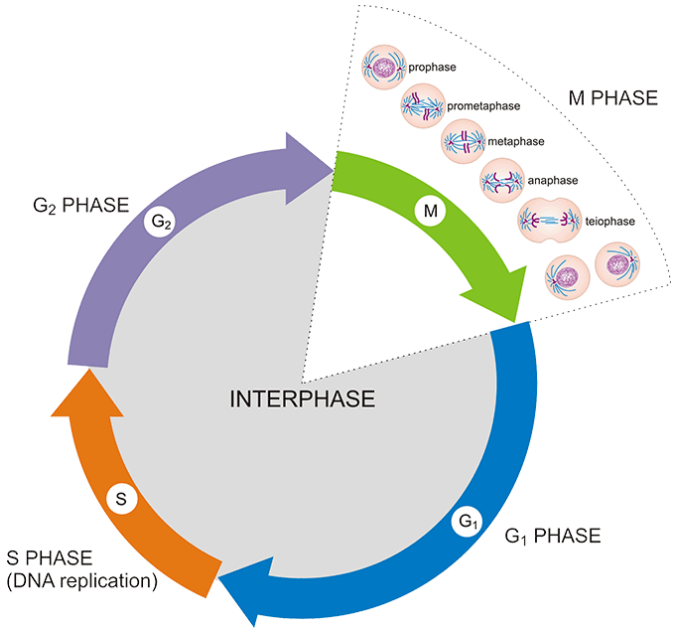

Figure 1: Eukaryotic cell cycle phases. Cell cycle in eukaryotes consists of the Interphase, where cells undergo cell growth and DNA replication, and the M phase, where chromosomes are segregated to the daughter cells, and cells undergo cytokinesis. Interphase occupies up to 95% of time of the cell cycle, and it is divided into the G1 phase, S phase and G2 phase. The M phase is divided into prophase, prometaphase, metaphase, anaphase, telophase and finally cytokinesis. (CUSABIO, n.d.)

Cell cycle is a complex regulatory process which is a defining feature of every cell. In eukaryotes, the cell cycle consists of a series of stages: two gap phases (G1, G2), a DNA synthesis phase, and an M phase, where the two daughter cells are created (Figure 1) (Resources, 2020).

1.1.2 Interphase

The two growth phases including the DNA synthesis phase (G1, S, G2) are called interphase. At this stage, the cell doubles its DNA, and it also synthesises mRNA and specific proteins that prepare the cell to enter mitosis. During the G1 phase, the cell expresses proteins that induce DNA synthesis, and also duplicates cellular contents (excluding chromosomes) (Watson, J. D., 2014). After the G1 phase, cells enter into the Synthesis phase, where DNA is replicated by tightly regulated processes (Takeda & Dutta, 2005). After the S phase concludes, the cell possesses twice the number of chromosomes, known as "sister chromatids." Following this, the cells proceed to the second and final growth phase, during which they examine any errors that may have arisen in the S phase. When all the necessary repairs are made, the cells then undergo mitosis, a process that involves chromosome separation and leads to generation of two daughter cells.

1.1.3 Mitosis

The last phase of the cell division is called Mitosis (M phase). Mitosis consists of five subphases.

The first phase of mitosis is called prophase, and it occupies over half the time of mitosis. During prophase of mammalian cells, the nuclear membrane breaks down and the nuclear envelope is destroyed. The centrosome is a cellular structure that consists of many proteins and acts as a nucleating site for microtubules, tubulin polymers that are essential for maintaining cell shape, intracellular protein transport and multiple cell division

processes. Centrosome-organised microtubules form spindle fibres that subsequently constitute the mitotic spindle (Resources, 2020) (CentroSome, 2023). After prophase, the centrosome duplicates, migrating to the opposite ends of the cell that are ought to be the new daughter cells (Resources, 2020).

The next phase of mitosis is called prometaphase. Here, chromosomes migrate to the middle of the cell, the cell equator. This movement is induced by the binding of microtubules to a protein complex that assembles on the centromeric region of chromosomes, called kinetochore. The next step is Metaphase, where chromosomes properly align themselves at a plane that lies in the middle of the spindle axis formed by the centrosomes (Resources, 2020), the metaphase plate.

When and if every chromosome is correctly aligned, the cell enters anaphase, where the spindle microtubules bound to the kinetochores pull the chromosomes to the opposite ends of the cell (CentroSome, 2023).

The final stage of mitosis is called Telophase. The nuclear membrane reforms around the chromosomes grouped at the two poles of the cell. Finally, the cells divide, creating two identical daughter cells. This stage is called cytokinesis (CentroSome, 2023).

1.1.4 The yeast life and cell cycle

1.1.4.1 Yeast life cycle

Cell cycle of every eukaryotic cell follows the same general principles, but differs between organisms. *Saccharomyces cerevisiae* is a unicellular eukaryotic organism, commonly known as baker's yeast, and it is used widely amongst researchers, as it provides a simplified model of the eukaryotic cell cycle and cell biology.

Yeast cells can exist in both forms (diploids and haploids). Haploids exist in two mating types, named MAT (mating-type): MATα and MATa. The main difference is found at MAT locus, which encodes transcriptional regulators, controlling the expression of specific genes that are responsible for the fusion of haploid cells of different mating types to form diploid cells (Figure 2) (Yamamoto et al., 2017).

In nutrient-deficient environments, diploid yeast cells have the ability to undergo meiosis and sporulation, a process that involves formation of 4 separate spores that each include a haploid genome. Meiosis is a biological phenomenon wherein a single cell undergoes two rounds of division, resulting in the generation of four cells, each containing half the original genetic content. This process is of paramount importance in sexual reproduction as it serves as a mechanism to introduce genetic variability. Meiosis comprises two key stages, known as meiosis I and meiosis II (Bhuiyan & Schmekel, 2004).

In yeast cells, the meiotic process shares fundamental similarities with that observed in other organisms. In yeast, the initiation of meiosis is triggered by specific environmental signals, committing the cells to the meiotic pathway, irreversibly separating them from the typical mitotic cell cycle, even if the initiating cues are removed (Bhuiyan & Schmekel, 2004).

A pivotal outcome of meiosis is the halving of the chromosome number, culminating in the production of haploid cells. In the context of the budding yeast *Saccharomyces cerevisiae*, meiosis results in the creation of four haploid spores. These spores engage in genetic recombination, facilitating the exchange of genetic material between homologous chromosomes, thereby fostering genetic diversity among the resultant spores (Börner, G. V., Hochwagen, A., & MacQueen, A. J., 2023).

Among these spores, two will possess the mating type a, while the other two will have the mating type α. When conditions become more favourable, these haploid spores can germinate and develop into haploid cells once again.

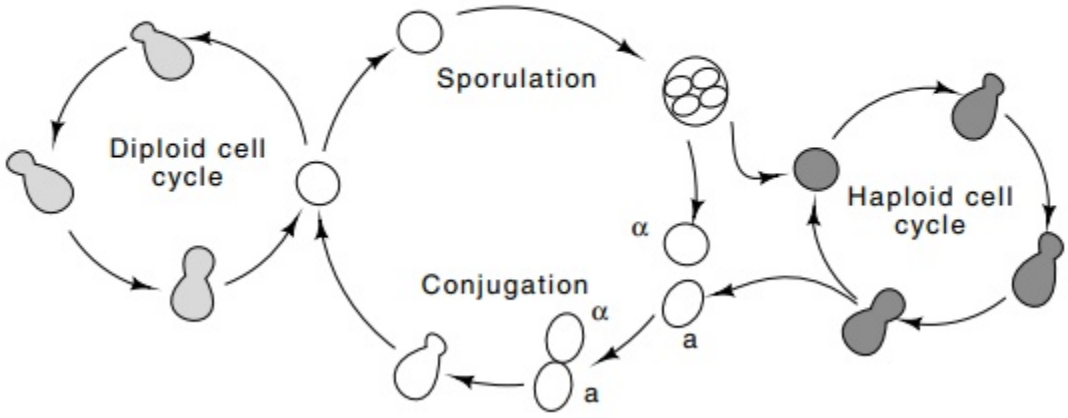

Figure 2: The yeast cell cycle. Yeast cells can exist in two forms: haploid cells, consisting of two mating types (a and α), and diploid a/α cells. When two haploids mate, they undergo "conjugation", but in nutrient-deficient environments they undergo meiosis, a phase that is called "sporulation" (Elements of Yeast Genetics, n.d.).

1.1.4.2 Yeast cell cycle differences

Many differences can be found between the cell cycle of mammalian cells and baker's yeast, regarding the duration, the regulation and overall cell cycle dynamics (Howes et al., 2017). Yeast cell division happens every 90 minutes under optimal laboratory conditions. During the yeast cell cycle, a small bud is formed that in the end will grow to be the daughter cell, hence the common name "budding yeast".

Fission yeast (*Schizosaccharomyces pombe*) and budding yeast (*Saccharomyces cerevisiae*) exhibit significant differences in their cell cycle processes, particularly in cytokinesis, growth, and cell-cycle control (Bähler, 2005).

Fission yeast divides through a process named medial fission, where the cell splits in two equal halves, where budding yeast undergoes asymmetric division, producing a daughter cell smaller than the mother cell. Fission yeast grows by elongating at the cell ends, while budding yeast initiates growth by forming a bud at a specific site, which enlarges during cell cycle (Gu & Oliferenko, 2015).

The bud remains attached to the mother cell until the end of the cell cycle (Figure 3). Through the actin network, mother and bud cells exhibit phenotypic differences in their proteins and organelles. One key protein is Ace2, along with Ash1p, which regulates genes essential for the daughter cell (bud), enhancing polarity through differential protein expression (Herrero et al., 2020). Ash1p also represses mating-type switching in the daughter cell, locking its mating type, ensuring that mother and daughter cells have different mating types. While the mother cell can change its mating type, the daughter cell remains fixed in its current mating type due to Ash1p repression (Chang & Drubin, 1996).

Asymmetric cell division also utilises cell polarity to guide and position the mitotic spindle correctly (Koca Caydasi Research Group - Ayşe Koca Çaydaşı, 2019). Furthermore, research by Fehrenbacher et al. has shown that due to cell polarity, organelles transferred to the bud are generally in better condition, allowing the bud to survive through more cell cycles compared to the mother cell (Fehrenbacher et al., 2004). Thus, asymmetry is crucial not only for mating-type differentiation, but also for maintaining the youth and health of newly formed bud cells compared to the ageing mother cells (Herrero et al., 2020).

Cell polarity plays a crucial role in the positioning and orientation of the spindle during cell division. As mentioned, budding yeast cells establish polarity by unevenly distributing proteins and organelles, creating distinct functional regions. The polarised cell cortex interacts with microtubules, which grow preferentially toward specific areas of

the cell aligned with polarity markers. Motor proteins such as dynein and kinesin facilitate spindle positioning by transporting cargo along the microtubules toward these polarised regions (McNally, 2013).

Budding yeast doesn't have a typical and distinct G2 phase in the cell cycle. Although fission yeast provides a clear G2 phase, where cells grow and prepare for mitosis, *S. cerevisiae* cells transition quickly from the S phase to mitosis, due to its specific cell cycle properties. These properties are characterised by a focus in various checkpoints, integrating signals such as cell polarity, spindle orientation and microtubule dynamics (Magliozzi & Moseley, 2021).

The centrosome in budding yeast is called the Spindle Pole Body (SPB), and instead of lying at the cytoplasm, it is embedded in the nuclear membrane (Figure 4). In yeast, even after the creation of the daughter cells, SPBs spindle poles exist and are connected to the kinetochore via kinetochore microtubules. During the S phase, a new SPB is assembled next to the old SPB that is carried on from the previous cell cycle, and becomes inserted into the nuclear membrane (Kilmartin, 2014).

Another significant distinction between budding yeast and other eukaryotes is that, in budding yeast, the S phase occurs concurrently with spindle assembly (Leisner et al., 2008). During this phase, DNA replication happens alongside spindle formation, facilitating efficient cell cycle progression and enhancing genomic stability. Moreover, the establishment of the spindle apparatus during the S phase ensures the proper organisation of newly replicated chromosomes, allowing them to be correctly positioned for accurate segregation (Juanes et al., 2013).

The formation of the yeast spindle pole body entails the initiation through the establishment of a satellite structure, encapsulating essential SPB components, including Spc42, Spc29, Spc110, and Spc72 (Kilmartin, 2014).

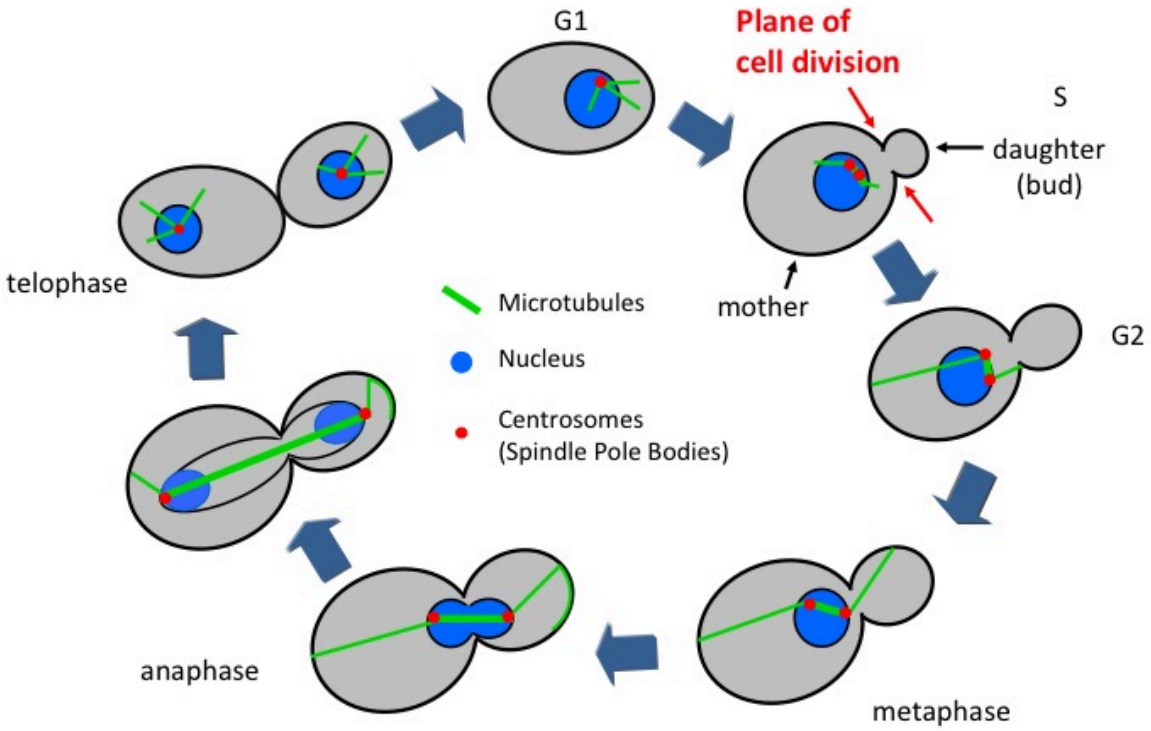

Figure 3: Budding yeast cell cycle. Yeast cells commit to division when they initiate budding, as a daughter cell forms on the mother cell and remains connected until telophase. Subsequently, the spindle pole body is duplicated and chromosomes are replicated, becoming attached to microtubules at kinetochores in a bipolar manner during metaphase. Chromosome segregation occurs in anaphase, driven by nuclear and cytoplasmic microtubules, assisted by binding proteins and molecular motors. Yeast undergoes a closed mitosis, maintaining the nuclear envelope intact during cell division (Koca Caydasi Research Group - Ayşe Koca Çaydaşı, 2019).

These proteins play integral roles in shaping SPB architecture and facilitating microtubule nucleation. Subsequent to satellite formation, its constituent elements undergo concerted assembly, culminating in the development of a larger and more complex structure recognized as the duplication plaque (Kilmartin, 2014). Within the duplication plaque, a significant transformation occurs as the embedded satellite undergoes crucial changes, driving the maturation of the spindle pole body.

The final steps involve inserting the plaque, now with the transformed satellite, next to the mother SPB while connected. This precise process ensures seamless integration into the nuclear envelope, completing the SPB duplication cycle (Kilmartin, 2014). Contrary to what is described for mammalian cells, the yeast nuclear membrane does not break down during mitosis and the budding yeast nucleus stays intact, resulting in a so-called closed mitosis (Tanaka et al., 2005).

The correct positioning of the spindle is ensured by feedback mechanisms, particularly the Spindle Assembly Checkpoint (SAC). The SAC activates to delay cell cycle progression until proper microtubule-chromosome attachments and correct spindle orientation are achieved (Barford, 2011). Incorrect chromosome attachments and misalignments driven by spindle positioning errors trigger the SAC, which coordinates adjustments in spindle alignment. Additionally, various signalling pathways integrate inputs from cellular cues, modulating cytoskeletal and motor protein activity to fine-tune spindle positioning according to the cell's polarised state (Stevermann & Liakopoulos, 2012).

1.2 The spindle assembly checkpoint (SAC)

1.2.1 Attachment issues and aneuploidy

Aneuploidy is the deviation from the correct ploidy (chromosome number) in cells. Aneuploid cells can lack one or more chromosomes or contain extra chromosome copies and/or chromosome fragments. Aneuploidy is linked to tumorigenesis, metastasis, and cancer (Hassold et al, 2007). Aneuploidy is often the consequence of errors in chromosome segregation. These in turn can be the result of erroneous attachment of chromosomes at spindle microtubules, at the site of kinetochores (Gladfelter & Berman, 2009).

Attachment issues are a frequent phenomenon in all eukaryotes and can easily be studied in yeast, as spindle poles and kinetochores are bound by only one microtubule (Figure 4) (Banerjee et al., 2020).

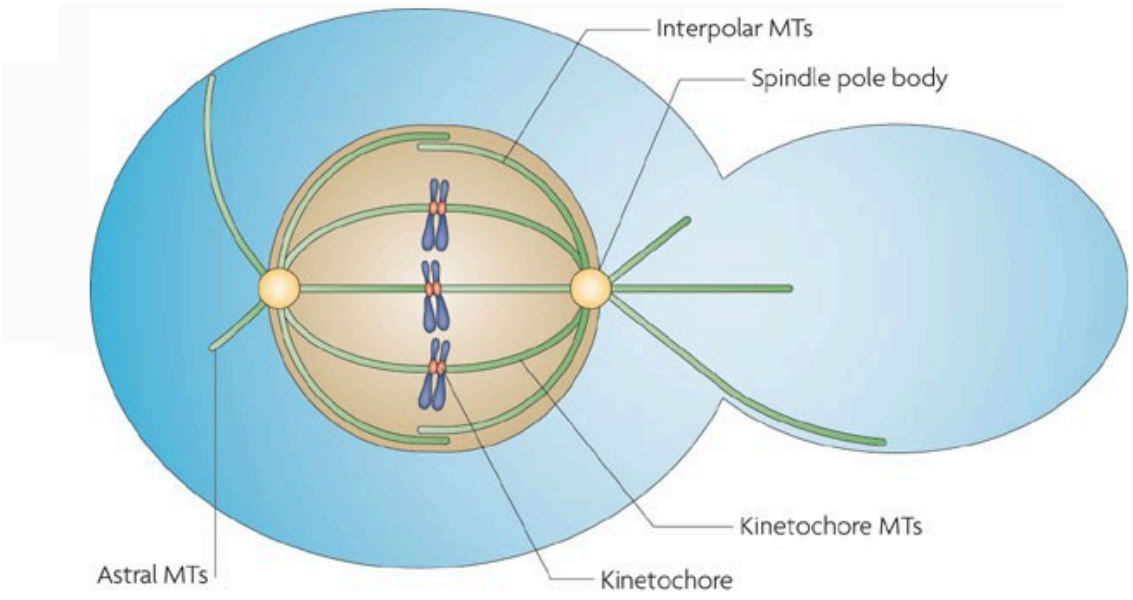

Figure 4: Illustration of Spindle Pole Bodies in yeast. Spindle poles (centrosome yeast homologue) are embedded into the nuclear membrane (Gladfelter & Berman, 2009).

In general, the following attachment issues could occur: a. one kinetochore is attached to microtubules from the same pole (syntelic), b. only one kinetochore is attached to a spindle pole (monotelic), and c. both kinetochores are bound to microtubules from their respective spindle poles but one is also attached to microtubules from the other spindle pole (merotelic) (Figure 5) (McVey et al., 2021). Merotelic attachment in yeast is not possible, since kinetochores are specifically designed to attach to a single microtubule, but all other errors may also arise here due to mechanical or molecular issues (Banerjee et al., 2020).

Cells enter anaphase when and if spindle microtubules are correctly attached to the kinetochores. Only when both kinetochores are bound to the correct pole, in a configuration called biorientation, can cells enter anaphase (Barford, 2011). Timing and accuracy of chromosome segregation is regulated by the Spindle Assembly Checkpoint (SAC), which is activated in response to errors regarding microtubule binding to kinetochores (Campbell & Desai, 2013).

To avoid generation of aneuploid cells during mitosis, the Spindle Assembly Checkpoint (SAC) delays anaphase until the microtubules are correctly attached to the kinetochores and the chromosomes are bioriented on the spindle. The checkpoint blocks or delays the cell cycle by inhibiting the Anaphase Promoting Complex (APC/Cyclosome, APC/C), an ubiquitin E3 enzyme that catalyses the ubiquitylation and destruction of proteins to ensure sister chromatid segregation, cell cycle progression after anaphase and exit from mitosis (Barford, 2011).

APC/C function is activated by binding to Cdh1 during interphase and Cdc20 is during mitosis. This function is crucial for substrate recognition by APC/C, catalysing the formation of ubiquitin chains on protein substrates, targeting them to degradation by the 26S proteasome. APC/C-dependent ubiquitylation and subsequent degradation of the protein Pds1 is the key event for anaphase entry. Termed also securin, Pds1 is an inhibitor

of separase, the protease that cleaves cohesin, the ring-shaped complex that wraps around chromatids, initiating the separation of sister chromatids (Barford, 2011).

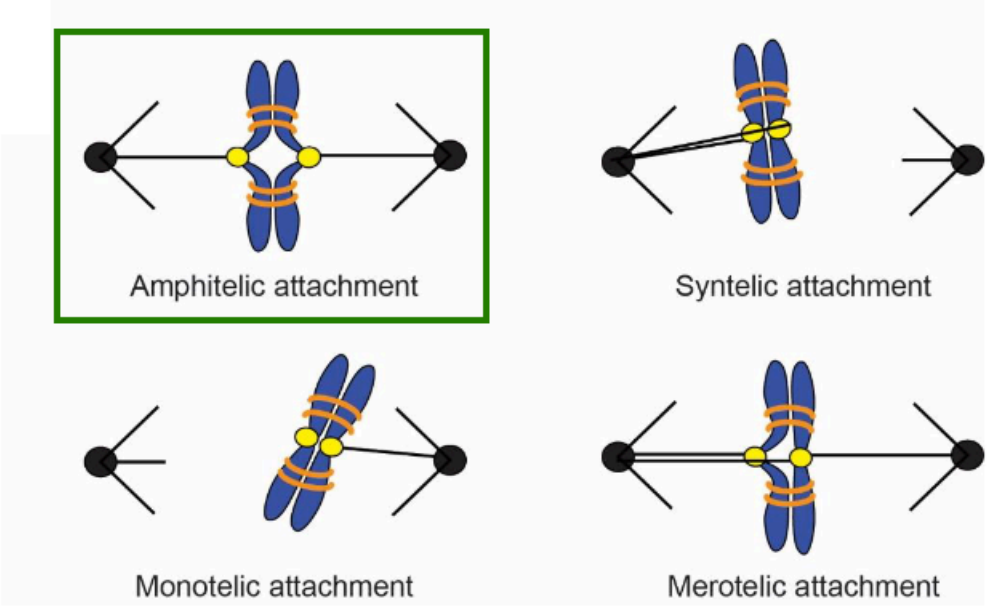

Figure 5: Simplified representation of kinetochore microtubules attachment to kinetochores (McVey et al., 2021). There are four ways for the microtubules to be attached to the kinetochores: amphitelic, when both kinetochores are bound to their respective spindle poles, syntelic when both kinetochores are bound to only one spindle pole, monotelic when only one kinetochore is bound to only one spindle, and merotelic when both kinetochores are bound to their respective spindle poles but one spindle pole is also attached to the other kinetochore.

As mentioned, SAC activates upon errors in microtubule-kinetochore attachments. These errors generate the formation of a protein complex, named Mitotic Checkpoint Complex (MCC), composed by Mad2, Cdc20. Bub3 and BubR1 (Jin & Wang, 2013). MCC assembly is performed in the highly conserved KMN network, which acts as a scaffold for the complex. KMN is an abbreviation from the first letter of its three subunits: Knl1 (Spc105 in *S. Cerevisiae*), Mis12 and Ndc80 complexes. Mis12 anchors KMN network to the kinetochore, Ndc80 binds to microtubules, initiating kinetochore-microtubule connections, and Knl1 is responsible for recruiting more SAC proteins (Corbett, 2017).

The mechanism by which the SAC functions in the inactivation of APC/C is straightforward. Bub3 bound to BubR1 stabilises the complex at the KMN network and, consequently, at the kinetochore, while Mad2 stabilises Cdc20 within the complex (Díaz-Martínez & Yu, 2007). The binding of Cdc20 to the MCC inhibits APC/C activation, since Cdc20 binding to APC/C is necessary for substrate recognition. (Corbett, 2017)

1.2.2 Ipl1 function in SAC

Scientists discovered that in budding yeast, cohesin deactivation activates SAC and leads to anaphase delay that depends on the kinase activity of Ipl1 (yeast homolog of Aurora B). Ipl1 is a serine/threonine kinase, an essential regulator for genomic stability, proper chromosome segregation, spindle assembly checkpoint (SAC), cytokinesis, and the attachment of microtubules to kinetochores (Figure 6) (Buvelot et al., 2003) (Gassmann et al., 2004).

The dependance of SAC on Ipl1 was demonstrated by Sue Biggins and Andrew W. Murray. They showed that incorrect localization of Ipl1 resulted in increased microtubule-attachment errors and disruption of SAC signalling in yeast (Biggins & Murray, 2001). In addition, Ipl1's mammalian homologue Aurora B inhibition causes a dramatic increase in both merotelic and syntelic attachments in mammalian cells (Gassmann et al., 2004).

Ipl1 phosphorylates outer kinetochore proteins, such as Knl1, Mis12 and Ndc80, destabilising and finally retracting kinetochore-microtubule attachments (Doodhi & Tanaka, 2022).

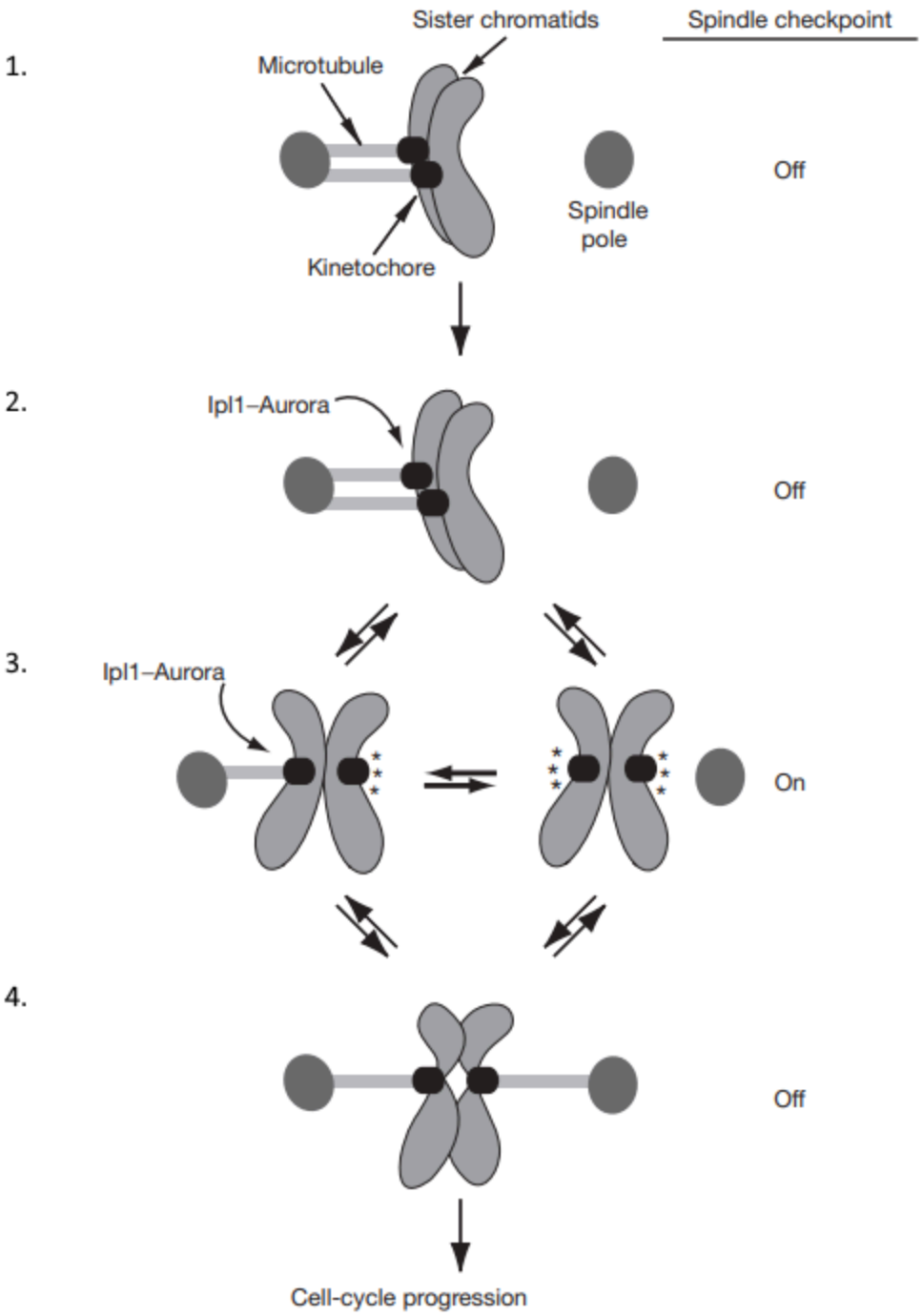

Figure 6: The Ipl1-Aurora B function involves correcting improper attachments and triggering the spindle checkpoint by inducing unattached kinetochores. Firstly, the spindle checkpoint does not directly detect mono-oriented attachments or kinetochore-microtubule interactions lacking tension. Secondly, Ipl1-Aurora identifies defects in tension and enhances the instability of inappropriate attachments. Thirdly, Ipl1-Aurora facilitates kinetochore detachment, resulting

in unoccupied microtubule binding sites, which serve as the primary signal for activating the spindle checkpoint. Finally, the checkpoint pauses the cell cycle until kinetochores establish bipolar attachments and experience tension (Pinsky et al., 2005).

Among outer kinetochore components, the Ndc80 complex (Ndc80C) and the Dam1 complex (Dam1C) directly interact with microtubules (MTs) and play major roles in creating the kinetochore–MT interface in budding yeast (Figure 7) (Doodhi & Tanaka, 2022).

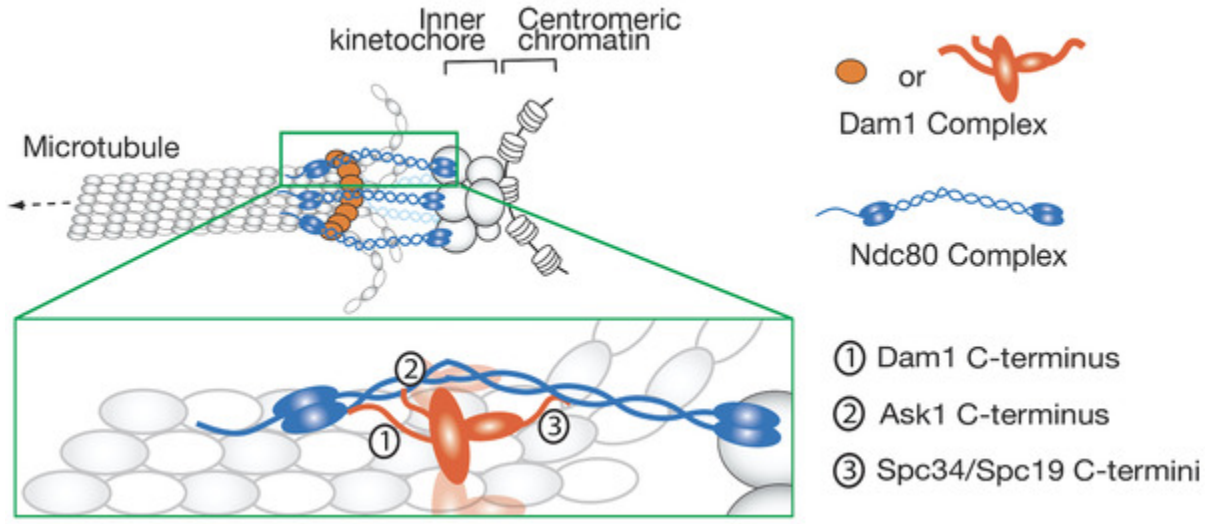

Figure 7: Visual representation about interactions between Dam1C and Ndc80C at the end‑of kinetochore - microtubule attachments in budding yeast. Three flexible regions of the Dam1C (Dam1C‑terminus, Ask1 C‑terminus and Spc34/Spc19 C‑termini) interact with different regions of the Ndc80. These regions are phosphorylated by Ipl1. (Doodhi & Tanaka, 2022)

Ndc80 phosphorylation electrostatically interferes with the complex dynamics, preventing its attachment to microtubules (Figure 8) (Doodhi & Tanaka, 2022). This is due to its positively charged N-terminus that interacts with the negatively charged microtubules. Phosphorylated Ndc80 shows a reduced positive charge, leading to a decreased affinity for microtubules (Vallardi et al., 2017).

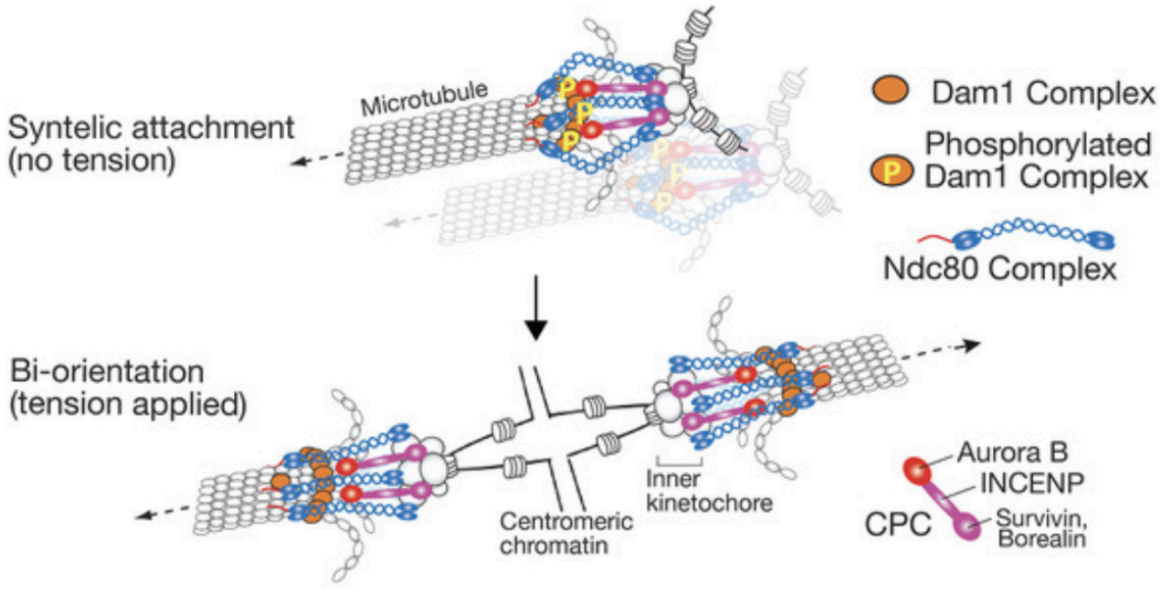

Figure 8: In the absence of tension on centromeres, Aurora B phosphorylates the Dam1 complex, destabilising microtubule-kinetochore attachments. When sister chromatids are bi-oriented, tension is applied and Dam1 complex interacts with Ndc80 to further stabilise microtubule - kinetochore attachments. (Doodhi & Tanaka, 2022)

1.2.3 Tension-sensing Ipl1

Apart from inducing the correction of microtubule-kinetochore attachments, Ipl1 is also said to activate the SAC (Papini et al., 2021) (Biggins & Murray, 2001). It was proposed that the correct attachment of kinetochore microtubules to chromosomes creates high levels of tension at kinetochores, which inactivates the SAC, while chromosomes that are incorrectly attached experience low-to-no tension at all (Figure 9). This difference in tension leads to the activation of SAC, which is regulated by Ipl1 (Biggins & Murray, 2001) (Pinsky et al., 2005).

A theoretical proposition posits that cellular awareness of attachment issues between microtubules and chromosomes is primarily mediated through tension (Biggins & Murray, 2001). This concept aligns with findings dating back to 1969 by Bruce Nicklas and Carol Koch, who observed that tension plays a crucial role in influencing the binding

dynamics between kinetochores and chromosomes. Specifically, they noted that interactions characterised by tension tend to result in stable binding (Nicklas & Koch, 1969).

The mechanism through which Ipl1 perceives tension is not fully understood, but the "Spatial Separation Model" provides a prominent theoretical framework. According to this model, Ipl1 kinase is stably localised and activated within the inner centromere. In conditions of low to no tension, Ipl1 substrates at kinetochores are in close proximity to the inner centromere (McVey et al., 2021).

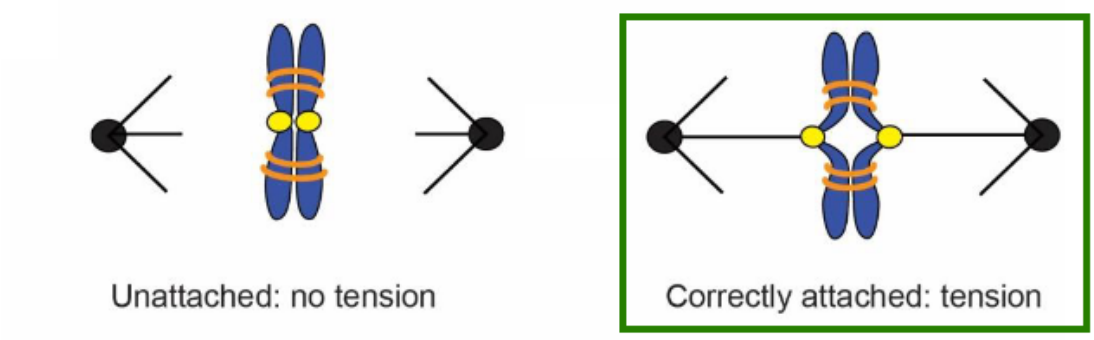

Figure 9: Correctly attachments between kinetochore microtubules and kinetochores exert levels of tension (McVey et al., 2021).

This allows the kinase to access and phosphorylate its targets at the kinetochore, destabilising kinetochore-MT interactions and facilitating the correction of improper attachments. In contrast, when microtubules are correctly attached, the kinetochore is distanced from the kinase due to stretching, preventing Ipl1 from phosphorylating its targets and thereby ensuring the stability of MT-kinetochore configurations (Figure 10) (Liu et al., 2009).

Other proteins that regulate the activity of Ipl1 depending on the tension at kinetochores are the phosphatases PP1 and PP2. Protein Phosphatase 1 (PP1) and 2 (PP2) are recruited to kinetochores, and oppose Ipl1 activity by dephosphorylating the kinase substrates. These dephosphorylation patterns appear only in bipolar attachments, further stabilising them, since tension-mediated stretching of centromeres shifts substrates away from Ipl1 and towards PP1 and PP2 (Akiyoshi et al., 2010).

Scientists suggest that Ipl1 is only active in environments that exhibit specific tension levels. This regulation of the kinase occurs with a protein that induces or inhibits Ipl1 activity depending on the kinetochore tension, due to the conformational change of the protein (McVey et al., 2021).

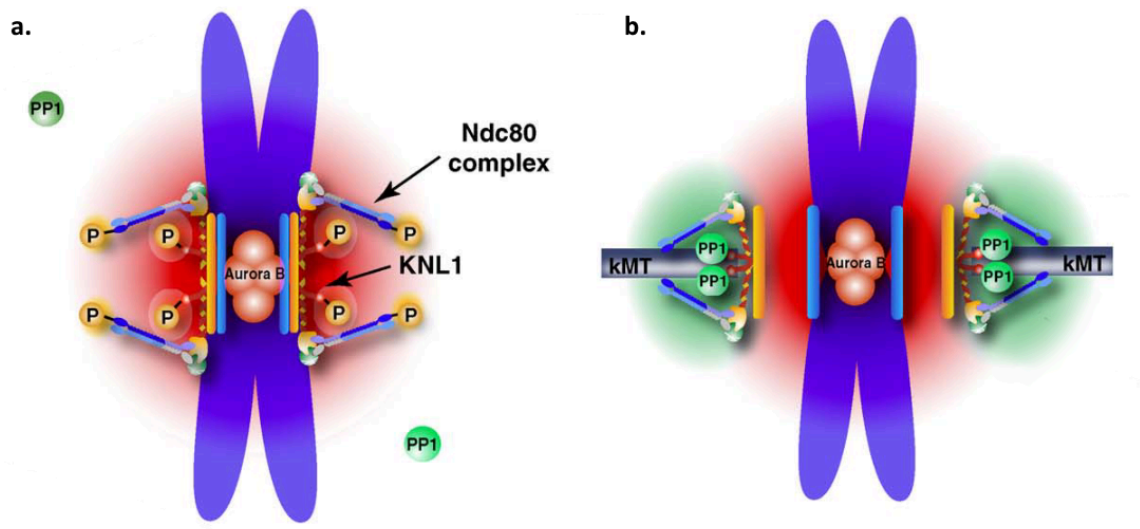

Figure 10: Spatial separation model: Kinetochore microtubules (kMT) are attached to kinetochores, exerting tension (Lampson & Cheeseman, 2011). When microtubules are incorrectly attached to kinetochores, (a.) the Ndc80 complex and KNL1 proteins are phosphorylated, thus kinetochore - kinetochore microtubule attachments are not stabilised. When microtubules are correctly attached to the kinetochores (b.), the centromeric stretch leads substrates away from Ipl1's homolog, Aurora B, towards a region full of phosphatases, such as PP1. This stabilises the kinetochore microtubule-kinetochore attachment.

The proteins proposed for the activation of Ipl1 are Sli15, a DNA translocase called PICH, and a kinesin-7 motor protein, called CENP-E (McVey et al., 2021). Yeast cells

lack a DNA translocase homologous and analogous to PICH (Biebricher et al., 2013), but this mechanism could be found in yeast cells within other protein interactions.

Although Ipl1's activity in microtubule-kinetochore attachments requires phosphorylation of its substrates in the kinetochore, Ipl1 localises at the inner centromere during mitosis (Broad & DeLuca, 2020). In human cells, this recruitment of Aurora B to the inner centromere relies on the phosphorylation of histones H3 and H2A (Yamagishi et al., 2010). This phosphorylation recruits Survivin by interacting with its BIR domain, thereby also facilitating the recruitment of Aurora B to the inner centromere (Broad & DeLuca, 2020).

1.3 CPC composition and function

CPC is highly conserved amongst eukaryotes. In mammalian cells, CPC composites of Aurora B, INCENP, Borealin and Survivin, when in *S. cerevisiae* Ipl1, Sli15, Nbl1 and Bir1 respectively (Table 1, Figure 11).

Homo Sapiens	***S. cerevisiae***
Aurora B	Ipl1
INCENP	Sli15
Borealin	Nbl1
Survivin	Bir1

Table 1: CPC homologues in *Homo Sapiens* and *S. cerevisiae* (Chromosomal Passenger Complex | SGD).

The four proteins that altogether comprise CPC can be oriented in two main groups by their main function: the kinase and localisation module (Carmena et al., 2012).

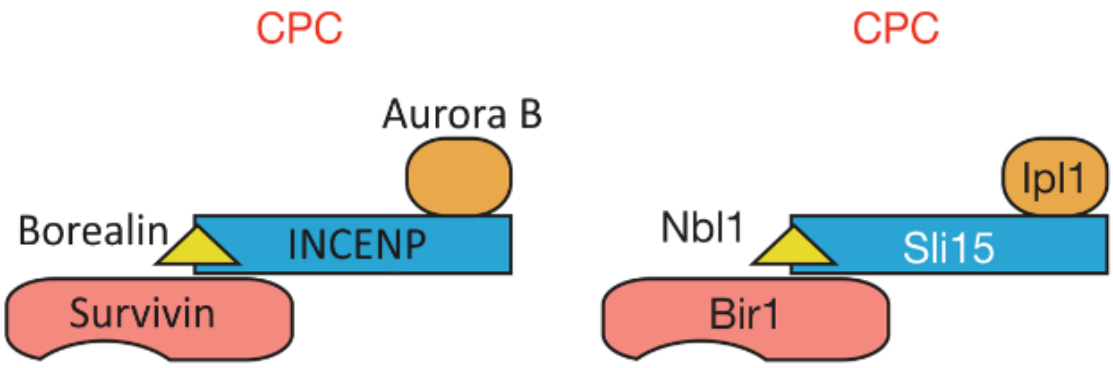

Figure 11: CPC in mammalian cells (left) and *S. cerevisiae* (right). Image made in photoshop.

The kinase module consists of the kinase Ipl1 and the carboxyl terminus of the protein Sli15. The localization module consists of the amino-terminus part of Sli15, the Bir1 and Nbl1 (Figure 12a). Sli15's N-terminal part is connected with the other two by a

three-helix bundle, while Ipl1 interacts by its C-terminal (Figure 12b) (Fischböck-Halwachs et al., 2019).

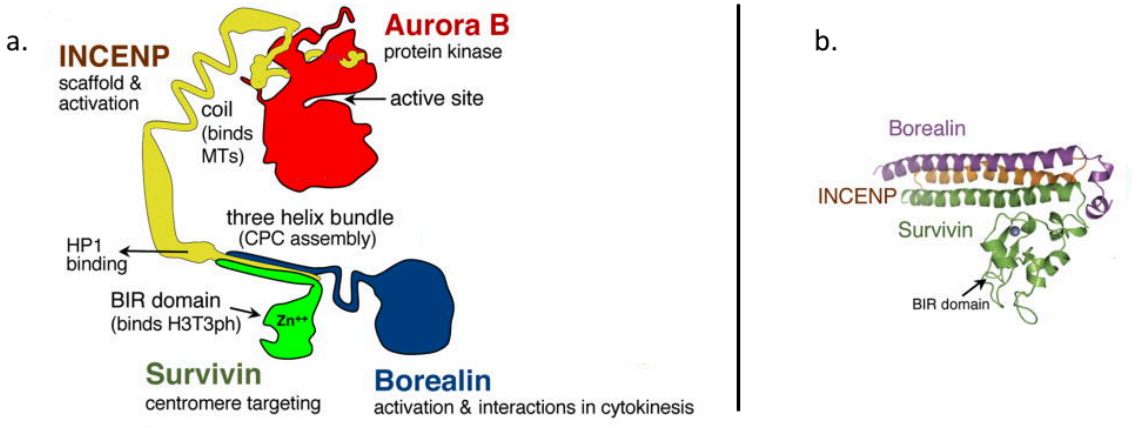

Figure 12: Structure of the CPC (a) and the three-helix bundle (b).The diagram represents the units of CPC, consisting of Aurora B kinase, INCENP, Survivin and Borealin, and their respective functions. In the picture b. is also demonstrated the BIR domain of Survivin, that is fundamental for the CPC localization to the centromere of the chromosomes, the mitotic spindle, and the anaphase midbody (Carmena et al., 2012).

1.3.1 Nbl1

Nbl1 is located on chromosome VIII in yeast. It is classified as a Borealin/Dasra/CSC-1-like protein, interacting with key proteins in chromosome segregation as previously mentioned (Sli15, Bir1) (NBL1 | SGD, n.d.). The importance of the engagement between these proteins was referenced by Yuko Nakajima and Randall G. Tyers, using a temperature-sensitive *nbl1* mutant in yeast. By studying this mutant, researchers observed abnormalities in the localization of Sli15 and Bir1. (Nakajima et al., 2009). The deficiency of functional Nbl1 disrupts Aurora B activity, thereby impacting both cell growth and the cell cycle. Furthermore, Nbl1 likely contributes to the coordination of actin and microtubule dynamics, critical for the precise execution of cell division (Marsoner et al., 2022).

Yeast's Nbl1 human homolog, Borealin, binds to the three helix bundle (with INCENP and Survivin) by its N-terminal domain, a highly conserved region amongst eukaryotes (Figure 13). Yeast Nbl1 consists of only the region involved in this bundle (Carmena et al., 2012).

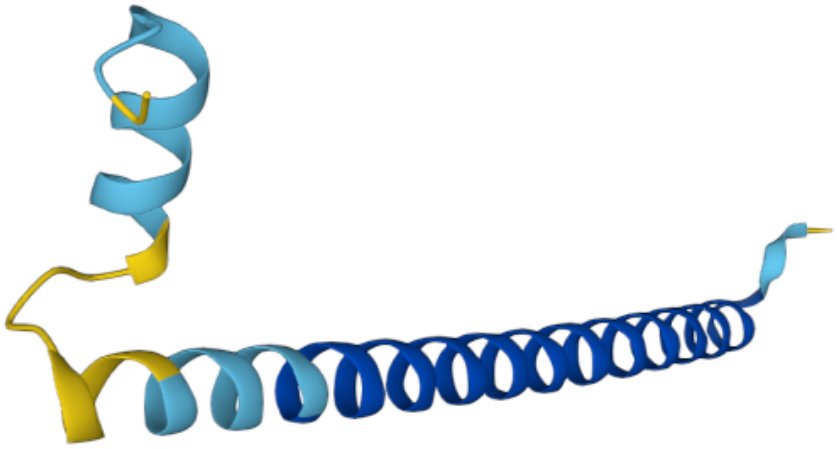

Figure 13: Suggested structure of Nbl1 monomer, using AlphaFold. The colours imply the model confidence of the calculative representation, where blue is very high (pLDDT > 90), pale blue is confident (90>pLDDT>70), yellow is low (70>pLDTT>50) and orange is very low (pLDDT<50) (NBL1 | SGD, n.d.).
(https://alphafold.ebi.ac.uk/entry/A0A1S7HRL5)

("pLDDT," stands for "per-residue local distance difference test, and it is used to evaluate the quality of predicted protein structures)

1.3.2 Bir1

Bir1 (Figure 14) human homolog, Survivin, functions as an anti-apoptotic protein, described originally as "Inhibitor of Apoptosis Protein" (IAP). In its free form it acts as a homodimer, having a "butterfly shape", but within the CPC, Bir1 forms a three-helix bundle with Sli15 and Nbl1, bound by its dimerization surface, neglecting any other Bir1 proteins. Therefore, Bir1 is unable to form a dimer when bound to CPC (Jeyaprakash et al., 2011).

In mammalian cells, survivin is overexpressed largely in numerous dysfunctions, with its levels being correlated with the respective disease aggression and clinical outcome (Jaiswal et al., 2015).

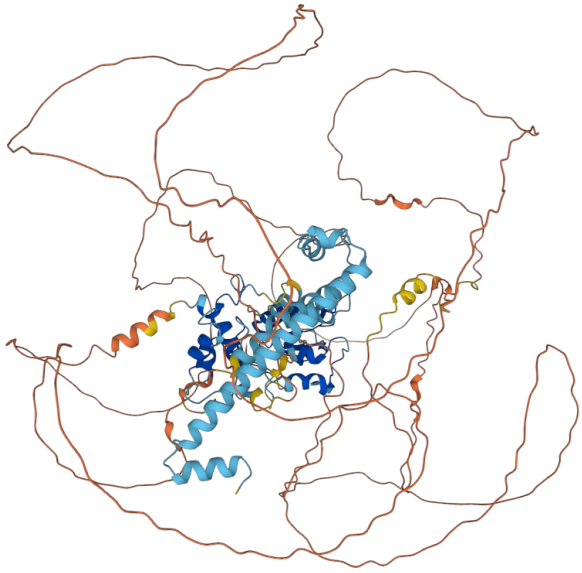

Figure 14: Suggested structure of Bir1 (YJR089W, monomer) protein, using AlphaFold. The colours imply the model confidence of the calculative representation, where blue is very high (pLDDT > 90), pale blue is confident (90>pLDDT>70), yellow is low (70>pLDTT>50) and orange is very low (pLDDT<50). (https://alphafold.ebi.ac.uk/entry/Q3E7Y6) (BIR1 | SGD, n.d.)

The region called /baculovirus IAP repeat/ (BIR) in the Bir1 protein, likely mediates protein-protein interactions within the CPC and with other kinetochore-associated proteins (Shimogawa et al., 2009). It is fundamental for the CPC localization to the centromere of chromosomes, the mitotic spindle, and the anaphase midbody, acting as a recognition site, allowing it to bind to specific regions or domains of other kinetochore proteins such as BubR1, Hec1 (Cormier et al., 2013). These interactions are instrumental in modulating the functionality and ensuring the stability of the Chromosomal Passenger Complex (CPC) to the kinetochores, thereby facilitating the proper operation of the complex (Jwa et al., 2008).

1.3.3 Sli15

Sli15 (Figure 15) acts as the scaffold between the localization and phosphorylation modules in CPC. Its N-terminal part is required for the CPC localization to the

centromeres, where the first 58 amino acids form the triple helix between Survivin/Borealin/INCENP (Carmena et al., 2012) (Jwa et al., 2008).

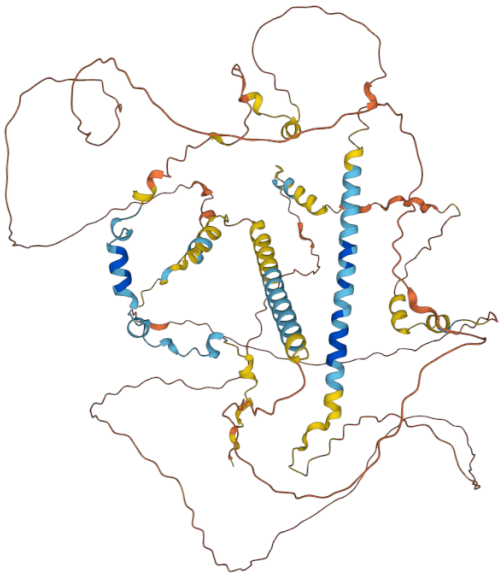

Figure 15: Suggested structure of Sli15 (YBR156C) protein, using AlphaFold. The colours imply the model confidence of the calculative representation, where blue is very high (pLDDT > 90), pale blue is confident (90>pLDDT>70), yellow is low (70>pLDTT>50) and orange is very low (pLDDT<50).

(SLI15 | SGD, n.d.)

Pereira and Schiebel's 2003 study found that inhibiting Sli15 phosphorylation causes premature localization to spindle microtubules in metaphase, regulating CPC transition to microtubules (Pereira & Schiebel, 2003).

Mutations that affect the phosphorylation of Sli15 do not affect the growth or viability of cells, but they decrease the rate of anaphase spindle elongation (Sandall et al., 2006). Notably, deletions in Sli15's microtubule-binding domain are lethal and severely disrupt CPC's chromosome segregation function, underscoring the importance of Sli15's microtubule interaction in the complex (Fink et al., 2017).

The microtubule-binding region in Sli15 is followed by the “IN-box” of Sli15 (Figure 16). This region interacts with Ipl1, and is implicated in linking the kinase to

microtubules and ensuring accurate attachment to the kinetochore, contributing to the dynamic regulation of mitotic processes in yeast (Makrantoni et al., 2014).

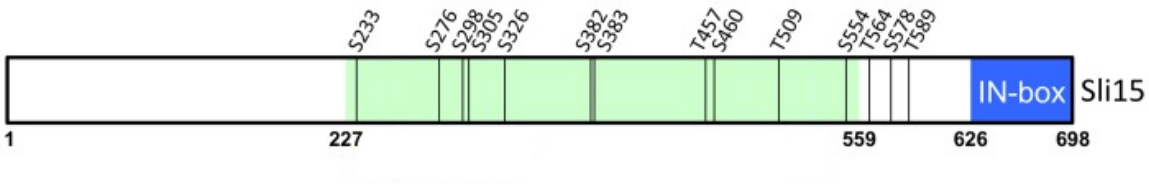

Figure 16: Visual representation of Sli15, illustrating the 14 phosphorylation sites, identified through in vitro mapping (black). The microtubule-binding region (residues 227–559) is highlighted in green, while the conserved IN box (residues 626–698) is shaded in blue (Makrantoni et al., 2014).

1.3.4 Ipl1

Ipl1 is a Serine/Threonine kinase, belonging to a highly conserved Aurora family of kinases (Figure 17). In all organisms studies so far, Aurora proteins are critical regulators of genomic stability and are crucial for the proper chromosome segregation, the spindle activating checkpoint (SAC), cytokinesis, and the correct attachments between microtubules and kinetochores (Buvelot et al., 2003).

Ipl1 localises to the kinetochores before and during metaphase, and later transfers to the mitotic spindle during anaphase (Buvelot et al., 2003). This translocation is crucial for the many functional aspects of Ipl1, since the kinase ensures proper attachments and segregation of chromosomes during mitosis.

Apart from regulating the SAC and MT-chromosome attachments, Ipl1 contributes to chromosome compaction during mitosis, through the phosphorylation of histone-3 at Ser10 (H3S10) (Hsu et al., 2000). It is also proposed to regulate the binding of condensin, by phosphorylating the kleisin protein Cnd2, that promotes the localization and recruitment of condensin to chromosomes (Carmena et al., 2012).

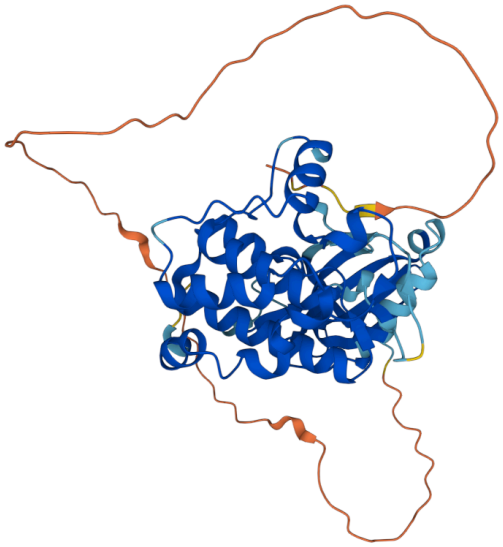

Figure 17: Suggested structure of Ipl1 protein, using AlphaFold. The colours imply the model confidence of the calculative representation, where blue is very high (pLDDT > 90), pale blue is confident (90>pLDDT>70), yellow is low (70>pLDTT>50) and orange is very low (pLDDT<50).
(IPL1 | SGD, n.d.)

1.4 Ipl1 activity and localisation

In human cells, the linkage between Ipl1 (Aurora B) and the "IN-box" of Sli15 (INCENP), as well as the phosphorylation of the second, induces conformational changes to the complex and the kinase, enhancing its enzymatic activity (Petsalaki et al., 2011). Surprisingly, in yeast, the phosphorylation of this region is not essential for the activation of Ipl1, rather the kinase is activated by the lack of tension to the kinetochores (Makrantoni et al., 2014).

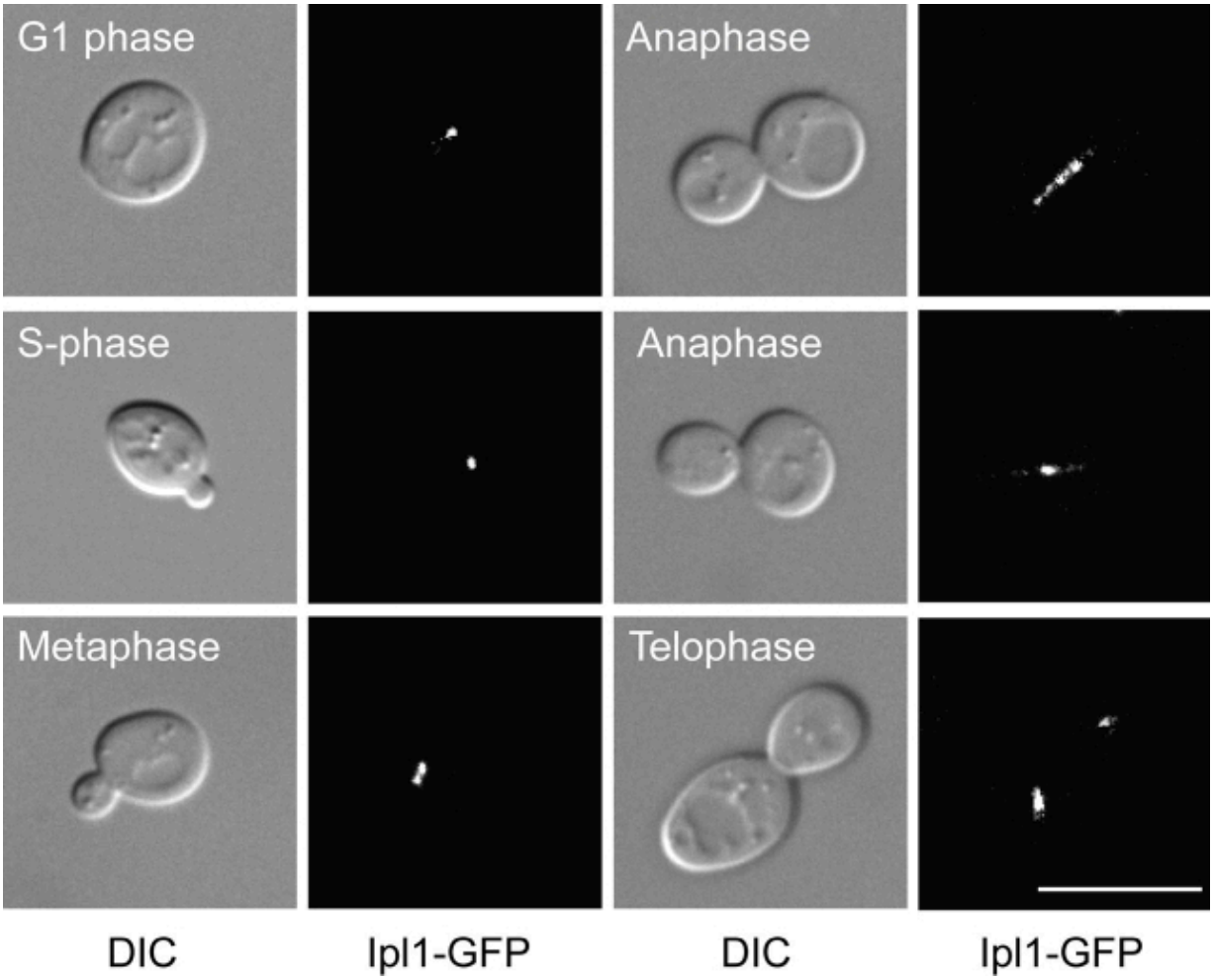

Figure 18: Ipl1's different localizations throughout the cell cycle in budding yeast. Images were taken and edited by Stephanie Buvelot et al. (Buvelot et al., 2003).

1.4.1 Ipl1/CPC localisation

In early mitosis, Ipl1 (along with CPC) localises to chromosome arms, while later in metaphase it is found at the centromere. During the late stages of anaphase, CPC translocates from the centromere to the anaphase spindle (Figure 18) (Buvelot et al., 2003) (Hadders & Lens, 2022). This translocation is essential for regulating microtubules of the central spindle involved in spindle dynamics, elongation, and cytokinesis (Argiros et al., 2012).

Changes in the localization of CPC from chromosome arms to the centromere is mediated by two histone kinases, namely Haspin and Bub1 (Boyarchuk et al., 2007). Disruption of either Haspin or Bub1 kinases results in reduced localization of Ipl1 at the inner centromere, leading to increased risk of aneuploidy (Cairo & Lacefield, 2020).

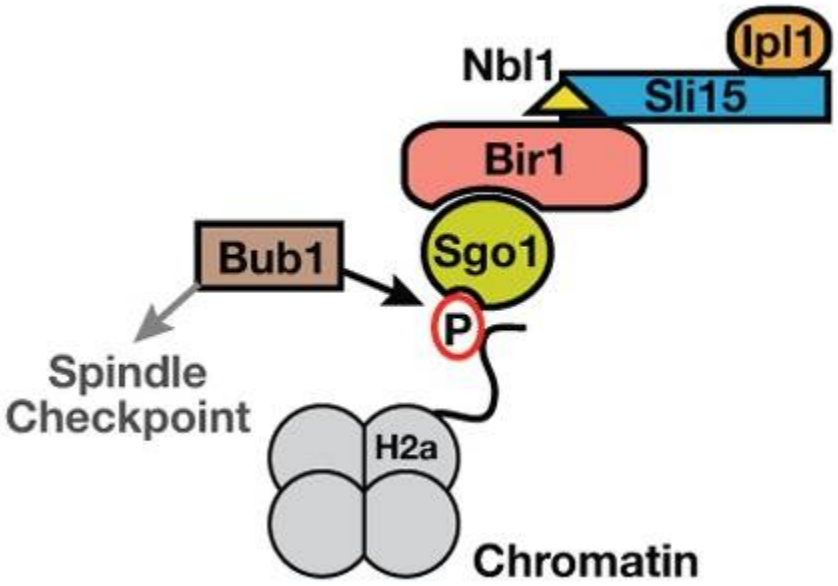

Figure 19: Graphical abstract demonstrating the regulatory mechanism that contributes to the localization of Sgo1 and Ipl1, involving Bub1-Bub3 (Kawashima et al., 2010).

Downstream of Bub1, Sgo1 serves as a molecular scaffold for Ipl1, and also facilitates the interaction between condensin and centromeric chromatin, ensuring the overall stability (Sane et al., 2021) (Peplowska et al., 2014). Bub1 phosphorylates histone H2A at Serine 121. This phosphorylated serine residue is recognised by Sgo1, which is bound to CPC by Bir1, therefore ensuring the stabilisation of the complex in the centromere (Figure 19) (Kawashima et al., 2010).

Stabilisation of Bub1 depends also on Mps1 activity both in yeast and human cells. In yeast, this recruitment is mediated via phosphorylation of the kinetochore protein Spc105 (Knl1 yeast homolog) by Mps1, which enhances binding of Bub1 to the kinetochore protein Knl1 (Van Der Horst & Lens, 2013).

In addition, activity of the CPC is required to enforce maintenance of CPC at centromeres: The CPC restricts loading of Sgo specifically onto centromeres. Finally, stabilisation of CPC in the centromere depends on the Sli15 centromere targeting domain (2-228 amino acids). Campbell and Desai revealed that the deletion of this domain (Sli15ΔN2-228) interfered with the localization of Sli15 -and therefore the whole CPC complex- to kinetochores (Campbell & Desai, 2013).

At the end of mitosis, CPC shifts its position from the chromosomes to the microtubules. Studies have revealed that specific protein interactions facilitate the CPC's transition from the chromosomes to the microtubules. Research by Gruneberg et al. demonstrated that Sli15 human homolog, INCENP, binds to the Kinesin-6 protein Mklp2 in order to translocate from the chromosomes to microtubules in HeLa cells (McKim, 2021) (Gruneberg et al., 2004). Mklp2 not only plays a critical role in CPC localization to the microtubules but also in its transport to the spindle midzone.

The switch from chromatin to microtubules is regulated by chromatin and Mklp2 competition for binding to STD, one of the two conserved INCENP domains that interact

with microtubules (known as STD and SAH (McKim, 2021)). The STD domain also engages with chromatin, stabilising CPC in its chromosomal location. Cdk1 activity regulates the timing of CPC translocation to microtubules. Prior to anaphase, high Cdk1 activity prevents association between INCENP and Mklp2 and prevents translocation of the CPC to the midzone (Hümmer & Mayer, 2009).

Cdk1 is highly active during mitosis, and its activity decreases at the onset of anaphase. This reduction in Cdk1 activity facilitates the translocation of the Chromosomal Passenger Complex (CPC) to the microtubules and spindle midzone at specific stages of the cell cycle (Kalous et al., 2020). In yeast, a similar mechanism operates and CPC translocation to the midzone is initiated by the activation of Cdc14 phosphatase, which leads to dephosphorylation of the Cdk1 sites on Sli15, facilitating relocalization of Sli15 and Ipl1 to the spindle midzone (Pereira & Schiebel, 2003) (D'Amours & Amon, 2004).

In late anaphase, CPC accumulates at the spindle midzone, where it plays a crucial role in promoting spindle disassembly and cytokinesis (Buvelot et al., 2003). Ipl1 substrates like Dam1, Sli15, and Ndc10 localise to spindle midzone, suggesting Ipl1 may regulate microtubule dynamics at this location to promote spindle disassembly (Buvelot et al., 2003).

Cells lacking functional Ndc10 exhibit spindle stability defects during anaphase and struggle with chromosome separation during cytokinesis (Biggins et al., 1999). Additionally, the transport of Ndc10 to the midzone in anaphase relies on CPC activity, highlighting the critical step of CPC translocation to the spindle midzone (Bouck & Bloom, 2005).

In mammalian cells, the localization of Aurora B at the midzone regulates spindle length through two opposing mechanisms. First, Aurora B phosphorylates KIF2A, a microtubule depolymerase, inhibiting its activity and keeping it anchored at the minus ends of

microtubules (Uehara et al., 2013). Additionally, Aurora B monitors chromosome positioning during anaphase to ensure that the nuclear envelope re-forms only after proper chromosome separation. This regulation occurs due to Aurora B removal from chromosomes, leaving phosphatases to dephosphorylate its substrates, including histone H3 and condensin complexes that hold chromosomes together (Afonso et al., 2016).

1.5 The SUMO system

Small ubiquitin-related modifier (SUMO) proteins constitute a diverse family of proteins with structural similarity to ubiquitin (Figure 20). SUMO proteins and ubiquitin exhibit only a modest degree of overlap in their amino acid sequences, sharing approximately 10-20% of their sequence (Geiss-Friedlander & Melchior, 2007).

1.5.1 SUMO homologs

In eukaryotic cells such as *S. cerevisiae*, only one SUMO gene is expressed, whereas mammals -and plants- can express up to eight different SUMO homologs. In vertebrates, three SUMO proteins are expressed: SUMO-1 (also known as Smt3c, PIC2, GMP1, sentrin, Ubl1), SUMO-2 (also known as Smt3a, Sentrin3) and SUMO-3 (also known as Smt3b and Sentrin2) (Table 2). SUMO-2 and SUMO-3 share the same amino acid sequence, where only three N-terminal residues differ from one another. They both form a subfamily known as SUMO-2/-3, and share 50% their motif with SUMO-1 (Hay, 2005).

Protein	*Homo Sapiens*	*S. cerevisiae*
Modifier	SUMO-1, -2, -3	Smt3
Activating Enzyme (E1)	SAE1/SAE2	Aos1/Uba2
Conjugating Enzyme (E2)	UBC9	Ubc9
SP-RING SUMO Ligases (E3)	PIAS1, -2b, -3, -4; ZMIZ1; NSE2a	Siz1, Siz2, Zip3,Mms21
SUMO proteases	SENP1, -2, -3, -5, -6, -7; DESI1, -2; USPL1	Ulp1, Upl2

Table 2: SUMO pathway homologs (Control of nuclear activities by substrate-selective and protein-group sumoylation) (Hay, 2005).

Similar to ubiquitin, SUMO proteins covalently modify specific lysine residues on their target proteins. This process known as sumoylation, plays a regulatory role in a wide

range of cellular processes including nuclear transport, transcriptional regulation, chromosome segregation, DNA repair, or the modulation of protein-protein interactions (Hegde, 2010).

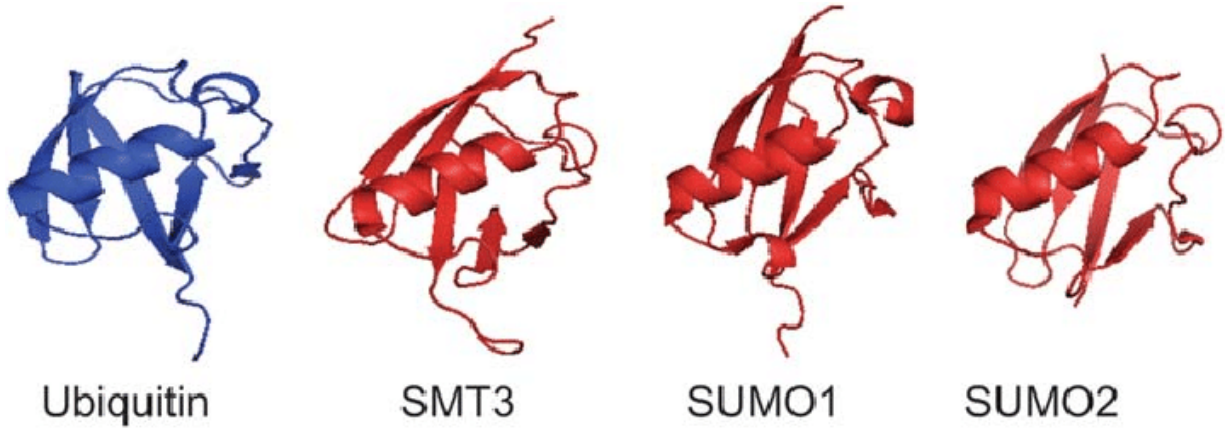

Figure 20: Structure of ubiquitin and SUMO proteins (Alonso et al., 2015).

1.5.2 Sumoylation cycle

The process that encompasses the addition and removal of SUMO proteins from a target protein is known as the "sumoylation cycle". This cycle involves a series of enzymatic events, including the activation, conjugation, and deconjugation of SUMO. Although the sumoylation cycle is mechanistically similar to ubiquitination, the sumoylation enzymes are unique and differ from the ones involved in ubiquitination (Figure 21) (Sajeev T. K. et al, 2021).

SUMO proteins are generated as inactive peptides that mature by proteolytic cleavage. Maturation and activation of the immature precursor SUMO protein involves enzymes that cleave the C-terminal part of the SUMO, in order to reveal a double glycine residue. These enzymes consist of a family of proteases, known as sentrin-specific proteases (SENPs) in mammals, and ubiquitin-like-protein specific proteases (Ulps - Ulp1 and Ulp2) in *S. cerevisiae* (De Albuquerque et al., 2018).

Ulp1 is known for desumoylating many intracellular proteins and is also responsible for SUMO maturation in yeast, while Ulp2 is a highly specific enzyme, having a distinct substrate profile (De Albuquerque et al., 2018). They share the 27% of their active domains, while their non catalytic structure and sequence shows no similarity. Ulp2 binds to three Smt3 units, cleaving only a single Smt3, while Ulp1 processes multiple Smt3 units (Eckhoff & Dohmen, 2015). This difference is occuring due to their difference in binding affinity to Smt3. Ulp1 binds to the C-terminal -GGATY sequence of the immature Smt3, relying on multiple hydrophobic and salt bridges for the stability, while the binding of Ulp2 in specifically three Smt3 units might be affected by its structure (Mossessova & Lima, 2000) (Eckhoff & Dohmen, 2015).

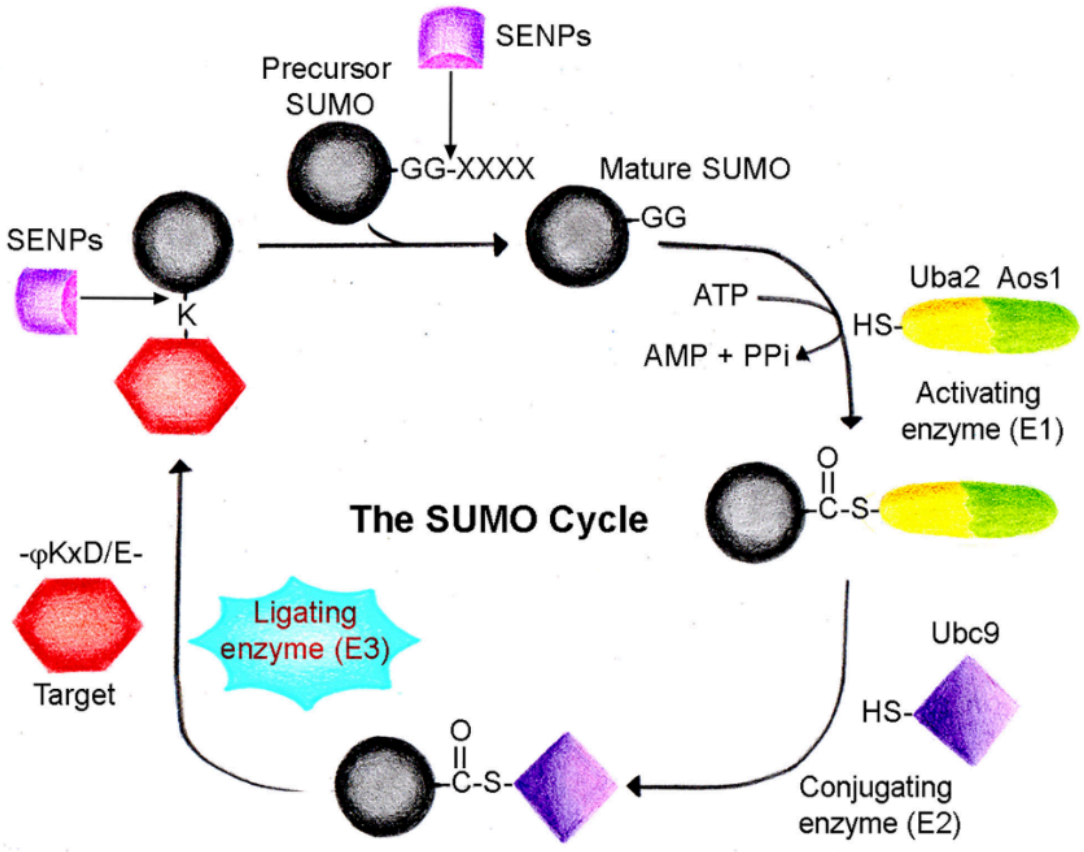

Figure 21: Sumoylation cycle. The cycle begins with the processing of immature SUMO proteins by the SENPs (Ulp1), which exposes a diglycine motif. This motif is then modified with adenylate and transferred to cysteine residues in SUMO E1 and E2 enzymes. Afterwards,

SUMO is attached to lysine residues on the target substrate directly through the E2 enzyme or with the aid of SUMO E3 ligases. This covalent attachment of SUMO modifies the substrate protein, leading to diverse effects such as changes in localization, stability, protein-protein interactions, or activity. To restore the substrate protein to its original state, the reverse process, known as desumoylation, occurs. SUMO-specific proteases (SENPs) are responsible for cleaving the SUMO moiety from the target protein (Sajeev T. K. et al, 2021).

The sumoylation cycle initiates with the activation of SUMO proteins by E1 enzymes. During this step, SUMO undergoes adenylation, resulting in the formation of a high-energy thioester bond between the C-terminus glycine of SUMO and the catalytic cysteine residue of the E1 enzyme (Figure 22b). Following activation, the activated SUMO molecule is then transferred to an E2 enzyme, forming a thioester intermediate (Talamillo et al., 2020).

The E2 enzyme plays a crucial role in the sumoylation process by mediating the transfer of SUMO from itself to a particular lysine residue on the target protein by an isopeptide bond (Figure 22a). This transfer is facilitated by the presence of E3 ligases, which interact with both the E2 enzyme and the target protein. E3 ligases contribute to the specificity and efficiency of the conjugation reaction, ensuring that SUMO is attached to the correct lysine residue on the target protein. It is important to note that while E3 enzymes are commonly involved in the finalisation of target protein modification in many organisms, not all organisms require E3 enzymes for this process (Cremona et al., 2012)

S. cerevisiae expresses three SUMO E3 ligases, Siz1, Siz2 (SAP and mIZ-finger DNA-binding domains), and Mms21 (methyl methanesulfonate sensitivity 21) (Nilsson et al., 2008). The differences between Siz1, Siz2, and Mms21 in are primarily associated with their roles and their substrates. The distinct functions of these ligases highlight their specific contributions to cellular processes, with Siz1/Siz2 affecting gene expression and Mms21 playing a pivotal role in DNA repair and growth (Jalal et al., 2017).

After the covalent attachment of SUMO to the target protein SUMO can impact the function, localization, stability, and interactions of the protein. SUMO serves as a signal that facilitates protein-protein interactions by attracting other proteins to the modified protein. This recruitment of other proteins further influences the behaviour and molecular interactions of the modified protein, contributing to the intricate network of cellular processes (Everett et al., 2013).

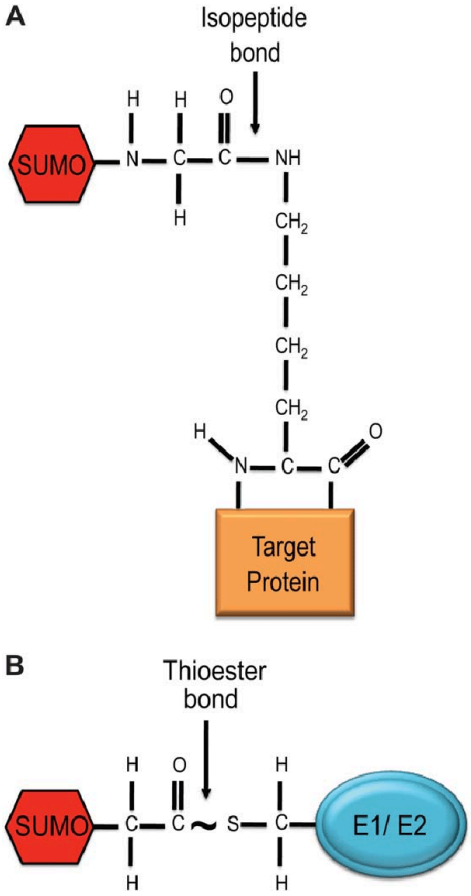

Figure 22: Sumoylation pathway chemical bonds. SUMO binds to target proteins by an isopeptide bond between a lysine residue on the substrate and the terminal SUMO glycine (A). The E1/E2 enzymes catalysing the sumoylation cycle form a thioester bond between the C-terminal glycine carboxyl group of SUMO and catalytic cysteine in the E1/E2 enzyme (SUMO-activating and conjugating enzymes) (B) (Alonso et al., 2015).

Finally, the dynamic character of sumoylation encompasses the removal of SUMO from the target protein by the SENPs/Ulps, that cleave the isopeptide bond connecting SUMO to the target protein, leading to the detachment of SUMO and the restoration of the target protein to its unmodified state. In yeast, Ulp1 confers the main SUMO deconjugation

activity. The enzymatic activity of SENPs plays a crucial role in maintaining the balance and reversibility of sumoylation (Wang & Dasso, 2009).

1.5.3 Sumoylation motifs

The lysine residue which SUMO proteins are attached, follows a specific amino-acid motif:

ΨKxE/D or **E/DxKΨ**

where Ψ is any hydrophobic amino acid, x is any amino acid, E is Glutamic and D is Aspartate Acid (Matic et al., 2010).

This motif provides an overall stability and recognitive framework for the binding of the SUMO protein to the targeted protein. The hydrophobic residue before or after the target lysine enhances the affinity between the SUMO-conjugating enzymes E3 or E2 and the lysine, thus stabilising the interaction and ensuring the proper positioning of the target lysine for conjugation (Matic et al., 2010). The negatively charged Glutamate and Aspartate enhance the interaction between the SUMO-conjugating enzyme (E2) and the target protein by electrostatic interactions caused by the said protein residues (Yang et al., 2006).

Two more sumoylation motifs have been identified: Phosphorylation-Dependent Sumoylation Motif (PDSM) and the Negatively Charged Aminoacid Dependent Sumoylation Motif (NDSM). The first motif is characterised by a foundational sequence motif followed by a phosphorylated serine residue and a proline residue (ψKxExxpSP). The second motif entails the core motif succeeded by two or more acidic amino acids located in the C-terminal tail (Yang et al., 2006). However, it is still unclear how the E2 enzyme recognizes these sites.

Finally, the structure of a protein can influence its susceptibility to sumoylation. The sumoylation affinity depends highly on the accessibility of these lysine residues, which is

influenced by the protein's three-dimensional structure (Lascorz et al., 2022). Additionally, the cellular context, the interactions of the protein with other molecules, and post-translational modifications can impact its sumoylation status. Some proteins may have specific domains or regions that facilitate or hinder the sumoylation. process (Wilkinson & Henley, 2010).

1.5.4 SUMO-chains

The diverse effects of SUMO proteins throughout the cell stem from the way they interact. Individual SUMO interactions typically participate in assembling protein complexes, regulating enzyme function, DNA binding, and protein-protein interactions. In contrast, multi- or polysumoylation can lead to significantly different outcomes (Keiten-Schmitz et al., 2020) (Békés et al., 2011).

Poly-SUMO chains involve the attachment of multiple SUMO molecules to a target protein, forming chains that can have distinct functional consequences. (Keiten-Schmitz et al., 2020). Poly-sumoylation can induce conformational changes in target proteins, altering their activity or stability (Bermúdez-López et al., 2016). SUMO-chains regulate the activity of cell cycle regulators, such as cyclins and cyclin-dependent kinases (CDKs), indirectly controlling cell cycle progression, ensuring accurate DNA replication and chromosome segregation (Keiten-Schmitz et al., 2020).

Furthermore, SUMO-chain interaction with a protein may serve as a signal for ubiquitin ligases or autophagy receptors, leading to protein degradation, thereby controlling protein levels and maintaining cellular homeostasis (Oeser et al., 2016).

Poly-sumoylation also contributes to the occupation and dynamics of chromatin, influencing the regulation of gene expression and genome stability overall (Keiten-Schmitz et al., 2020). This happens through several mechanisms, including altering chromatin accessibility by promoting changes in histone-DNA interactions

(compacting chromatin), making certain genomic regions less accessible for transcription factors and regulatory proteins, affecting gene expression (Bannister, A., Kouzarides, T., 2011).

Poly-sumoylation also serves as a recruitment signal for chromatin remodelling complexes, regulating histone modifications by crosstalking with modifications such as acetylation, methylation and ubiquitination, interfering with chromatin dynamics (What Is Histone SUMOylation?- CUSABIO, n.d.).

A great example of poly-sumoylation in action is illuminated by a coordinated and simultaneous sumoylation of an entire cluster of interconnected homologous recombination (HR) and DNA damage checkpoint proteins upon DNA damage. The exposure of long single-stranded DNA recruits repair factors such as Siz2, an E3 SUMO ligase found in *S. cerevisiae* (Pasupala et al., 2012). Siz2 is bound to DNA by its SAP domain, carrying the SUMO conjugating enzyme Ubc9 (Figure 23) (Jentsch & Psakhye, 2013).

The HR proteins bound to DNA undergo sumoylation upon interaction with Siz2 at their respective sumoylation sites. This collective sumoylation process contributes to the stabilisation of HR proteins within the region of damaged DNA. Moreover, it enhances the retention of Siz2 alongside HR proteins, facilitated by the presence of multiple SUMO-Interactive -Motifs (SIMs-see below) on the HR proteins themselves (Jentsch & Psakhye, 2013).

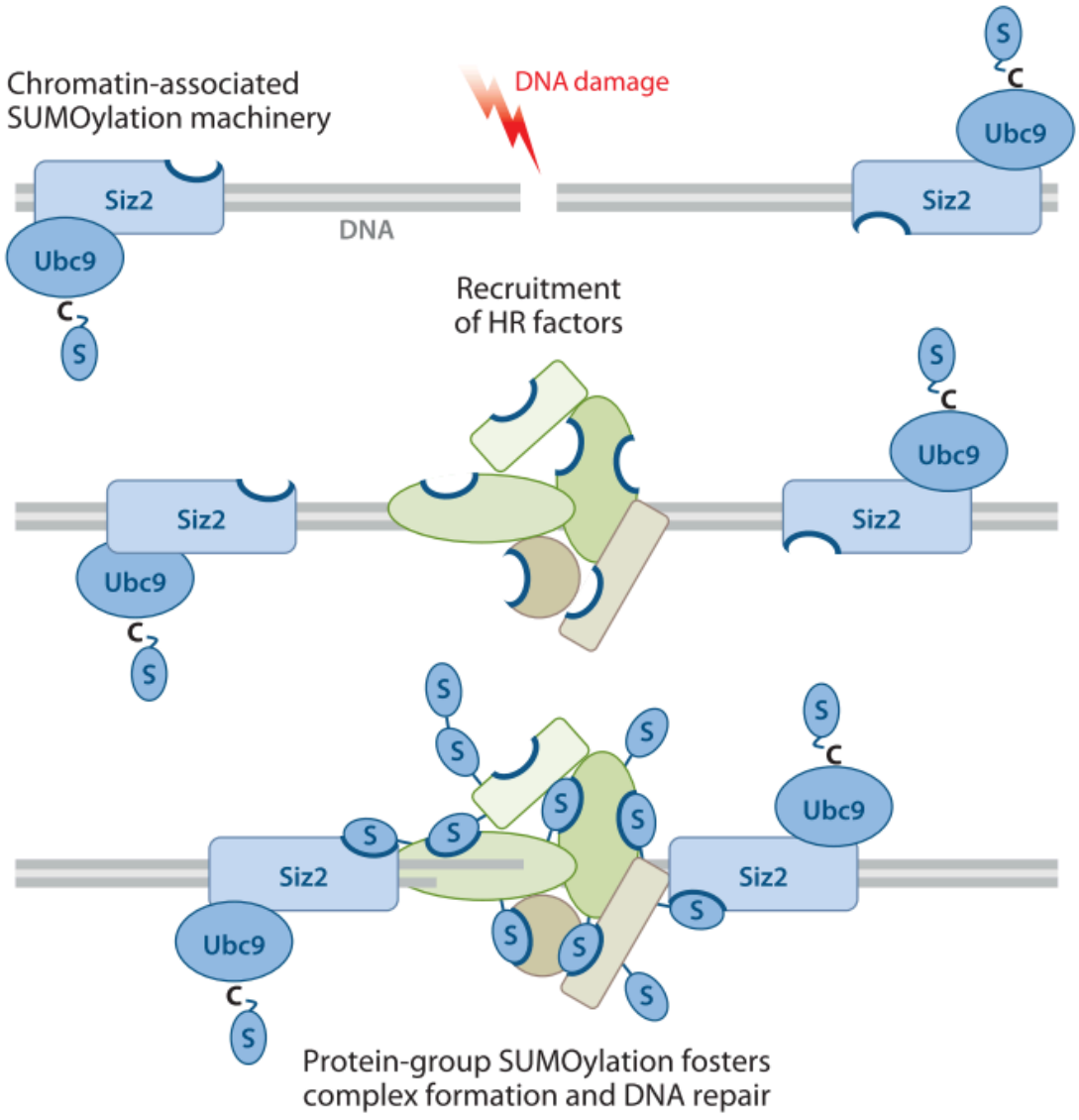

Figure 23: Illustration of protein-group sumoylation in action. Upon DNA damage, a coordinated and simultaneous sumoylation of interconnected homologous recombination (HR) and DNA damage checkpoint proteins occurs. Long stretches of single-stranded DNA recruit repair factors such as Siz2, an E3 SUMO ligase found in *S. cerevisiae*. Siz2, bound to DNA by its SAP domain, carries the SUMO conjugating enzyme Ubc9. HR factors bound to DNA are subsequently sumoylated upon encountering Siz2, leading to the stabilisation of HR proteins in the damaged DNA area. This group sumoylation further stabilises the localization of Siz2 with the HR proteins, facilitated by multiple SIMs located on them (Jentsch & Psakhye, 2013).

1.5.5 SUMO-interacting motifs

As mentioned above, taking into consideration the relatively simple motif that encapsulates the lysine residue that can be sumoylated within a protein, SUMO proteins can also be sumoylated. This creates poly-SUMO chains, which are recognized by an area on specific proteins, called SUMO Interacting Motifs (SIM) (Yau et al., 2021).

SIMs contain a hydrophobic core, but are also composed of a sequence of amino acids with a negative charge, such as aspartate and glutamate (Yau et al., 2021). The negatively charged residues can establish electrostatic interactions with positively charged residues present in SUMO proteins, thereby facilitating the binding between SIMs and SUMO. These interactions significantly contribute to the stability and specificity of the SUMO-SIM complex (Lascorz et al., 2022).

Apart from the group sumoylation paradigm during DNA repair, another great example of the effect of SUMO-SIM interaction are PML nuclear bodies. Within the nuclei of mammalian cells exist a membraneless organelle called the PML nuclear body or promyelocytic leukaemia nuclear body. PML bodies serve as versatile and active nuclear compartments, fulfilling significant functions in different cellular processes such as the regulation of gene expression, DNA repair, defence against viruses, and suppression of tumour formation (Liu et al., 2023).

These structures contain the promyelocytic leukaemia (PML) protein, which undergoes extensive sumoylation and possesses a SUMO-interacting motif (SIM). SUMO proteins bound to PML are subsequently recognized by the SIM within the same PML protein, leading to an accumulation of PML and the formation of mature and dynamic PML-NBs (Bernardi & Pandolfi, 2007). The dynamic functionality of this organelle is achieved through its ability to form droplets, creating a specialised compartment within the nucleus (Figure 24). This compartment facilitates the recruitment and localization of specific

proteins to the PML-NBs, enabling their interactions and functions within this unique nuclear environment (Lallemand-Breitenbach & De, 2010).

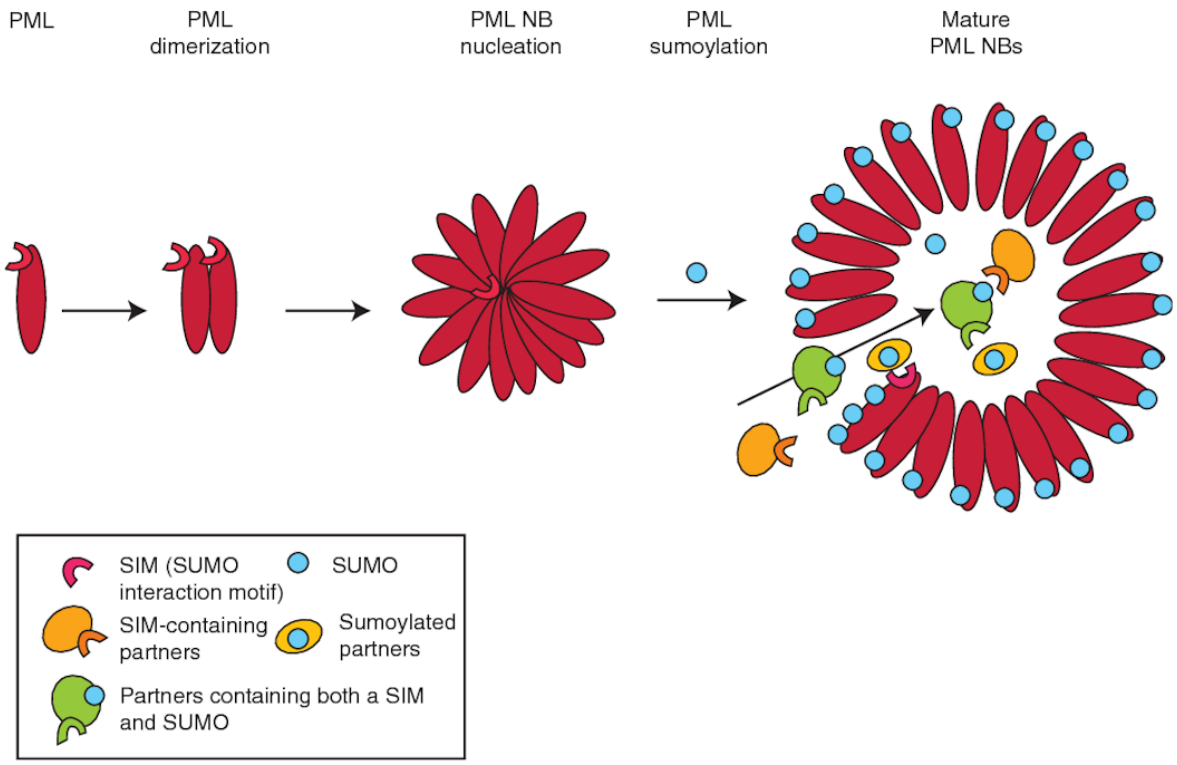

Figure 24: Schematic representation of the PML-NBs formation. PML proteins first dimerize through protein-protein interactions, and then multimerize to nucleate NBs. PML sumoylation then leads to organisation in a spherical body, due to the twofold existence of both SUMO proteins and SIMs. The dynamic function of PML NBs is achieved by the recruitment of SIM-containing or sumoylated proteins (or both) by the SUMO or SIM of PML into the inner core of the body (Lallemand-Breitenbach & De, 2010).

1.5.6 Sumoylated lysines

Identifying Lysine residues within a protein as "sumoylation sites" *in silico* can be really difficult. The attachment of SUMO to a Lysine residue within a protein necessitates the presence of a specific amino acid motif, as mentioned previously. Although this motif is relatively simple and can be found multiple times within a protein, several additional

factors must be considered for successful Lysine sumoylation (Da Silva-Ferrada et al., 2012). The activity of E2 and E3 enzymes, which play crucial roles in the sumoylation process, are highly dependent on the target protein. While Lysine residues may appear to be suitable sites for SUMO binding, the structural characteristics of the protein at these specific sites often pose significant challenges (Munk et al., 2017).

The difficulties encountered in identifying sumoylation sites are also due to the characteristics of SUMO itself. In cell lysates, numerous SUMO isopeptidases are present, which can lead to the release of SUMO from its target proteins. Additionally, SUMO can non-covalently interact with other proteins, as indicated by the presence of SUMO Interacting Motifs (SIMs) (Impens et al., 2014). According to Gareau and Lima, nickel chromatography under denaturing conditions effectively inactivates SUMO isopeptidases and prevents contamination from non-covalent SUMO-protein interactions (Gareau & Lima, 2010).

The most common method for isolating sumoylated proteins involves His-tagged SUMO proteins. Following isolation, the sumoylated proteins are analysed using mass spectrometry (MS), however identifying specific sumoylation sites remains challenging due to the complexity of the SUMO modification process. Unlike ubiquitination sites, which are aided by a small di-amino acid GlyGly tag that remains on lysine residues after tryptic digestion (Da Silva-Ferrada et al., 2012), SUMO modifications often leave larger peptide fragments, complicating the MS analysis. These fragments can obscure the identification of the target peptide sequence (Gareau & Lima, 2010) (Da Silva-Ferrada et al., 2012).

To bypass these challenges, Impens et al. developed a method involving the substitution of the threonine residue immediately following the GG motif with arginine. This modification allows for digestion with proteases such as trypsin or Lys-C that leave the lysine residue with the GG tag intact. Following cleavage, they enriched sumoylated

peptides using specific antibodies, which were then subjected to mass spectrometry, providing detailed mass and sequence information that pinpoints the exact lysine residues modified by SUMO (Impens et al., 2014).

Another approach involves site-directed mutagenesis, where lysine residues are replaced with arginine. This substitution does not alter the protein's overall structure or charge but prevents SUMO binding. SUMO cannot attach to arginine due to the presence of a guanidinium group, as opposed to the ε-amino group in lysine, which is recognized by the enzymatic machinery facilitating the attachment of SUMO to the protein substrate (Alonso et al., 2015).

1.5.7 SUMO involvement in CPC localization and activity

The SUMO system is required for proper cell cycle progression and spindle function in yeast cells. Deletion of Smt3 leads to early mitotic arrest in large-budded cells with short spindles. *Δsmt3* cells don't arrest due to SAC but fail to activate APC/C post-SAC, a defect shared with *Δubc9* cells. Temperature-sensitive uba2 mutants exhibit hypersensitivity to microtubule destabilising drugs, causing early mitotic arrest with short, misaligned spindles at high temperatures (Dasso, 2008) (Musacchio & Desai, 2017).

There have been suggestions that sumoylation of midzone components could affect their proper localization on the midzone during mitosis. Montpetit et al. showed that the inner kinetochore protein and midzone protein Ndc10 is sumoylated. Lack of Ndc10 sumoylation abrogates its proper localization to the anaphase mitotic spindle (Montpetit et al., 2006).

However, Ndc10 mislocalization does not affect the CPC: whereas Ndc10 colocalizes with Bir1 to mitotic spindle, the non-sumoylated Ndc10 strain shows no defects in the localization of Bir1, as the latter remains spindle-bound (Montpetit et al., 2006).

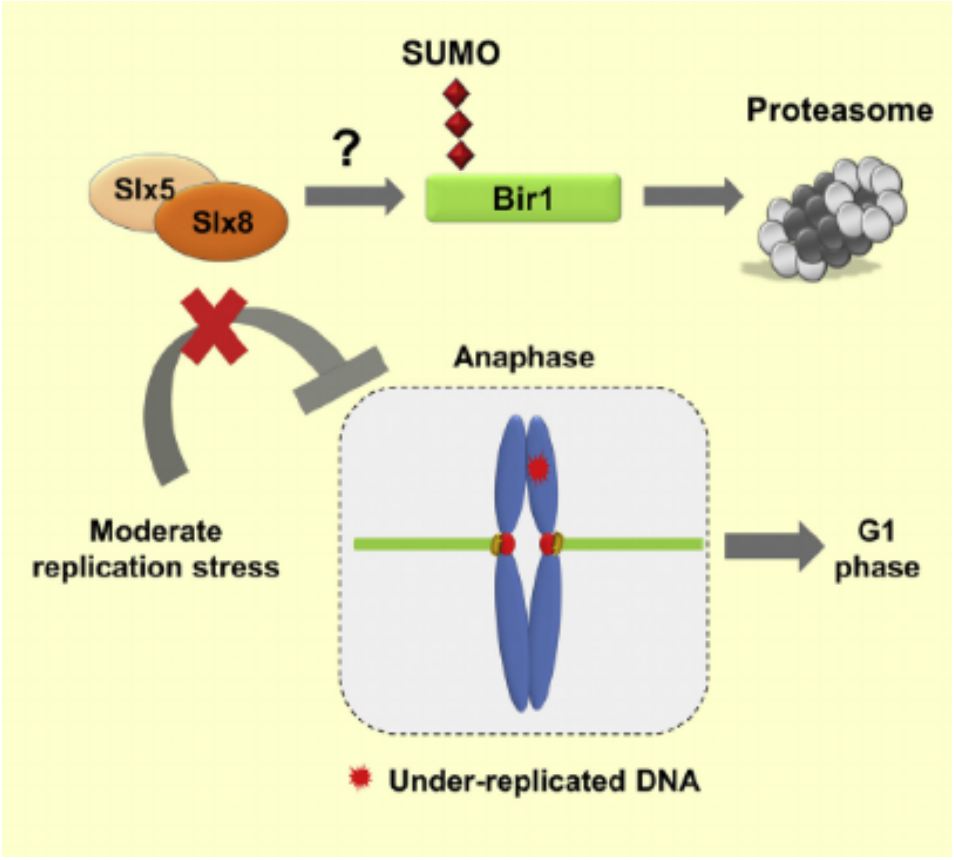

Figure 25: Moderate replication stress leads to the degradation of sumoylated Bir1. In this context, Slx5/8 reduces mitotic checkpoint activation, promoting cell survival. (Thu et al., 2016)

They also observed that the loss of sumoylation of Ndc10 has an impact on the sumoylation of Bir1. These findings suggest that Bir1 sumoylation requires the Ndc10 machinery, but that Bir1 sumoylation does not affect its relocalization from the kinetochores to the midzone (Montpetit et al., 2006).

In HeLa cells, Fernández-Miranda et al. indicated that preventing Aurora B sumoylation reduced cell viability, led to abnormal chromosome segregation and caused CPC to spread across chromosome arms during prometaphase and metaphase (Fernández-Miranda et al., 2010). Furthermore, INCENP failed to localise to inner centromeres, indicating that Aurora B sumoylation is crucial for CPC localization. Same

experiment stated that Aurora B showed no reduction in its kinase activity, suggesting that this phenotype stemmed from its mislocalization, highlighting the importance of sumoylation in Aurora B positioning (Fernández-Miranda et al., 2010).

In addition, other data indicate that sumoylation could regulate CPC through the sumo-targeted ubiquitylation by the STUbLs. Yee Mon Thu et al., induced replication stress in budding yeast cells, and showed that Slx5 targets sumoylated Bir1 and Sli15 for ubiquitylation, subsequently destabilising and directing them towards the proteasome for degradation (Figure 25) (Thu et al., 2016). Elimination of CPC activity was part of the mechanisms that enable cells to recover from mild replication stress.

Taken together, this data suggest that sumoylation could indeed have a yet poorly characterised role in the regulation of CPC activity, interactions in the cell, as well as its localization throughout mitosis.

2. Aim of study

The purpose of this research is to understand the involvement of sumoylation in function and localization of the CPC complex in yeast. The main questions that will be answered are whether a non-sumoylated CPC is viable for yeast, and how does it affect the localization or activity. To investigate this, the goal was to create a CPC that was not able to undergo sumoylation. CPC mutants lacking several identified sumoylation sites were created. Yeast strains expressing wild-type and potentially non-sumoylatable variants of the CPC components Sli15, Bir, Nbl1 tagged with GFP (Sli15) and mCherry (Bir1) were also created, and the localization of the tagged proteins using time-lapse fluorescent microscopy was observed. Cell growth under different conditions was monitored and compared between mutants and wild-type strains, and spindle dynamics and lengths were measured during late metaphase and anaphase.

3. Materials and Methods

3.1 Materials

3.1.1 Chemical Resources

Name	Manufacturer
Acetic acid	Sigma-Aldrich
Agarose	Invitrogen
Ammonium persulfate (APS)	USB Corporation
Ampicillin sodium salt	Sigma-Aldrich
b-mercaptoethanol	Sigma-Aldrich
Bacto(TM) Agar	Becton Dickinson
Bacto(TM) Tryptone	Becton Dickinson, Sparks, US
Bacto(TM) yeast extract	Becton Dickinson, Sparks, US
Bromophenol blue	Waldeck
Cycloheximide (CHX)	Sigma-Aldrich
Deoxyribonucleotides (dNTPs)	New England Biolabs
Dithiothreitol (DTT)	ThermoFisher Scientific
Ethanol	Sigma-Aldrich
Ethylenediaminetetraacetic acid (EDTA)	Merck
G-418 sulphate	Merck
Galactose	Sigma-Aldrich
GelRedTM	Biotium
Glucose	Merck
Glucose	Formedium
Glycerol	VWR
Glycine	Euromedex
Hydrochloric (HCl)	Merck
Immobilon Western ECL	Merck
Isopropanol	Roth
Lithium Acetate (LiAc)	Sigma-Aldrich

Methanol	Sigma-Aldrich
Peptone	Biomedicals
PhastGel Blue R (Coomassie brilliant blue)	GE Healthcare
Polyethylene glycol (PEG-3250)	Sigma-Aldrich
Ponceau S	Sigma-Aldrich
Salmon sperm DNA (ssDNA)	Sigma-Aldrich
Sodium Chloride (NaCl)	Applichem
Sodium Hydroxide (NaOH)	Merck
Synthetic complete drop out mixtures (SC)	Formedium
tetramethylethylenediamine (TEMED)	Roth
Trichloroacetic acid (TCA)	Sigma-Aldrich
Tris(hydroxymethyl)aminomethane	Roth
Tween-20	Roth
Unsweetened powdered milk	Régilait
Urea	Euromedex
Yeast nitrogen base without amino acids	Formedium

Table 3: Chemical resources

3.1.2 Enzymes

3.1.2.1 Restriction enzymes

Restriction enzymes	Reaction buffer
AscI	CutSmart
BamHI	CutSmart
BglII	CutSmart
BstXI	CutSmart
ClaI	CutSmart
EagI	CutSmart
EcoRV	CutSmart
HpaI	CutSmart
KpnI	CutSmart

NdeI	CutSmart
NotI	CutSmart
NotI HF	CutSmart
PacI	CutSmart
PmeI	CutSmart
SacII	CutSmart
SnaBI	CutSmart
SnaBI	CutSmart
SwaI	CutSmart
XbaI	CutSmart

Table 4: Restriction enzymes

3.1.2.2 DNA editing enzymes

DNA editing enzymes	Reaction buffer
OneTAQ Polymerase	OneTAQ reaction Buffer
Q5 HF Polymerase	Q5 reaction buffer
T4 DNA Ligase	T4 buffer
Antarctic Phosphatase	(Antarc. phosph. buffer)

Gibson Assembly Mastermix	Components
	T5 Exonuclease
	Phusion High-Fidelity DNA Polymerase
	Taq DNA Ligase

Table 5: DNA editing enzymes

3.1.3 Buffers

Buffer	Components
SDS-PAGE running buffer	25mM TRis-HCl, pH 8.3
	190mM glycine
	0.1% w/v SDS
TAE buffer (1x)	40mM Tris
	1.14% v/v acetic acid
	1mM EDTA
TBS	50mM Tris-HCl, pH 8.0
	0.9% w/v NaCl
TBS-Tween	50mM Tris-HCl, pH 8.0
	0.9% w/v NaCl
	0.1% v/v Tween-20
Transfer Buffer	50mM Tris-HCl, ph 8.0
	200mM glycine
	20% v/v methanol
	0.2% w/v SDS
Yeast transformation buffer	200mM LiAc
	40% v/v PEG-3250
	0.7% v/v beta-mercaptoethanol

Table 6: Buffers

3.1.4 Plasmids

Gene	Plasmid name	Backbone	What for?
Plasmids created			
Smt3	pSmt3	pST	isolate smt3 to form pSTE1E2Smt3
Smt3	pSTE1E2Smt3	pST	changed from pSTE1E2S1, for SUMO1 to be changed to Smt3
Sli15	pRS306_Sli15_4R	pRS306	mutated Sli15, not sumoylated

Sli15	pRS306_Sli154R_mRuby2_His5	pRS306	mutated Sli15, not sumoylated with mRuby2 tag
Sli15	pRS306_Sli15-4R_3HA_His3Mx6	pRS306	mutated Sli15, not sumoylated with 3HA tag
Sli15	pRS306_Sli15_KanMx6	pRS306	Sli15 to be transferred in yeast
Plasmids used			
His3	pDL8_pFA6a_3HA_His3MX6	pDL8_pFA6a	to tag Sli15
mRuby	pDL1265_pFA6a-link-yomRuby2-SpHis5	pDL1265_pFA6a	isolate mRuby2
Sli15	pRS306_Sli15 full locus	pRS306	to create pRS306_Sli15_KanMx6
Smt3	pET11a_Smt3	pET11a	to isolate Smt3
SUMO	pSTE1E2S1	pST	as a backbone to create pSTE1E2Smt3
Cas9	pSP_1658	pSP	for CrispR
Bir1	pRS305-Bir1-GFP	pRS304	to create yeast strains with non-sumoylated CPC components
Bir1	pRS305-Bir1_4R-GFP	pRS304	to create yeast strains with non-sumoylated CPC components
Bir1	pRS304-BIR1-TRP1	pRS304	as a control
Bir1	pRS304-Bir1_4R-mCherry	pRS304	to create yeast strains with non-sumoylated CPC components
Bir1	pRS304-Bir1-mCherry	pRS304	to visualise Bir1 in yeast

Table 7: Plasmids

3.1.5 Primers

Gene	Primer name	Sequence	What for?
Sli15	KanMX6 + 298R	CCTGGAATGCTGTTTTGCCGGG	Colony PCR for the insertion of Sli15_KanMx6 in yeast cells
Sli15	Sli15_1f	GACCATCGAGAAATAATCGG	Colony PCR for the insertion of Sli15_KanMx6 in yeast cells
Sli15	Sli15 + 1652f	AAGGATGTCGCATTTGGAAC	Colony PCR for the insertion of Sli15_KanMx6 in yeast cells
Kan	Kan-Ctf	gtttcatttgatgctcgatgag	Colony PCR for the insertion of Sli15_KanMx6 in yeast cells

Sli15	Sli15-3'UTRr	CCGCATTAATTATGTACCCC	Colony PCR for the insertion of Sli15_KanMx6 in yeast cells
Sli15	Sli15_829f	cgataaatagtcctgctataa	Enhance the Sli15-4R gene
Sli15	Sli15_2r	ttgatttaatgttaaccagt	Colony PCR for the mutation of lysines in Sli15
Sli15	Sli15_R1_CrispR	gtgaacgatatacgtaatgcaggggaataccagagtatttaaagtgtacGAATTCGAGCTCGTTTAAAC	Enhance mRuby2 and 3HA to transform them to pRS306_Sli15_KanMx6
Sli15	Sli15_S3frameshift	aatcctaggctaaacaggttgaaaccgcgtcaaattgtgcccaaaaggtctgCGTACGCTGCAGGTCGAC	Enhance mRuby2 and 3HA to transform them to pRS306_Sli15_KanMx6
GFP	GFP_ApaI_f	GCGAGGGCCCagtaaaggagaagaacttttc	To enhance GFP for its insretion in Sli15-4R
GFP	GFP_ApaI_r	GCGAGGGCCCccggtagaggtgtggtcaata	To enhance GFP for its insretion in Sli15-4R
Sli15	Sli15_829f	TCTACGATAAATAGTCCTGC	To confirm GFP insertion in Sli15
GFP	GFP rev	AACAAGAATTGGGACAACTCC	To confirm GFP insertion in Sli15

Table 8: Primers

3.1.6 Media

Medium Name	Components
SOB Medium (500ml)	2 % (w/v) Bacto tryptone: 10 g
	0.5 % Yeast extract: 2.5 g
	10 mM NaCl: 1 ml (5 M stock)
	2.5 mM KCl: 416.7 µl (3 M stock)
	10 mM MgCl2: 1.02 g (MgCl2 x 6 H2O)
	10 mM MgSO4: 1.23 g (MgSO4 x 7 H2O)
Transformation Buffer (TB) (500ml)	10 mM Pipes: 1.51 g (pKa = 6.8)
	55 mM MnCl2: 5.44 g (MnCl2 x 4 H2O) or 4.45 g (MnCl2 x 2 H2O)
	15 mM CaCl2: 7.5 ml (1 M stock) or 1.1 g (CaCl2 x 2 H2O)

	250 mM KCl: 41.67 ml (3 M stock)

Table 9: Media

3.1.7 Yeast strains

Yeast name	Backbone	Mating type	Genotype	What for?
Yeast strains created				
YDL4790 (588a sli15_kanmx6)	*YDL588*	a	*SLI15_kanMx6 ade2-101 ura3-52 lys2-801 his3-Δ200 trp1-Δ63 leu2*	To mutate Sli15, using the PAM sequence of kanMx6
YDL4791 (590alpha sli15_kanmx6)	*YDL590*	alpha	*SLI15_kanMx6 ade2-101 ura3-52 lys2-801 trp1-Δ63 his3-Δ200 leu2*	To mutate Sli15, using the PAM sequence of kanMx6
YDL4830 (sli15-4R-mRuby)	*YDL588*	a	*Sli15-4R-mRuby2:SpHis5 ade2-101 ura3-52 lys2-801 his3-Δ200 trp1-Δ63 leu2*	To visualise Sli15-4R in yeast
YDL4831 (sli15-mRuby)	*YDL588*	a	*Sli15-mRuby2:SpHis5 ade2-101 ura3-52 lys2-801 his3-Δ200 trp1-Δ63 leu2*	To visualise Sli15 in yeast
YDL4895 (sli15-4R-GFP)	*YDL590*	alpha	*Sli15-4R-GFP:SpHis5 ade2-101 ura3-52 lys2-801 his3-Δ200 trp1-Δ63 leu2*	To check cell viability and create more mutated strains
YDL4901	cross 4627,4895	alpha	*Sli15-4R-GFP:SpHis5 Nbl1-R-URA3 ade2-101 ura3-52 lys2-801 his3-Δ200 trp1-Δ63 leu2*	To create the triple mutant *bir1-4R sli15-4R nbl1R*
YDL4902	cross 4627,4895	alpha	*Sli15-4R-GFP:SpHis5 Nbl1-R-URA3 ade2-101 ura3-52 lys2-801 his3-Δ200 trp1-Δ63 leu2*	Check viability and growth, and create the triple mutant
YDL4903	cross 4627,4895	a	*Sli15-4R-GFP:SpHis5 Nbl1-R-URA3 ade2-101 ura3-52 lys2-801 his3-Δ200 trp1-Δ63 leu2*	Check viability and growth, and create the triple mutant

YDL4904	cross 4627,4895	a	*Sli15-4R-GFP:SpHis5 Nbl1-R-URA3 ade2-101 ura3-52 lys2-801 his3-Δ200 trp1-Δ63 leu2*	Check viability and growth, and create the triple mutant
YDL4917 (bir1-4R-mCherry)	*YDL588*	a	*Bir1-4R-mCherry:LEU2 ade2-101 ura3-52 lys2-801 his3-Δ200 trp1-Δ63 leu2*	To visualise bir1-4R and create the triple mutant *bir1-4R sli15-4R nbl1R*
YDL4918 (bir1-mCherry)	*YDL588*	a	*Bir1-mCherry:LEU2 ade2-101 ura3-52 lys2-801 his3-Δ200 trp1-Δ63 leu2*	To visualise bir1
YDL4926	cross 4901x4917	a	*Bir1-4R-mCherry:LEU2 Sli15-4R-GFP:SpHis5 Nbl1-R-URA3 ade2-101 ura3-52 lys2-801 his3-Δ200 trp1-Δ63 leu2"*	Check cell viability, CPC localization, spindle dynamics
YDL4927	cross 4901x4917	alpha	*Bir1-4R-mCherry:LEU2 Sli15-4R-GFP:SpHis5 Nbl1-R-URA3 ade2-101 ura3-52 lys2-801 his3-Δ200 trp1-Δ63 leu2"*	Check cell viability, CPC localization, spindle dynamics
YDL4930	cross 4896x4918	a	*Bir1-mCherry:LEU2 Sli15-GFP:SpHis5 ade2-101 ura3-52 lys2-801 his3-Δ200 trp1-Δ63 leu2*	Check cell viability, CPC localization, spindle dynamics
YDL4931	cross 4896x4918	alpha	*Bir1-mCherry:LEU2 Sli15-GFP:SpHis5 ade2-101 ura3-52 lys2-801 his3-Δ200 trp1-Δ63 leu2*	Check cell viability, CPC localization, spindle dynamics
Yeast strains used				
YDL588	*S288C wildtype*	a	*ade2-101 ura3-52 lys2-801 his3-Δ200 trp1-Δ63 leu2*	To create Sli15_kanmx6
YDL590	*S288C*	alpha	*ade2-101 ura3-52 lys2-801 trp1-Δ63 his3-Δ200 leu2*	To create Sli15_kanmx6
S288C	*EM93, EM126, NRRL YB-210*	alpha	*MATα SUC2 gal2 mal2 mel flo1 flo8-1 hap1 ho bio1 bio6*	Multiple creations
YDL4627	*YDL588*	a	*Nbl1-R-URA3 ade2-101 ura3-52 lys2-801 his3-Δ200*	To create the double mutant Sli15-4R_GFP::Nbl1-R

			trp1-Δ63 leu21	
YDL4643 (ipl1-2R)	*YDL4630*	a	*ade2-101 ura3-52 lys2-801 his3-Δ200 trp1-Δ63 leu2*	To create the double mutant *sli15-4R ipl1-2R*
YDL4666	cross 4629, 4630	alpha	*ade2-101 ura3-52 lys2-801 his3-Δ200 trp1-Δ63 leu2*	To create *bir1-gfp* strain

Table 10: Yeast strains

3.1.8 Microscopes

Microscope Name	Properties
Inverted Nikon TiE wide-field microscope	100X Plan Apochromat 1.40NA oil\ sCMOS back-illuminated Prime95B Photometrics Lumencor LED Illumination Controlled by NIS Elements.
Spinning disk OLYMPUS SR Olympus IX83 inverted microscope	Inverted microscope coupled to Yokogawa W1 spinning disk unit, including a SoRa disk, 60X UPLXAPO 1.42 NA WD 0.15mm oil camera, sCMOS Fusion BT Hamamatsu Laser Illumination

Table 11: Microscopes

3.2 Protocols

3.2.1 Chemically competent cells

The following protocol covers the inoculation and growth of bacterial cultures, the preparation of cells for transformation, and the steps required to render them competent.

Materials used:

- SOB Medium (500ml)
- Transformation Buffer (TB) (500ml)
- Desired bacterial strain
- Antibiotics
- Falcon Tubes
- Eppendorf's tubes
- DMSO
- Liquid nitrogen

The four-day procedure follows:

Day 1:

1. Two microliters of the desired bacterial strain, previously stored at -80°C, are inoculated into SOB medium.
2. The appropriate antibiotic is added at a final concentration of 1x. For XL1-Blue competent cells, tetracycline is used at a concentration of 12.5 µg/ml.

Day 2:

3. The overnight culture is inoculated to achieve an OD600 of 0.03 in 250 ml of SOB medium, supplemented with additional antibiotic to maintain a final concentration of 1x.

4. The culture is incubated at 18°C until it reaches an OD600 of 0.6. This process may extend up to two days, requiring periodic monitoring to adjust the overnight dilution and ensure proper cell preparation.

Day 4:

5. The culture at the appropriate OD is placed on ice for 10 minutes.
6. It is then centrifuged at 2500 x g for 10 minutes at 4°C using several 50 ml Falcon tubes.
7. The cell pellet is gently resuspended in 80 ml of ice-cold TB buffer and transferred to a beaker on ice for an additional 10 minutes.
8. The mixture is centrifuged again at 2500 x g for 10 minutes at 4°C.
9. The cells are then gently resuspended in 20 ml of ice-cold TB buffer,
10. The resuspension is followed by the addition of DMSO to achieve a final concentration of 7%, and it is transferred to a beaker on ice for another 10 minutes.
11. The cell suspension is aliquoted into 100 µl portions, rapidly frozen in liquid nitrogen, and stored at -80°C.

3.2.2 QIAGEN® Miniprep DNA extraction protocol

To prepare the culture for DNA extraction:

- Incubate the culture at 37°C with continuous shaking overnight to the respective medium.
- Ensure all centrifugation steps are carried out at 15,000xg
- Handle the lysate gently to avoid shearing chromosomal DNA, which may co-purify as a contaminant.
- Add the provided RNase A solution to Buffer P1, mix thoroughly, and store at 2–8°C. Add ethanol (96–100%) to Buffer PE as indicated on the bottle label.

Materials used:

- RNase A
- Buffer P1
- Buffer P2
- Buffer N3
- Elution Buffer
- 70% ethanol
- 96% isopropanol
- Cell Culture

The procedure follows:

1. Divide 3 mL of the overnight culture into two Eppendorf tubes (1.5 mL each). Centrifuge at 13,000 rpm (~17,900 x g) for 2.5 minutes. Discard the supernatant as completely as possible.
2. Resuspend the cell pellet in 200 µL of resuspension buffer solution (Buffer P1) by vortexing thoroughly, then transfer to a microcentrifuge tube.
3. Add 200 µL of lysis solution (Buffer P2) and gently invert the tube until the solution becomes clear. Let it stand for 2 minutes.
4. Add 350 µL of neutralisation solution (Buffer N3) and mix thoroughly by inversion. Centrifuge at 13,000 rpm for 20 minutes. Retain the supernatant and discard the pellet.
5. Add 450 µL of 96% isopropanol to the supernatant and mix well. Centrifuge at 13,000 rpm for 30 minutes. Discard the supernatant as completely as possible.
6. Add 500 µL of 70% ethanol to the pellet and gently mix. Centrifuge at 13,000 rpm for 5 minutes. Carefully remove all the supernatant and allow the pellet to air dry.
7. Resuspend the dried pellet in 50 µL of elution buffer EB (10 mM TrisCl, pH 8.5). Store the eluted DNA at 4°C.

Note that this protocol is not the one provided by QIAGEN, and it is adjusted to the lab needs.

3.2.3 DNA precipitation

On subjection of bacterial cell suspension to a highly alkaline environment, the high molecular weight bacterial chromosomal DNA and proteins are denatured. When the lysis is carried out at a pH environment of 12-12.5, it leads to an irreversible denaturation of the high molecular weight chromosomal DNA, the cell lysate is neutralised by the addition of a high molecular weight acidic salt which acidifies the alkaline environment. This slight change in pH of the environment leads to rapid selective renaturation of the small molecular weight plasmid DNA but is unable torenature the bacterial chromosomal DNA. The use of Ammonium acetate for protein and high molecular weight DNA precipitation has been already reported for the purification of buccal DNA. The use of Ammonium acetate for selective precipitation of bulk RNA and high molecular weight DNA from plasmid DNA has been reported to be of high effectiveness.

Materials used:

- DNA Solution
- Ammonium Acetate ($NH_4CH_3CO_2$) 6M
- Ethanol 70% v/v
- Ethanol 96% v/v

The procedure follows:

1. Add ammonium acetate to the DNA solution at a 1:10 ratio of the DNA solution volume and vortex briefly.
2. Add cold 96% ethanol at 2.5 times the volume of the DNA solution, vortex, and let the mixture rest on ice for 10 minutes.

3. Centrifuge at maximum speed for 20 minutes using a refrigerated centrifuge (4-6°C recommended).
4. Remove the supernatant.
5. Add 700 μL of 70% ethanol (v/v) and centrifuge at maximum speed for 5 minutes.
6. Remove the ethanol and allow the pellet to dry completely.
7. Resuspend the pellet in 20 μL of Elution Buffer or TE buffer.

3.2.4 Colony PCR

In order to check if the recombination of a gene is successful, Culture PCR can be used, amongst other techniques. This one is based on the difference between the genome that occurs when the recombination happens. Using that difference, specific primers that target the recombinated sequence are used in a PCR assay, and after the PCR products run together in an Agarose gel. If the recombination is successful, the PCR should only enhance the correct cultures.

Materials used:

- LB/YP Agar plates
- Tips (or toothpicks)
- Specific PCR primers (forward and reverse)
- Polymerase
- Polymerase buffer

The procedure follows:

1. In an LB (or YP) agar plate, all of the cultures of the plate that should be tested are picked with tips (or toothpicks) and they are spreaded in a single line (between 3-4 cm) in a new plate. They are all numbered.
2. The agar plate should be incubated at 37 ºC (or 28 ºC for yeast). It should be ready the next day.

3. The next day procedure should be followed as the specific protocol of the polymerase that will be used, adjusted to 20µl. The only difference is that instead of the DNA template, the exact volume is replaced by distilled water. It is recommended that a master-mix will be created for even results.

3.2.5 Gibson Assembly protocol

Gibson Assembly is a widely adopted method in synthetic biology due to its simplicity, versatility, and effectiveness for assembling large DNA constructs. This method allows for the successful assembly of multiple DNA fragments, regardless of their length or end compatibility, in a single-tube isothermal reaction.

The Gibson Assembly Master Mix contains an exonuclease that generates single-stranded 3′ overhangs, enabling the annealing of complementary DNA fragments, a polymerase that fills in gaps within the annealed fragments, and a DNA Ligase, sealing the nicks in the assembled DNA.

3.2.6 LB agar plates

For the preparation of LB agar plates, the following ingredients are mixed in a big 1L flask:

- 20 g agar
- 10 g tryptone
- 5 g yeast extract powder
- 10 g NaCl
- dH_2O up to 1 litre

The mixture is then sterilised and stirred, with an antibiotic added at a 1:1000 ratio if required. Once the medium has slightly cooled, approximately 50 mL is dispensed into each plate. The plates are allowed to cool on the bench before being stored in the cold room.

3.2.7 Agarose gel

In a 500 mL flask, the following ingredients are combined:

- 150 mL TAE (1x) buffer
- 1.354 g agarose.

The mixture is heated with continuous stirring, allowing it to boil for only a few seconds. Once the temperature slightly decreases, 7.5 µL of Gel Red (at a 1:200 ratio) is added. The solution is then poured into an appropriate agarose gel casting tray.

3.2.8 Transformation of ligation product in competent cells

The frozen competent cells are allowed to thaw slightly on ice. 100 µL of these cells are transferred to the ligation product. After a 30-minute incubation on ice, the cells undergo heat shock at 42°C for exactly 1 minute. Subsequently, 1 mL of liquid LB medium is added, and the cells are removed from the heat. The mixture is gently and carefully shaken, then incubated at 37°C for 30 minutes. Following incubation, the cells are centrifuged at 4,500 x g for 2 minutes, and as much supernatant as possible is discarded. Finally, the cells are gently resuspended in a small amount of distilled water and plated onto LB agar plates, ensuring even distribution across the surface.

3.2.9 DNA isolation with “NucleoSpin Gel and PCR Clean-up Mini Kit”

The NucleoSpin Gel and PCR Clean-up Mini Kit is a commercially available kit used to purify DNA fragments from agarose gels and isolating/cleaning PCR products.

The kit contains:

- Silica Membrane Columns, containing silica membranes that selectively bind DNA during the purification process.
- Collection Tubes to collect flow-through during centrifugation steps.
- Specific buffers:

- Binding Buffer (NTI), facilitating the binding of DNA to the silica membrane.
- Wash Buffer (NT3), used to wash away impurities and contaminants. It is often provided as a concentrate that requires the addition of ethanol before use.
- Elution Buffer (NE), eluting the purified DNA from the silica membrane.

The procedure for cleaning a PCR product (liquid extraction):

1. 2 volumes of NTI are added per every 1 volume of the PCR product
2. The mixture is then added to a Silica Membrane Column, grouped with one Collection Tube, and it is centrifuged at 11,000xg for 30s, removing the liquid that is extracted.
3. 700μl of NT3 are added to the Silica Membrane Column, to further clean the binded DNA. The sample is centrifuged at 11,000xg for 30s twice, removing the extracted liquid.
4. The sample is centrifuged to dry completely at 11,000xg for 1m.
5. The Collection Tube is exchanged with a clean eppendorf. 20μl of NE buffer are added to the Silica Membrane Column and left for 1m to dilute the DNA. The mixture is centrifuged at 11,000xg for 1m.

The clean PCR product is found diluted in 20μl NE Buffer inside the eppendorf.

The procedure for cleaning a gel (gel extraction):

After running the DNA product on an agarose gel, the region containing the desired DNA fragment is excised and placed in an Eppendorf tube. The gel piece is then weighed. and an amount of 2 μL of NTI buffer per milligram of gel is added. The sample is dissolved at 50°C, with vortexing if necessary to facilitate the process. Once fully dissolved, the procedure continues as with liquid extraction.

3.2.10 Yeast Transformation

Yeast transformation is an important technique in which exogenous DNA is introduced into S.Cerevisiae, resulting in genetic modification of the organism. The materials used for this method are mentioned below:

- Fresh yeast culture (OD: 0.6/mL)
- ssDNA (salmon sperm DNA)
- Yeast Transformation Buffer
    - PEG
    - Lithium acetate
    - β-mercaptoethanol
- YPD
- Agar plates

The procedure follows:

1. Preparation of ssDNA:
   1.1 Incubate the salmon sperm ssDNA at 90 ºC for exactly 10m
   1.2 After 10 minutes, the ssDNA is stored on ice until used
2. LiAc:PEG is created in 1:5 analogy, storing it at room temperature.
3. Assembly of Yeast Transformation Buffer (YTB):
    - Only when the transformation will occur, LiAc:PEG must me mixed with β-mercaptoethanol, at an analogy of 7µl/1ml, so is advised that 200µl of the buffer is made:

Product	Amount (µl)
LiAc:PEG	199
β-mercaptoethanol	1.4

   The buffer is stored in ice until used.
4. 1 - 1.5 mL of the culture is centrifuged at 1,000 x g for 2 minutes.

5. The supernatant is thoroughly discarded.
6. 8 µL of the prepared ssDNA is added and mixed gently.
7. 2 µL of the insert DNA is added and mixed gently with the sample.
8. 100 µL of the prepared YTB is added and mixed gently.
9. The mixture is incubated at room temperature for 30 minutes with gentle rotation.
10. The sample undergoes heat shock by incubating at 42°C for exactly 15 minutes.
11. Centrifuge the sample at 1,500 x g for 3 minutes.
12. The supernatant is thoroughly discarded.
13. The pellet cells are resuspended in 1 mL of YPD.
14. (Optional) The mixture is allowed to rotate at room temperature for at least 5 hours.
15. Centrifuge the sample at 1,500 x g for 2 minutes and discard a portion of the supernatant.
16. Resuspend the pellet in the remaining supernatant and plate on agar plates under appropriate conditions.
17. Incubate the plates at 28°C.

3.2.11 PCR - Polymerases Protocols

PCR is a technique that amplifies a specific DNA segment using primers—short, single-stranded DNA sequences complementary to the start and end points of the target region. To complete a PCR successfully, the process requires primers, a DNA template, a polymerase enzyme that synthesises the new complementary DNA strand, dNTPs as a nucleotide source, and a buffer to create the optimal environment for the reaction. (Mullis & Faloona, 1987)

Each PCR cycle follows a three-step sequence (MERCK | Polymerase Chain Reaction, 2024):

1. Initial denaturation/Denaturation: The mixture is heated to separate the DNA strands.

2. Annealing: The temperature is lowered around 50-65°C, allowing the primers to bind (anneal) to their complementary sequences on the single-stranded DNA template.
3. Extension: The complementary DNA strands are synthesised during this step.
4. Final extension: This step ensures that every new synthesised DNA is completely extended.

The polymerases used in this research are TAQ polymerase and Q5 polymerase.

3.2.11.1 TAQ polymerase protocol

Taq polymerase is a thermostable DNA polymerase I named after the thermophilic eubacterial microorganism *Thermus aquaticus*, from which it was originally isolated by Chien et al. in 1976. Its name is often abbreviated to Taq or Taq pol. *T. aquaticus* is a bacterium that lives in hot springs and hydrothermal vents, and Taq polymerase was identified as an enzyme able to withstand the protein-denaturing conditions (high temperature) required during PCR. Therefore, it replaced the DNA polymerase from E. coli originally used in PCR (Chien et al., 1976).

The PCR mixture using TAQ polymerase consists of the following components:

Product	Amount (µl)
double distilled H_2O	35.75
TAQ Buffer	1.0
DNA template	1.0
primers (2x)	1.0
dNTPs	1.0
TAQ polymerase	0.25
Final mixture	50

This final product is 50µl, but analogous changes can be made in order for the PCR to be completed in other volumes. The procedure happens in PCR tubes. The temperature and time conditions used with TAQ Polymerase are written below:

Step		Temperature	Time
1	Initial Denaturation	95 ºC	30s
2	Denaturation	95 ºC	20s
3	Annealing	55 ºC	35s
4	Extension	68 ºC	1m per 1kb
5	Final extension	68 ºC	5m
6	Hold	4 ºC	indefinitely

Steps 2 to 4 repeated at least 30 times, to ensure the synthesis of a lot of DNA.

3.2.11.2 Q5® polymerase protocol

Q5 polymerase is an engineered enzyme from New England Biolabs (NEB), expressed from a mutated polymerase gene derived from organisms such as *Thermococcus* or *Pyrococcus*. While the exact mutations in Q5 polymerase are proprietary to the manufacturer, it generally provides superior accuracy and performance compared to traditional DNA polymerases. (New England Biolabs, 2024)

The PCR mixture using TAQ polymerase consists of the following components:

Product	Amount (µl)
double distilled H_2O	31
Q5 Buffer	10.0
DNA template	2.5

Product	Amount (μl)
primers (2x)	2.5
dNTPs	1.0
Q5 polymerase	0.5
Final mixture	50

The final product is 50μl, but analogous changes can be made in order for the PCR to be completed in other volumes, in PCR tubes. The temperature and time conditions used with TAQ Polymerase are written below:

Step		Temperature	Time
1	Initial Denaturation	95 ºC	30s
2	Denaturation	95 ºC	20s
3	Annealing	55 ºC	35s
4	Extension	68 ºC	1m per 1kb
5	Final extension	68 ºC	5m
6	Hold	4 ºC	indefinitely

Steps 2 to 4 repeated at least 30 times, to ensure the synthesis of a lot of DNA.

3.2.12 DNA insert with T4 DNA Ligation

T4 ligase is an enzyme isolated from the *T4 bacteriophage,* catalysing the formation of phosphodiester bonds between two adjacent nucleotides in DNA strands. It is used to join cut DNA with blunt or sticky ends, primarily for cloning and recombination purposes.

In cases where the technique is used for the insertion of a DNA segment, the following components are utilised:

Product	Amount (µl)
double distilled H_2O	~ (to 10)
T4 Ligase Buffer	1
DNA insert:DNA template	3:1
T4 Ligase	1.0
Final mixture	10

The final product is left for 1h to incubate at room temperature. Then it is stored at 4 ^{o}C.

4. Results: Clonings and strain construction

To create a CPC complex that cannot undergo sumoylation, it is essential to identify the specific lysine residues where SUMO binds. In this case, unpublished laboratory data were used and analysed to determine these residues, using bioinformatics tools such as JASSA, GPS-SUMO, and SUMOgo, as well as experimental data obtained through mass spectrometry.

Sumoylation sites in CPC		
Protein	**Lysine**	**Sequence**
Bir1	**732**	ILEDVSV**K**NETPNNE
	785	VEIKKVI**K**PEFEPVP
	707	VKELSGL**K**KETDDDK
	708	KELSGLK**K**ETDDDKY
	608	SNITAIP**K**EEQRRGN
	910	NLKVQSI**K**REFIDDC
	421	VNGDNKD**K**DLVIDFT
Ipl1	**133**	TGYICAL**K**VMEKEEI
	137	CALKVME**K**EEIIKYN
	229	NIIHRDI**K**PENILIG
	337	DLILKLL**K**YDPKDRM
	112	ELGKKLG**K**GKFGKVY
	114	GKKLGKG**K**FGKVYCV
Sli15	**324**	SRGNVGH**K**YSSSSID
	338	DLTGSPM**K**KVSQKFK
	339	LTGSPMK**K**VSQKFKS
	381	PKGKNSR**K**SSIPRFD

	315	PTKSFEN**K**ISRGNVG
	153	VEPLNSV**K**VDANESE
	169	SSPWSPY**K**VEKVLRE
Nbl1	36	EKLIENI**K**EETLKKL

Table 12: Sumoylation sites according to lab data, using JASSA, SUMOgo, GPS-SUMO and mass spectrometry. Highlighted with grey and bold are the data that were verified via mass spectrometry (Lani D., 2022).

These programs take into consideration the sumoylation motif around the lysine, also taking into account the tertiary structure of the protein, which contributes to the SUMO-binding affinity of each residue. However, as mentioned, it is not guaranteed that a lysine residue will be sumoylated just because it follows the specific motif, and it was observed that the experimental data verified sumoylation on some of the predicted lysines.

It was decided to introduce mutations in the highlighted lysine residues with grey and bold in Table 12. Bir1 and Nbl1 and Ipl1 have already been mutated in specific plasmids. Yeast strains containing the mutated Nbl1 (Nbl1-R) were also created beforehand. Sli15 was the only protein that had not been mutated yet, and thus the experiments began with the Sli15-4R

4.1 Creating Sli15-4R using CRISPR/Cas9

The *KANMX6* gene (conferring resistance to G418, a kanamycin analog) was cloned at the 3′ end of *SLI15.* It was inserted in order for its PAM sequence to be detected by the sgRNA in a specific CrispR/Cas9 assay to mutate Sli15 to Sli15-4R. It will be used as a further tag to separate the mutated gene, lacking G418 resistance, from the wild type after the CrispR/Cas9 experiment (Figure 27).

4.1.1 pRS306_Sli15_KanMx6

To clone *SLI15*, the *S. cerevisiae* INCENP homolog, the plasmid pRS306 was selected as a backbone, which confers ampicillin resistance. The *SLI15* gene was amplified from yeast genomic DNA using custom primers Sli15_Xho1 and Sli15_Not1, which incorporate specific restriction sites for XhoI and NotI, respectively. The enzyme utilised for the ligation process was T4 DNA ligase.

The ligation product was transformed into *XL1-Blue* competent cells and plated on LB agar containing ampicillin (LBAmp plates). A liquid culture was inoculated overnight at 37°C continuously, followed by plasmid isolation using the QIAGEN® Miniprep DNA Kit. The isolated plasmid was then subjected to digestion with multiple restriction enzymes to verify its correctness against the theoretical construct predicted by SerialCloner. The results confirmed the correct insertion of *SLI15* in pRS306, named pRS306_Sli15.

After enhancing the PCR products, pRS306_SLI15 was amplified using the primer pairs 1F+2R and 5F+6R, which have overhanging ends to facilitate seamless assembly with the *KANMX6* PCR product. Then a Gibson assembly was carried out, successfully achieving the desired construct. The plasmid acquired was named pRS306_Sli15_kanMx6 (Figure 26). The product was tested with the restriction enzymes ClaI, EcoRI, HindIII, PstI and BglII, since their sites are also found within the *KANMX6* sequence.

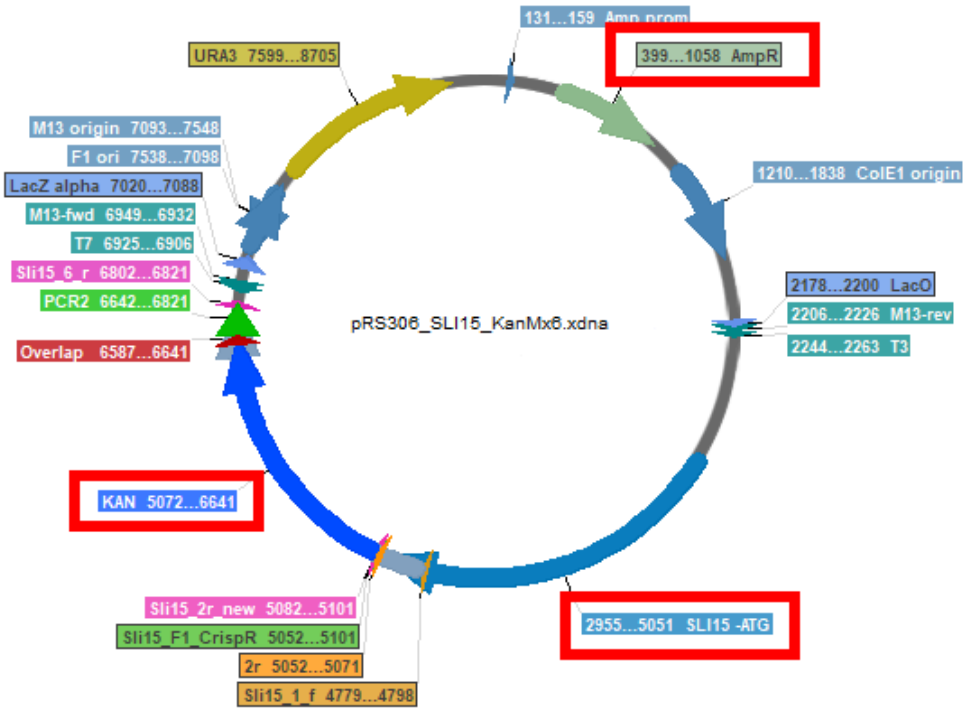

Figure 26: Graphical map of pRS306_Sli15_KanMx6, made by serial cloner.

4.1.2 CrispR/Cas9 mutagenesis

To insert the *KANMX6* at the *SLI15 3'UTR,* the pRS306_Sli15_kanMX6 was digested with SalI/NotI and was transformed into the yeast strains *S288C MATa* and *S288C MATalpha* (*YDL588* and *YDL590* respectively). Afterwards, the transformed cells were plated on G418 plates, successfully obtaining several colonies. Colony PCR was performed on ten of these colonies using the primers KanMx6 + 298R and Sli15_1f with Taq polymerase, with wild-type yeast as a control, and a band of expected size was obtained.

The insertion of the *KANMX6* at the *SLI15 3'UTR* was also verified with further PCR tests using the primer pair Kan-Ctf and Sli15-3'UTRr with Taq polymerase were carried

out. Additionally, the primer Sli15 + 1652f was designed and ordered, which when paired with Sli15-3'UTRr produced the expected results based on theoretical calculations. Both mating types of the G418-resistant yeast were then stored for future use, and named *YDL4790* and *YDL4791*.

The *SLI15-4R* gene with the specific lysine-to-arginine mutations was designed in Serial Cloner, and then was ordered to be synthesised. After PCR amplification of the received *SLI15-4R* DNA with primers Sli15_829f)/Sli15_6r (1758/1629), this was co-transformed with plasmid pSP_1658, containing the Cas9 enzyme and guide RNA targeting the PAM sequence of *KANMX6*, into the *588a SLI15_kanmx6* and *590alpha SLI15_kanmx6* yeast strains. These transformed cells were plated on -LEU plates to select for the corresponding marker on the plasmid.

After numerous attempts, a few colonies appeared on the plates. These were scraped onto G418 plates, alongside appropriate controls, to test whether the CRISPR/Cas9 system had successfully removed G418 resistance (figure 2). The absence of growth in the CRISPR/Cas9-treated colonies (and the backbone control 590), combined with robust growth in the *588a SLI15_kanmx6* and *590alpha SLI15_kanmx6* strains, suggested that the colonies might be correct, but further verification was required.

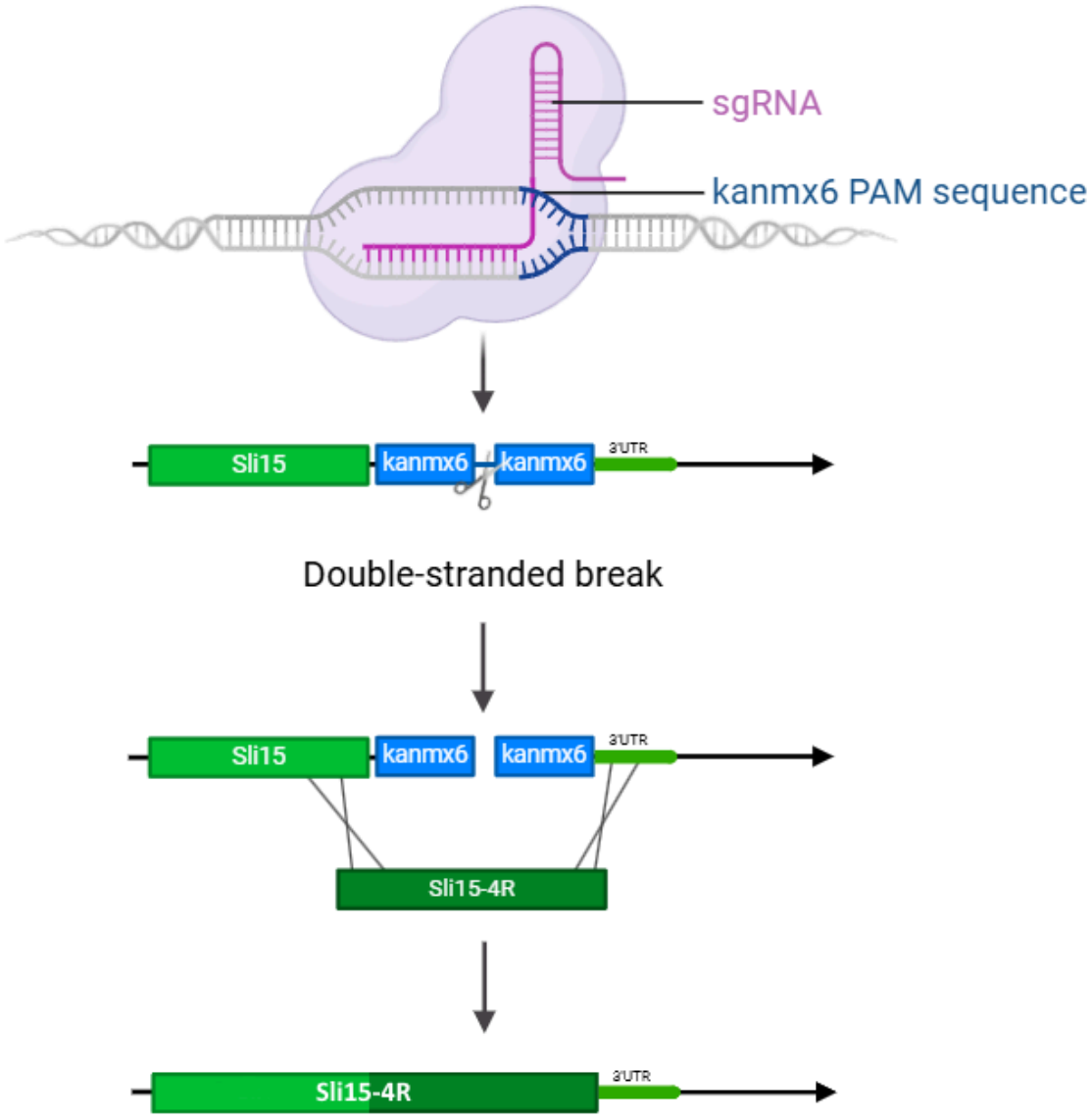

Figure 27: Graphical representation of the CRISPR/Cas9 system to insert sli15-4R gene into Sli15. sgRNA directs the enzyme to the PAM sequence of kanmx6 in the yeast genome, snips the DNA and the mutated gene is recombinated, creating a yeast strain with a Sli15 that cannot be mutated. Image created in BioRender and edited in Photoshop.

Colony PCR was performed using OneTaq polymerase with the primers Sli15_829f and Sli15_2r to check for the presence of the KAN sequence. The PCR results matched the theoretical size, indicating that the CRISPR/Cas9 system successfully excised the kanMx6 sequence from the genome. However, further PCR tests followed by sequencing

revealed that the 4R mutations had not been inserted into the genome. Therefore, the CrispR approach was abandoned and it was decided to create the mutated strains using classical homologous recombination (figure 3).

4.2 Creating the Double Mutant (*sli15-4R_GFP bir1-4R_mCherry*)

4.2.1 pRS306_Sli15_4R

Using the synthesised *SLI15-4R* gene containing specific lysine mutations in Sli15 to prevent sumoylation, the pRS306_Sli15_4R plasmid was created. The mutated gene fragment replaced the wild type sequence of the pRS306_Sli15 plasmid through cloning with ClaI and HpaI using Gibson assembly.

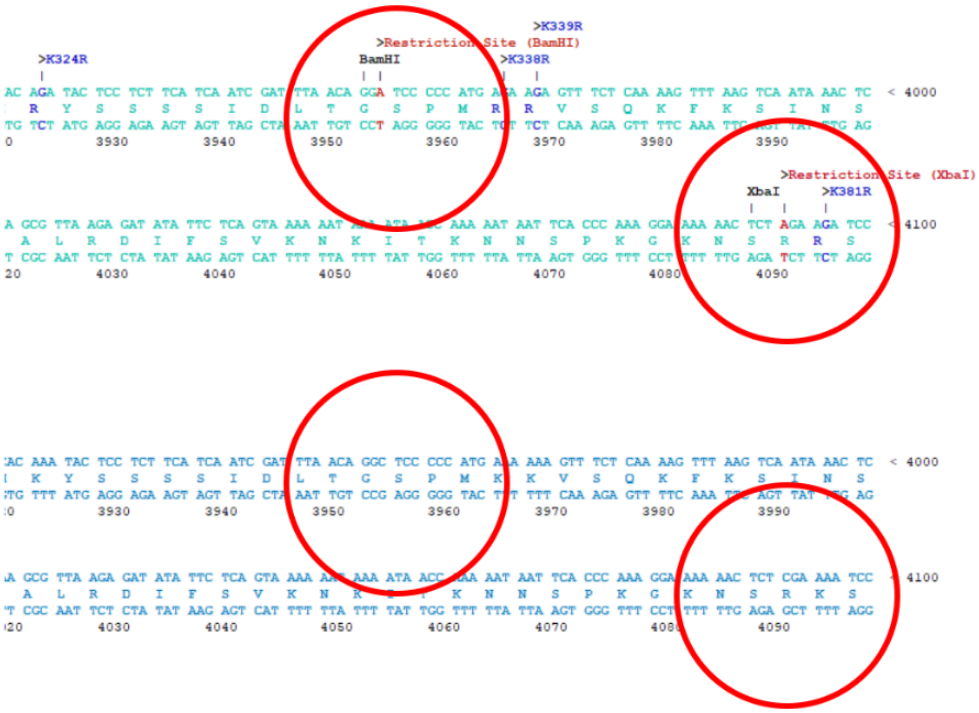

Figure 28: pRS306_Sli15_4R (up) and pRS306_Sli15 (down) sequence. Highlighted are the inserted restriction sites Xho1 and Not1. Made by SerialCloner.

To verify the introduction of mutations and the success of the Gibson assembly, the designed *SLI15-4R* gene includes two new and specific restriction sites, XbaI and BamHI, as seen on figure 28.

Multiple digestions were conducted with various restriction enzymes, the results consistently matched the theoretical predictions, confirming that the desired pRS306_Sli15-4R plasmid was obtained.

4.2.2 The *sli15-mRuby bir1-GFP* strains

To visualise Sli15 within yeast cells, determine its localization, and compare the sumoylated and non-sumoylated versions, the fluorescent tag encoding mRuby was both introduced into the pRS306_Sli15-4R and the wild-type RS306_Sli15.

The yomRuby2-SpHis5 gene cassette was amplified from the pDL1265_pFA6a-link-yomRuby2-SpHis5 plasmid using the primers Sli15_R1_CrispR and Sli15_S3frameshift with OneTaq polymerase. After purification, the pRS306_Sli15-4R and pRS306_Sli15 were digested with HpaI and SnaBI to prepare for Gibson assembly. Since both leave blunt ends, digested plasmids were treated with Antarctic phosphatase to further reduce self-ligation. From the resulting colonies, plasmids were isolated and the insertion of mRuby was verified by a restriction digest with NotI and AscI, since the yomRuby2-SpHis5 insert contains an AscI restriction site not present in the control. Correct plasmids were sent for sequencing. The confirmed plasmids were named pRS306_Sli15-4R_mRuby_His3Mx6 and pRS306_Sli15_mRuby_His3Mx6.

Both the plasmids were transformed in the *YDL588* yeast strain, and selected in -His plates. Transformants were tested with colony PCR, in order to ensure the insertion of the Sli15-4R-mRuby and Sli15_mRuby in *YDL588*. The strains were named *YDL4830 (sli15-4R-mRuby)* and *YDL4831 (sli5-mRuby).*

Examined under the microscope, the mRuby fluorescence intensity in the cells was too low, rendering experimental observations from challenging to impossible. Consequently,

Sli15 was tagged with GFP and Bir1 with mCherry to enhance signal detection and facilitate subsequent experiments.

4.2.3 The lethality of *ipl1-2R* strain

To create a CPC that cannot be sumoylated, it was necessary to create the yeast strain *ipl1-2R sli15-4R*. The Sli15-4R_mRuby_His3Mx6 plasmid was digested with KpnI and EcoRV, the resulting fragment purified and then transformed into the yeast strain *YDL4643* that was supposed to be *ipl1-2R MATa*. However, the resulting transformants did not contain any of the mutations in Sli15 and Ipl1, as checked by colony PCR. Future experiments also provided no *ipl1-2R* transformants, meaning that introducing i*pl1-2R* as a single source of Ipl1 in cells is possibly lethal. This might be due to the fact that the 2R mutation is a loss-of-function variant, hence the failure to recover viable colonies.

4.2.4 The correct double mutant

4.2.4.1 The *sli15-4R-GFP* strain

To insert the GFP tag into Sli15-4R, a PCR was conducted to amplify the specific GFP segment of the pFA6a-GFP(S65T) plasmid using primers GFP_ApaI_f and GFP_ApaI_r and the amplified GFP PCR product was cloned into ApaI-cut pRS306_Sli15-4R plasmid.

To create the *sli15-4R-GFP* strain the newly-cloned plasmid pRS306_Sli15-4R_GFP (S65T)_SpHis5 was digested with SacII, and the resulting Sli15-4R_GFP fragment directly transformed into the wild-type strain *YDL590*. Homologous recombination generated Sli15-4R-GFP, resulting in the creation of the *YDL4895*, and *YDL4896* strains, both of them in mating type alpha (MATa). This recombination luckily resulted in both the mutated *SLI15* gene (*YDL4895)* and the wild type *(YDL4896),* both resulting in the insertion of GFP. The strains were investigated and the recombination was confirmed by sequencing, using primers Sli15_829f and GFPrev.

4.2.4.2 Bir1-4R_mCherry

The Bir1-4R-mCherry construct was integrated into the *BIR1* locus of yeast strain *YDL588,* a mating type of the wild type yeast also used to create the *sli15-4R-GFP* strain. The transformation used the plasmid Bir1-4R-mCherry, which was digested with the restriction enzyme SwaI. Colony PCR was employed to confirm the integration of the Bir1-4R-mCherry construct. Positive colonies were subsequently verified by microscopy and the strains were named *YDL4917 (bir1-4R-mCherry)* and *YDL4918 (BIR1-mCherry)*, both in mating type a (MATa). The mutations were verified by sequencing.

Two of the newly created strains (*YDL4917* MATa *bir1-4R-mCherry:LEU2* and *YDL4895* MATalpha *sli15-4R-GFP:SpHis5)* were crossed. After sporulation and tetrad dissection, double mutant strains were selected in SDC-Leu and SDC-His plates.

4.3 Creating the triple mutant (*bir1-4R sli15-4R nbl1R*)

4.3.1 The *sli15-4R-GFP nbl1-R* strain

The existing *nbl1-R* strain (*YDL4627 MATa*), created by Dimitra Lani, was crossed with *YDL4895* (*sli15-4R-GFP*, MATalpha). This resulted in the generation of *YDL4901* and *YDL4902* on mating type alpha, and *YDL4903* and *YDL4904* with mating type a, selected on -Ura -His plates to identify *sli15-4R-GFP nbl1-R* double mutants.

4.3.2 The final triple mutant

The MATalpha strain *YDL4901* was crossed with the MATa strain *YDL4917*. This cross resulted in the creation of strains *YDL4926* and *YDL4927*, corresponding to mating types a and alpha, respectively of s*li15-4R-GFP bir1-4R-mCherry nbl1-R* selected on -Ura -Leu and -His plates (Figure 29).

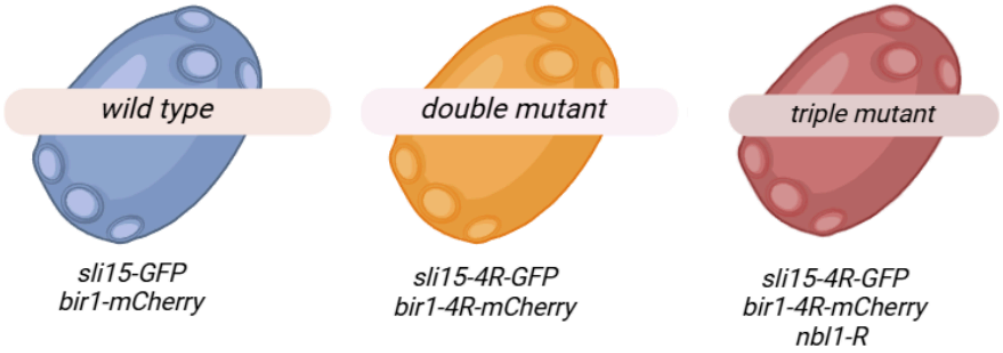

Figure 29: Yeast strains created.

5. Results: analysis of strain phenotypes

5.1. Culture behaviour

5.1.1 Growth tests

To test whether CPC mutants display any growth phenotypes, we plated serial dilutions of the different yeast strains on YPD full media plates and tested colony formation at different temperatures. Two growth tests are presented below, at 30°C and 37°C. Neither the double nor the triple mutant strain exhibit differences in the conditions tested (Figure 30).

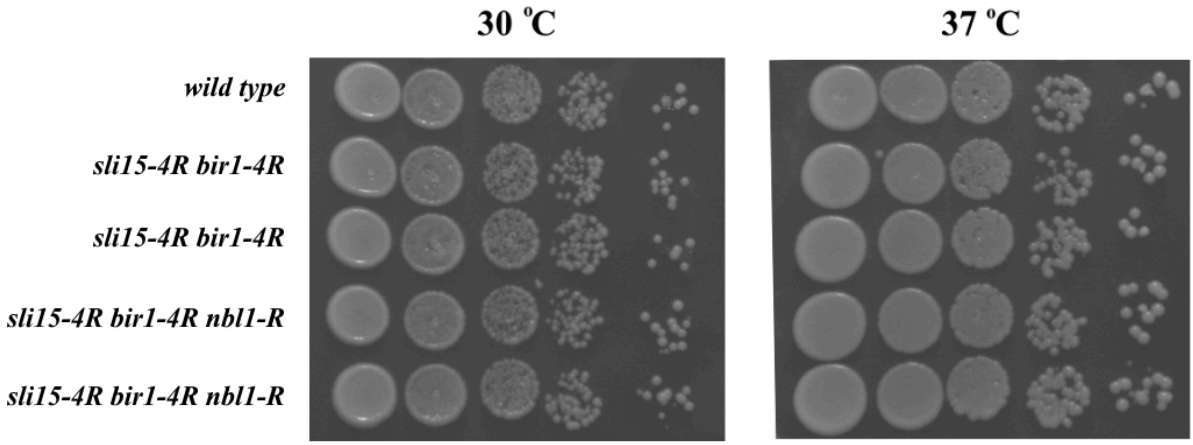

Figure 30: Yeast cell growth at various temperatures. From top to bottom: Wild Type, Double Mutant (*sli15-4R bir1-4R*), Double Mutant (*sli15-4R bir1-4R*), Triple Mutant (*sli15-4R bir1-4R nbl1-R*), Triple Mutant (*sli15-4R bir1-4R nbl1-R*).
From left to right: 30 ℃ and 37 ℃

This suggests that CPC sumoylation does not severely interfere with CPC function, since this would result in cell growth defects. Single-mutant strains (*sli15-4R*, *bir1-4R*, and *nbl1-R*) that were tested previously exhibited similar behaviour, showing no significant growth difference to wild type cells.

5.1.2 Hydroxyurea tests

Subsequently, experiments were conducted with incubation at various concentrations of hydroxyurea (HU). Hydroxyurea inhibits the production of nucleotides by targeting

ribonucleotide reductase, an enzyme crucial for the synthesis of deoxynucleotides and nucleotides. Cells exposed to hydroxyurea are susceptible to DNA damage, leading to replication stress (Charton et al., 2019). Under wild-type conditions, various mechanisms, including those involving the Chromosomal Passenger Complex (CPC) and specifically Aurora B kinase, help mitigate this stress (Luna-Maldonado et al., 2021).

Similar to the growth tests conducted above, serial dilutions of the different yeast strains on YPD full media were plated, containing different concentrations of hydroxyurea, and colony formation was tested. Only minor differences were observed between wild-type cells and the double and triple mutant strain, in terms of colony size and number, in 75 mM hydroxyurea (Figure 31).

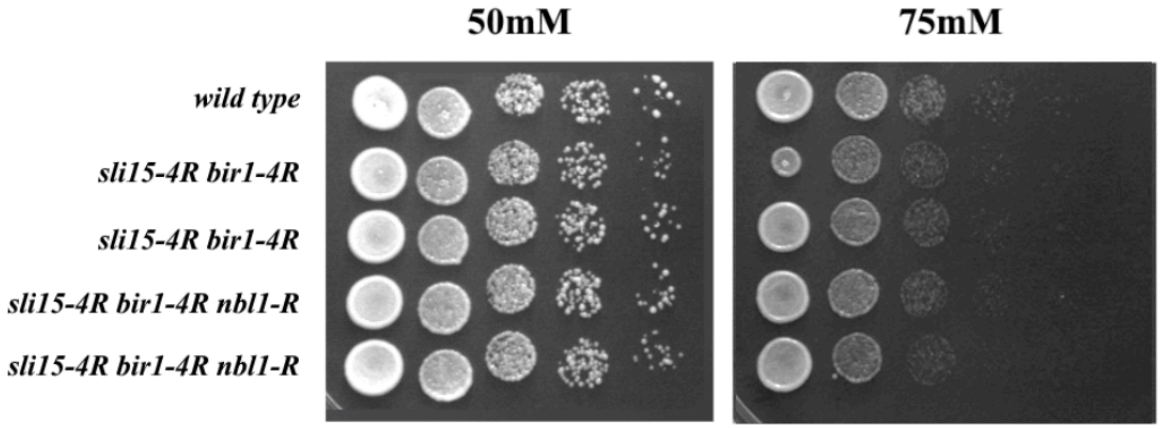

Figure 31: Yeast cells incubated with hydroxyurea. From top to bottom: Wild Type, Double Mutant (*sli15-4R bir1-4R*), Double Mutant (*sli15-4R bir1-4R*), Triple Mutant (*sli15-4R bir1-4R nbl1-R*), Triple Mutant (*sli15-4R bir1-4R nbl1-R*).

This suggests that the sumoylation of Sli15, Bir1, Nbl1 or a combined sumoylation of these components (Sli15, Bir1, and Nbl1) may be required for their function under replication stress caused by hydroxyurea.

5.2 Sli15-GFP/Bir1-mCherry colocalization

To quantify the colocalization between Bir1 and Sli15 in the wild type and the mutant strains, ImageJ was used, analysing images taken by the Inverted Nikon TiE wide-field microscope. This open-source program allows for everyone to reform its code, in order to create plugins that adapt to specific processes of an image, such as colocalization, data analysis and image analysis (Colocalization Analysis, ImageJ.net).

The plugin that was interpreted is named "Just Another Colocalization Plugin", proposed and submitted by Fabrice P. Cordelières and Susanne Bolte at the ImageJ forum. This plugin allows calculating a set of commonly used co-localization indicators, such as Pearson's coefficient and Manders' M1&M2 coefficient (Figure 32) (ImageJ.net).

Pearson's coefficient was chosen for assessing protein colocalization, due to its capability to analyse intensity variations between selected regions of interest. This method aligned well with the visual observation of protein overlap in the images analysed.

Manders' coefficient was avoided because it detects and analyses pixels with intensities above a specific threshold, which proved difficult to standardise across the microscopy conditions used, and it could lead to inconsistent results across different cells (ColocalizationTheory | Scientific Volume Imaging, n.d.).

The formula for Pearson's correlation coefficient r between two variables x and y is:

$$r = \frac{\sum(x_i - \bar{x})(y_i - \bar{y})}{\sqrt{\sum(x_i - \bar{x})^2 \sum(y_i - \bar{y})^2}}.$$

- r: Pearson's correlation coefficient (r value) which ranges from -1 to +1, meaning the perfect negative and perfect positive correlation respectfully. 0 also means no linear correlation, meaning that variables are independent of each other.

- x_i and y_i: individual data points or observations for variables x and y respectfully

- $\bar{x}$ and $\bar{y}$: average of values x and y respectively

- n: number of data points or observations

(Numeracy, Maths and Statistics - Academic Skills Kit, n.d.)

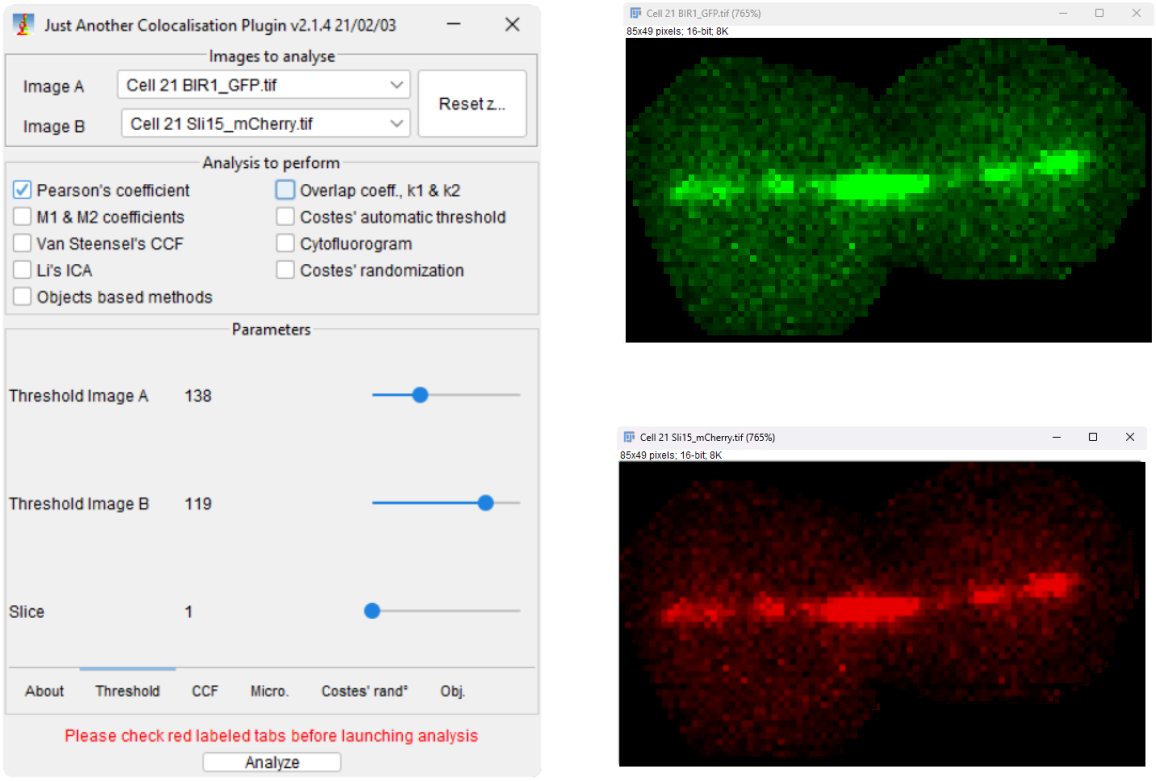

Figure 32: JACoP plugin (ImageJ, left) and the fluorescence of GFP and mCherry (right). The images on the right portrait a yeast cell, containing Sli15-4R-GFP and Bir1-4R-mCherry

This formula evaluates how well data from x and y fit in a straight line, assessing the degree of linear association between two variables by comparing their deviations from their means. In the context of the image colocalization analysis performed, the two values (x and y) represent the pixel intensity from one fluorescent channel of the image analysed, therefore the r value quantifies how the intensity varies across both images. A higher r indicates stronger linear association, suggesting greater colocalization of the proteins represented (Dunn et al., 2011).

Therefore, utilising JACoP, which analyses intensity based on Pearson's equation, the data were acquired and counted.

Average Pearson's R values					
wild type average		**2r average**		**3r average**	
late metaphase	late anaphase	late metaphase	late anaphase	late metaphase	late anaphase
0.972	0.955	0.808	0.942	0.991	0.989

The double mutant late metaphase measures were difficult to analyse, due to corrupted files. The results are consistent with expectations and visual analysis, confirming that Bir1 and Sli15 colocalize in every yeast strain.

Nevertheless it's crucial to interpret R values with caution. Pearson's coefficient provides a strong numerical measure, but overlooks differences in how microscopy images are captured, which can subtly influence the mean intensity values (X or Y), potentially leading to erroneous conclusions. Ensuring consistency in intensity thresholding and defining regions of interest (ROIs) is crucial for reproducibility, but the potential for human error in these processes must also be considered (Dunn et al., 2011) (ColocalizationTheory | Scientific Volume Imaging).

In conclusion, while Pearson's coefficient provides a robust method for quantitative analysis of the different yeast strains discussed, it's important to recognize its limitations. These include the limit in fully capturing protein colocalization dynamics, and other interfering factors such as the human element and constraints imposed by the microscopy setup.

Despite the limitations and cautions, it can be concluded that there is a strong likelihood that sumoylation does not affect the colocalization of Sli15 and Bir1.

5.3. Spindle length

5.3.1 Spindle length measurements in metaphase and late anaphase

Changes in CPC activity increase the maximum spindle length and delay the time of spindle disassembly in anaphase (Buvelot et al., 2003). We thus measured these 2 parameters in the double and triple CPC mutants.

Spindle length analysis was conducted using the fluorescence of Sli15-GFP in both wild type and in triple mutant cells (*sli15-4R bir1-4R nbl1-R*), analysing images taken from the Inverted Nikon TiE wide-field microscope, using ImageJ. As previously mentioned, at the end of anaphase, the spindle reaches its final size. By measuring the length of the fluorescent line of Sli15 with ImageJ (Figure 33b), which localises along the entire length of the spindle, the spindle length was determined, from the end of metaphase until spindle breakage (Figure 33a) (late anaphase).

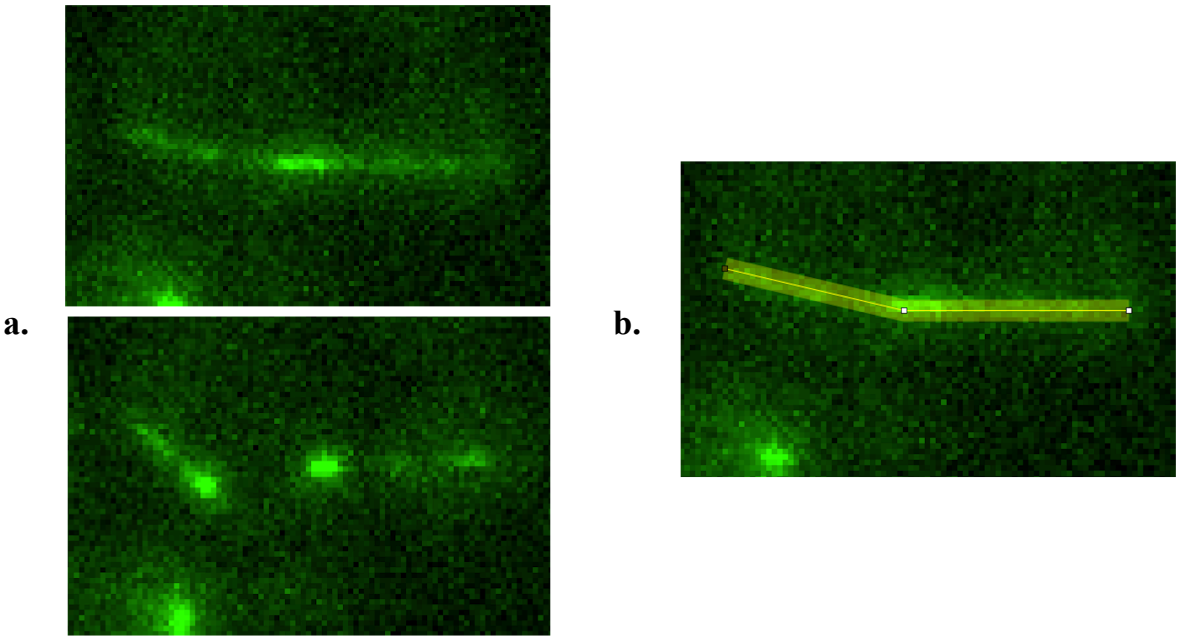

Figure 33: Sli15_GFP fluorescence. Spindle length was calculated by the "Segmented Line" tool and the "Measure" option by the "ROI manager" of ImageJ. Image showing (a.) moments before and after spindle breakage (up and down respectively), and the region of interest (ROI) used to measure spindle length.

An initial analysis was conducted to compare spindle length in wild-type and triple mutant cells during metaphase (M) and late anaphase (A), just before spindle breaking. A total of 16 cells from each strain were measured. There seemed to be a difference between the spindle length of wild type and triple mutant cells. The significance of these differences were calculated using both a ANOVA test for multiple comparisons and student's t-test (Figure 34). Both tests confirmed no significant difference in spindle length during metaphase.

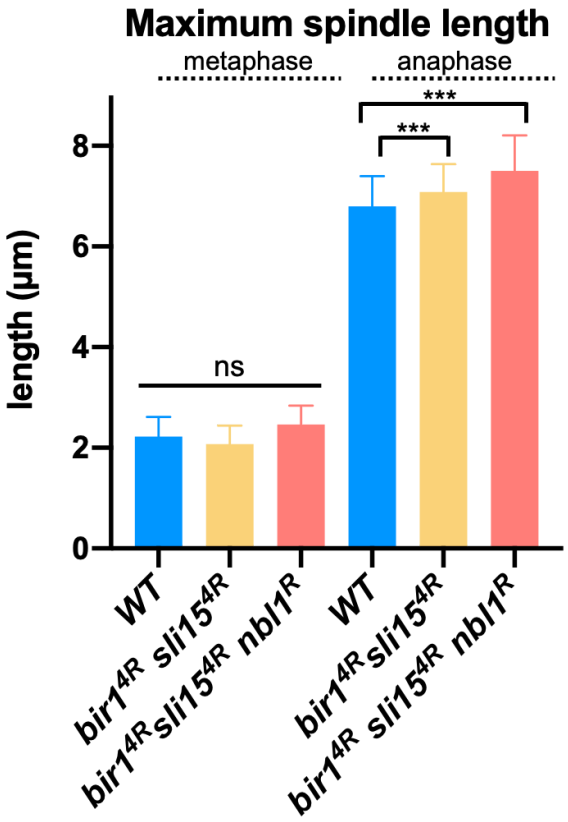

Figure 34: Measurements of max. metaphase and anaphase spindle lengths for different strains. The length of the spindle just before the beginning of anaphase spindle elongation (max metaphase length) as well as before spindle disassembly was measured from time-lapse images with 1 min temporal resolution. Sli15-GFP was used as a spindle marker. N>30 cells for each strain WT, *sli15-4R-GFP bir1-4R-mCherry* and *sli15-4R-GFP bir1-4R-mCherry nbl1-R*. Means of two biological replicates (one MATa and one MATalpha strain) are shown. P-value (***<0.0001) was calculated using the Brown-Forsythe and Welch ANOVA multiple comparison as well as student's t tests).

However, a significant difference was observed in late anaphase. These findings prompted the need for additional samples, focusing solely on the analysis of maximum spindle size. A total of 41 wild-type cells, 30 double mutant cells, and 45 triple mutant

cells were analysed from images captured using the Inverted Nikon TiE wide-field microscope.

The results confirmed the initial findings. No significant difference in spindle lengths was observed for metaphase spindles, whereas in their maximum anaphase spindle length the double and triple mutants displayed significant differences of 0.3µm and 0.7µm compared to wild-type, respectively.

A similar observation was made by Buvelot et al. in the *ipl1-321* mutant, a temperature-sensitive variant that loses its function at elevated temperatures. They reported that loss of Ipl1 function results in elongated spindles compared to wild-type cells, a phenomenon also observed in the present experiment. Since both Sli15/Bir1/Nbl1 and Sli15/Bir1 mutants display a similar phenotype, the sumoylation of Sli15 and Bir1 and/or Nbl1 may reduce Ipl1 activity.

5.3.2 Spindle dynamics

For approximately 35 cells in each strain, the time from anaphase onset (spindle elongation) to spindle breakage was measured, as seen on figure 35. The mean time was calculated for each strain and the results were compared, using t-tests to determine whether the observed differences were significant.

Significance test (t.test) between times from anaphase onset to spindle breakage			
strains	**WT vs 2R**	**WT vs 3R**	**2R vs 3R**
t.test value	0.3606	0.5831	0.727
conclusion	not significant	not significant	not significant
	Average time		
time (minutes)	18.5	18.3	18.4

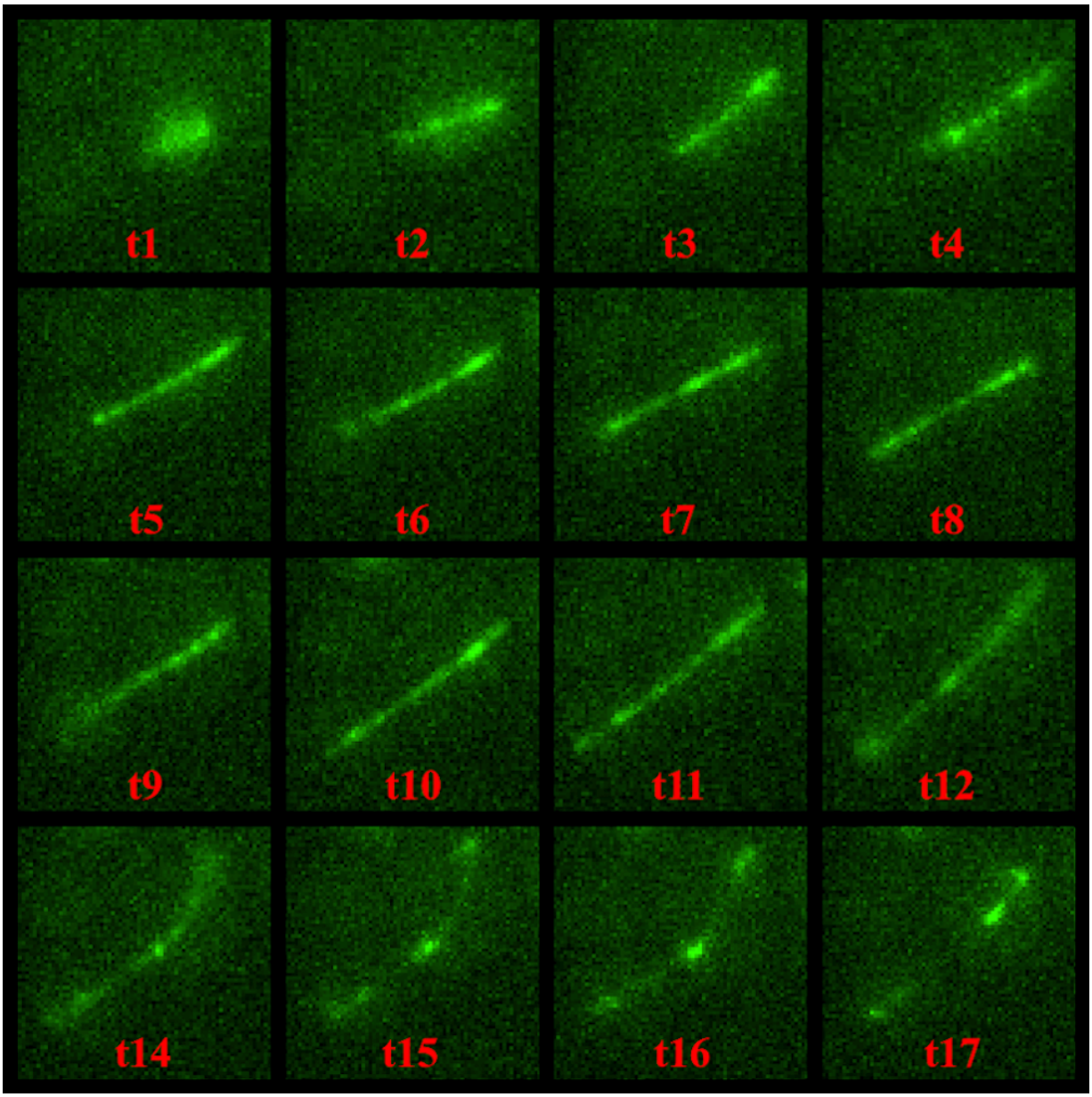

Figure 35: Sli15-GFP fluorescence in YDL4930 cells (*sli15-GFP bir1-mCherry*), as seen by Image J. Images taken with Inverted Nikon TiE wide-field microscope

As seen, cells show no significant variation in overall anaphase duration. However, differences in specific stages of spindle elongation may exist, as cells provide differences in the final spindle size. To investigate this, spindle lengths from 6 cells of each strain (18 cells in total) were measured with ImageJ at one-minute intervals throughout

anaphase for all three strains, in cells with a maximum spindle length corresponding to the average spindle length for each strain.

The average length was measured at each time point (Figure 36), and the following graph was generated:

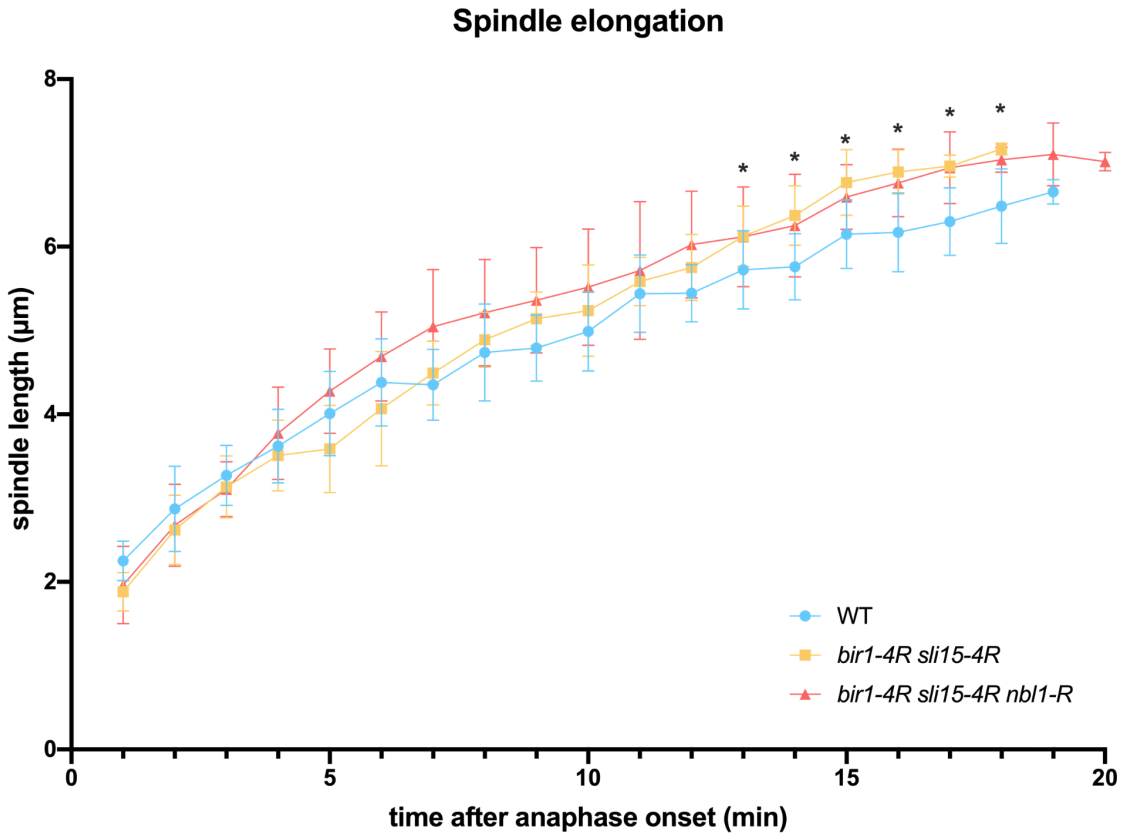

Figure 36: This graph depicts the average spindle lengths for the three strains analysed (light blue: Wild Type, yellow: *bir1-4R sli15-4R,* red: *bir1-4R sli15-4R nbl1-R*). A significant difference was observed as shown by measuring the data and their respective standard deviation from 14 minutes onward. suggesting that the two mutants show significant difference in spindle length, compared to the wild type cells.

A gradual increase in spindle length difference can be observed, particularly in the measurements from 14 minutes onward. At the initial stages, especially in the triple mutant spindle elongation also lasts longer (7 min vs 5 min compared to WT). In addition, the triple mutant seemed to have a faster rate of the initial, fast phase of spindle

elongation. Linear regression analysis of the time points 1-4 min confirms this assessment, showing a growth rate of 0.45±0.04 µm/min (R=0.98) and 0.58±0.04 µm/min (R=0.99) for the wild-type and the triple mutant, respectively (Figure 37).

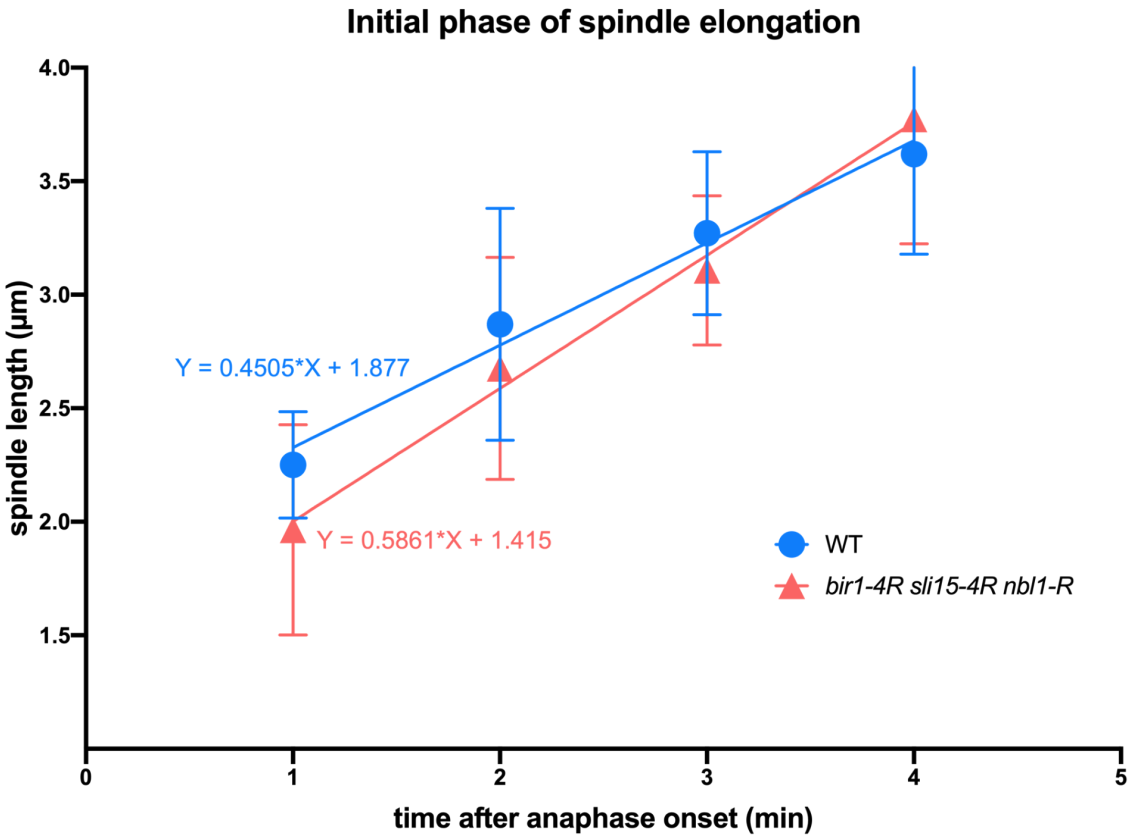

Figure 37: Linear regression analysis for the first four minutes of spindle growth, as mentioned. The analysis provides a growth rate of 0.45±0.04 µm/min (R=0.98) for the wild type, and 0.58±0.04 µm/min (R=0.99) for the triple mutant.

6. Discussion

The main point of caution with the data and experiments showcased, is that no further analysis was conducted to confirm the absence of CPC sumoylation in mutant strains. Immunoprecipitation of the mutant proteins and followed by detection of their sumoylation status using anti-SUMO antibodies or inversely, isolation of their sumoylation status after isolation under denaturing conditions are the two techniques needed to ensure the inability of the mutated CPC components to be sumoylated (Nie et al., 2015).

The following results are presented, proceeding with the assumption that the mutants exhibit the inability of the CPC to be sumoylated.

The inability to develop mutants with the Ipl1-2R variant suggests that Ipl1 sumoylation is crucial for *Saccharomyces cerevisiae* cells. If the 2R mutation represents a loss-of-function variant, it may explain the failure to recover viable colonies. This issue may arise from the inability of Ipl1 to localise to the centromeres or from general errors in chromosome segregation. All other CPC other mutants did not show any growth issues under normal conditions (30°C and 37°C).

The hydroxyurea assay provided useful information about the effect of CPC sumoylation on DNA damage and replication stress. The results showed that sumoylation of Sli15, Bir1, Nbl1, or a combined sumoylation of these, seem to have a slight defect in cell growth under conditions of replicative stress. This effect may be attributed to the disruption of SUMO-mediated interactions, causing inability of critical proteins to interact with the CPC due to the lack of sumoylation. One other possibility is that lack of CPC sumoylation prevents sumo-dependent degradation of CPC components like Bir1, which was proposed to be required for recovery from moderate replication stress (Thu et al., 2016).

According to the results presented here, we conclude that SUMO does not affect the localization of Sli15 and Bir1 in *Saccharomyces cerevisiae* cells. The Pearson's correlation values align with the qualitative observation of GFP and mRuby fluorescence, leading to the conclusion that none of the mutated strains (*sli15-4R bir1-4R nbl1-R* and *sli15-4R bir1-4R*) exhibit differences compared to the wild type. This finding corroborates the earlier report by Montpetit et al. that localization of unsumoylated Bir1 in the non-sumoylatable *ndc10-4R* mutant was not affected. and now suggests that sumoylation may be not required for correct localisation of the entire CPC .

There remains a possibility that the localization of Ipl1 and Nbl1 could be influenced, although this was impossible to detect in the current experiment due to lack of the required resolution. However, Gassmann et al. proposed that disruptions on Ipl1 localization during metaphase would typically lead to cell growth defects, a phenomenon not observed in this study (Gassmann et al., 2004).

SUMO may affect the activity of Ipl1. Ipl1 acts as a microtubule plus-end regulator, by phosphorylating its substrates with microtubule regulating activities, localised in spindle midzone (Buvelot, 2003). Previous findings state that loss of Ipl1 function in *ipli-321* mutants led to spindle elongation and delayed cytokinesis compared to wild type cells (Buvelot et al., 2003). Therefore, the observed differences in final spindle size between our mutants and the wild-type are consistent with a model indicating that the sumoylation of Sli15, Bir1, and/or Nbl1 may reduce Ipl1 activity.

To confirm that Ipl1 activity is indeed decreased, it would be necessary to further compare *ipl1-321* cells with the mutant strains created in this experiment and analyse spindle elongation and dynamics, in order to draw more reliable conclusions. Additionally, a phosphorylation analysis of Ipl1 substrates during metaphase and anaphase could provide stronger support for this hypothesis.

A caveat in this hypothesis is that reduced CPC/Ipl1 kinase activity would affect anaphase timing, resulting in prolonged spindle growth and delayed spindle disassembly. However, (Figure 35), the time required for spindle disassembly remained unchanged in CPC mutants. Therefore, sumoylation may not influence the activity of the CPC in general, but only its interaction with specific substrates involved in regulation of microtubule/spindle dynamics and spindle size.

Benitez et al. reported that delays in spindle disassembly are driven by two key Ipl1 substrates, Bim1 and She1 (Ibarlucea-Benitez et al., 2018). Additionally, Zimniak et al. demonstrated that Bim1 phosphorylation is essential for proper spindle dynamics and midzone disassembly *in vivo*, with an increase in spindle length during late anaphase (Zimniak et al., 2009). These results point to the possibility that impaired phosphorylation of Bim1 and She1 may underlie these observed alterations in spindle dynamics in our CPC mutants.

7. References

1. Abed, M., Bitman-Lotan, E., & Orian, A. (2018). The biology of SUMO-Targeted ubiquitin ligases in drosophila development, immunity, and Cancer. Journal of Developmental Biology, 6(1), 2. https://doi.org/10.3390/jdb6010002

2. Afonso, O., Figueiredo, A. C., & Maiato, H. (2016). Late mitotic functions of Aurora kinases. Chromosoma, 126(1), 93–103. https://doi.org/10.1007/s00412-016-0594-5

3. Akiyoshi, B., Sarangapani, K. K., Powers, A. F., Nelson, C. R., Reichow, S. L., Arellano-Santoyo, H., Gonen, T., Ranish, J. A., Asbury, C. L., & Biggins, S. (2010). Tension directly stabilizes reconstituted kinetochore-microtubule attachments. Nature, 468(7323), 576–579. https://doi.org/10.1038/nature09594

4. Alonso, A., Greenlee, M., Matts, J., Kline, J., Davis, K. J., & Miller, R. K. (2015). Emerging roles of sumoylation in the regulation of actin, microtubules, intermediate filaments, and septins. Cytoskeleton, 72(7), 305–339. https://doi.org/10.1002/cm.21226

5. Argiros, H., Henson, L., Holguin, C., Foe, V., & Shuster, C. B. (2012). Centralspindlin and chromosomal passenger complex behavior during normal and Rappaport furrow specification in echinoderm embryos. Cytoskeleton, 69(10), 840–853. https://doi.org/10.1002/cm.21061

6. Bähler, J. (2005). Cell-Cycle control of gene expression in budding and fission yeast. Annual Review of Genetics, 39(1), 69–94. https://doi.org/10.1146/annurev.genet.39.110304.095808

7. Ballmer, D., & Akiyoshi, B. (2024). Dynamic localization of the chromosomal passenger complex is controlled by the orphan kinesins KIN-A and KIN-B in the kinetoplastid parasite Trypanosoma brucei. eLife, 13. https://doi.org/10.7554/elife.93522

8. Banach, M., Fabian, P., Stapor, K., Konieczny, L., & Roterman, A. I. (2020). Structure of the hydrophobic core determines the 3D protein Structure—Verification by single mutation proteins. Biomolecules, 10(5), 767. https://doi.org/10.3390/biom10050767

9. Banerjee, A., Adames, N., Peccoud, J., & Tyson, J. J. (2020). A stochastic model for error correction of kinetochore-microtubule attachments in budding yeast. PLoS ONE, 15(8), e0236293. https://doi.org/10.1371/journal.pone.0236293

10. Bannister, A., Kouzarides, T. (2011). Regulation of chromatin by histone modifications. Cell Res 21, 381–395. https://doi.org/10.1038/cr.2011.22

11. Barford D. (2011). Structural insights into anaphase-promoting complex function and mechanism. Philosophical transactions of the Royal Society of London. Series B, Biological sciences, 366(1584), 3605–3624. https://doi.org/10.1098/rstb.2011.0069

12. Békés, M., Prudden, J., Srikumar, T., Raught, B., Boddy, M. N., & Salvesen, G. S. (2011). The dynamics and mechanism of SUMO chain deconjugation by SUMO-specific proteases. Journal of Biological Chemistry, 286(12), 10238–10247. https://doi.org/10.1074/jbc.m110.205153

13. Bermúdez-López, M., Villoria, M. T., Esteras, M., Jarmuz, A., Torres-Rosell, J., Clemente-Blanco, A., & Aragon, L. (2016). Sgs1's roles in DNA end resection, HJ dissolution, and crossover suppression require a two-step SUMO regulation dependent on Smc5/6. Genes & Development, 30(11), 1339–1356. https://doi.org/10.1101/gad.278275.116

14. Bernardi, R., & Pandolfi, P. P. (2007). Structure, dynamics and functions of promyelocytic leukaemia nuclear bodies. Nature Reviews Molecular Cell Biology, 8(12), 1006–1016. https://doi.org/10.1038/nrm2277

15. Bhuiyan, H., & Schmekel, K. (2004). Meiotic chromosome synapsis in yeast can occur without SPO11-Induced DNA Double-Strand breaks. Genetics, 168(2), 775–783. https://doi.org/10.1534/genetics.104.029660

16. Biebricher, A., Hirano, S., Enzlin, J. H., Wiechens, N., Streicher, W. W., Huttner, D., Wang, L. H., Nigg, E. A., Owen-Hughes, T., Liu, Y., Peterman, E., Wuite, G. J. L., & Hickson, I. D. (2013). PICH: a DNA translocase specially adapted for processing anaphase bridge DNA. Molecular cell, 51(5), 691–701. https://doi.org/10.1016/j.molcel.2013.07.016

17. Biggins, S., & Murray, A. W. (2001). The budding yeast protein kinase Ipl1/Aurora allows the absence of tension to activate the spindle checkpoint. Genes & development, 15(23), 3118–3129. https://doi.org/10.1101/gad.934801

18. Biggins, S., Severin, F. F., Bhalla, N., Sassoon, I., Hyman, A. A., & Murray, A. W. (1999). The conserved protein kinase Ipl1 regulates microtubule binding to kinetochores in budding yeast. Genes & Development, 13(5), 532–544. https://doi.org/10.1101/gad.13.5.532

19. BIR1 | SGD. (n.d.). https://www.yeastgenome.org/locus/S000003849

20. Bokros, M., Sherwin, D., Kabbaj, M., & Wang, Y. (2021). Yeast Fin1-PP1 dephosphorylates an Ipl1 substrate, Ndc80, to remove Bub1-Bub3 checkpoint proteins from the kinetochore during anaphase. PLOS Genetics, 17(5), e1009592. https://doi.org/10.1371/journal.pgen.1009592

21. Börner, G. V., Hochwagen, A., & MacQueen, A. J. (2023). Meiosis in budding yeast. Genetics, 225(2). https://doi.org/10.1093/genetics/iyad125

22. Bouck, D. C., & Bloom, K. S. (2005). The kinetochore protein Ndc10p is required for spindle stability and cytokinesis in yeast. Proceedings of the National Academy of Sciences, 102(15), 5408–5413. https://doi.org/10.1073/pnas.0405925102

23. Boyarchuk, Y., Salic, A., Dasso, M., & Arnaoutov, A. (2007). Bub1 is essential for assembly of the functional inner centromere. The Journal of cell biology, 176(7), 919–928. https://doi.org/10.1083/jcb.200609044

24. Broad, A. J., & DeLuca, J. G. (2020). The right place at the right time: Aurora B kinase localization to centromeres and kinetochores. Essays in Biochemistry, 64(2), 299–311. https://doi.org/10.1042/ebc20190081

25. Buvelot, S. (2003, January 27). The dynamic localization and novel functions of the Ipl1/Aurora protein kinase. FOLIA - Fribourg Open Library and Archive. https://folia.unifr.ch/unifr/documents/299830

26. Buvelot, S., Tatsutani, S. Y., Vermaak, D., & Biggins, S. (2003). The budding yeast Ipl1/Aurora protein kinase regulates mitotic spindle disassembly. The Journal of cell biology, 160(3), 329–339. https://doi.org/10.1083/jcb.200209018

27. Cairo, G., & Lacefield, S. (2020). Establishing correct kinetochore-microtubule attachments in mitosis and meiosis. Essays in biochemistry, 64(2), 277–287. https://doi.org/10.1042/EBC20190072

28. Campbell, C. S., & Desai, A. (2013). Tension sensing by Aurora B kinase is independent of survivin-based centromere localization. Nature, 497(7447), 118–121. https://doi.org/10.1038/nature12057

29. Cao, L., Wang, Z., Yang, X., Xie, L., & Yu, L. (2008). The evolution of BIR domain and its containing proteins. FEBS Letters, 582(27), 3817–3822. https://doi.org/10.1016/j.febslet.2008.09.058

30. Carmena, M., Wheelock, M., Funabiki, H., & Earnshaw, W. C. (2012). The chromosomal passenger complex (CPC): from easy rider to the godfather of mitosis. Nature reviews. Molecular cell biology, 13(12), 789–803. https://doi.org/10.1038/nrm3474

31. CentroSome. (n.d.). Genome.gov. https://www.genome.gov/genetics-glossary/Centrosome

32. Chang YC, Oram MK, Bielinsky AK. SUMO-Targeted Ubiquitin Ligases and Their Functions in Maintaining Genome Stability. Int J Mol Sci. 2021 May 20;22(10):5391. doi: 10.3390/ijms22105391. PMID: 34065507; PMCID: PMC8161396.

33. Chang, F., & Drubin, D. G. (1996). Cell division: Why daughters cannot be like their mothers. Current Biology, 6(6), 651–654. https://doi.org/10.1016/s0960-9822(09)00440-0

34. Chang, Y., Oram, M. K., & Bielinsky, A. (2021). SUMO-Targeted ubiquitin ligases and their functions in maintaining genome stability. International Journal of Molecular Sciences, 22(10), 5391. https://doi.org/10.3390/ijms22105391

35. Charton, R., Muguet, A., Griesenbeck, J., Smerdon, M. J., & Conconi, A. (2019). In yeast cells arrested at the early S-phase by hydroxyurea, rRNA gene promoters and chromatin

are poised for transcription while rRNA synthesis is compromised. Mutation Research/Fundamental and Molecular Mechanisms of Mutagenesis, 815, 20–29. https://doi.org/10.1016/j.mrfmmm.2019.04.003

36. Chen, L., Yin, T., Nie, Z. W., Wang, T., Gao, Y. Y., Yin, S. Y., Huo, L. J., Zhang, X., Yang, J., & Miao, Y. L. (2018). Survivin regulates chromosome segregation by modulating the phosphorylation of Aurora B during porcine oocyte meiosis. Cell cycle (Georgetown, Tex.), 17(21-22), 2436–2446. https://doi.org/10.1080/15384101.2018.1542894

37. Chien A, Edgar DB, Trela JM. Deoxyribonucleic acid polymerase from the extreme thermophile Thermus aquaticus. J Bacteriol. 1976;127(3):1550-1557. doi:10.1128/jb.127.3.1550-1557.1976

38. Coffman J. A. (2004). Cell cycle development. Developmental cell, 6(3), 321–327. https://doi.org/10.1016/s1534-5807(04)00067-x

39. Colocalization analysis. (n.d.). ImageJ Wiki. https://imagej.net/imaging/colocalization-analysis

40. ColocalizationTheory | Scientific Volume Imaging. (n.d.). Scientific Volume Imaging. https://svi.nl/ColocalizationTheory

41. COMA complex | SGD. (n.d.). https://www.yeastgenome.org/go/GO:0000817

42. Corbett, K. D. (2017). Molecular mechanisms of spindle assembly checkpoint activation and silencing. Progress in Molecular and Subcellular Biology, 429–455. https://doi.org/10.1007/978-3-319-58592-5_18

43. Cormier, A., Drubin, D. G., & Barnes, G. (2013). Phosphorylation regulates kinase and microtubule binding activities of the budding yeast chromosomal passenger complex in vitro. Journal of Biological Chemistry/˜the œJournal of Biological Chemistry, 288(32), 23203–23211. https://doi.org/10.1074/jbc.m113.491480

44. Cremona, C. A., Sarangi, P., & Zhao, X. (2012). Sumoylation and the DNA damage response. Biomolecules, 2(3), 376–388. https://doi.org/10.3390/biom2030376

45. D'Amours, D., & Amon, A. (2004). At the interface between signaling and executing anaphase—Cdc14 and the FEAR network. Genes & Development, 18(21), 2581–2595. https://doi.org/10.1101/gad.1247304

46. Da Silva-Ferrada, E., Lopitz-Otsoa, F., Lang, V., Rodríguez, M. S., & Matthiesen, R. (2012). Strategies to identify recognition Signals and Targets of SUMOylation. Biochemistry Research International, 2012, 1–16. https://doi.org/10.1155/2012/875148

47. Dasso, M. (2008). Emerging roles of the SUMO pathway in mitosis. Cell Division, 3(1), 5. https://doi.org/10.1186/1747-1028-3-5

48. De Albuquerque, C. P., Suhandynata, R. T., Carlson, C. R., Yuan, W., & Zhou, H. (2018). Binding to small ubiquitin-like modifier and the nucleolar protein Csm1 regulates substrate specificity of the Ulp2 protease. Journal of Biological Chemistry/the Journal of Biological Chemistry, 293(31), 12105–12119. https://doi.org/10.1074/jbc.ra118.003022

49. Deshaies, R. J., & Joazeiro, C. A. (2009). RING Domain E3 Ubiquitin Ligases. Annual Review of Biochemistry, 78(1), 399–434. https://doi.org/10.1146/annurev.biochem.78.101807.093809

50. Díaz-Martínez, L. A., & Yu, H. (2007). Running on a treadmill: dynamic inhibition of APC/C by the spindle checkpoint. Cell Division, 2(1), 23. https://doi.org/10.1186/1747-1028-2-23

51. Lani D. (2022). Study of the regulation of the Chromosomal Passenger Complex (CPC) by SUMO-targeted ubiquitin ligases in the yeast Saccharomyces cerevisiae [MSc thesis, University of Ioannina], Laboratory of Biology Department of Biological Applications and Technology

52. Doodhi, H., & Tanaka, T. U. (2022). Swap and stop – Kinetochores play error correction with microtubules. BioEssays, 44(5). https://doi.org/10.1002/bies.202100246

53. Dunn, K. W., Kamocka, M. M., & McDonald, J. H. (2011). A practical guide to evaluating colocalization in biological microscopy. AJP Cell Physiology, 300(4), C723–C742. https://doi.org/10.1152/ajpcell.00462.2010

54. Eckhoff, J., & Dohmen, R. J. (2015). In vitro studies reveal a sequential mode of chain processing by the yeast SUMO (Small ubiquitin-related modifier)-specific protease ULP2. Journal of Biological Chemistry/˜the œJournal of Biological Chemistry, 290(19), 12268–12281. https://doi.org/10.1074/jbc.m114.622217

55. Edgerton, H. D., Mukherjee, S., Johansson, M., Bachant, J., Gardner, M. K., & Clarke, D. J. (2023). Low tension recruits the yeast Aurora B protein Ipl1 to centromeres in metaphase. Journal of Cell Science, 136(16). https://doi.org/10.1242/jcs.261416

56. Elements of yeast genetics. (n.d.). BrainKart. https://www.brainkart.com/article/Elements-of-Yeast-Genetics_16821

57. Everett, R. D., Boutell, C., & Hale, B. G. (2013). Interplay between viruses and host sumoylation pathways. Nature Reviews Microbiology, 11(6), 400–411. https://doi.org/10.1038/nrmicro3015

58. Fehrenbacher, K. L., Yang, H., Gay, A. C., Huckaba, T. M., & Pon, L. A. (2004). Live Cell Imaging of Mitochondrial Movement along Actin Cables in Budding Yeast. Current Biology, 14(22), 1996–2004. https://doi.org/10.1016/j.cub.2004.11.004

59. Fink, S., Turnbull, K., Desai, A., & Campbell, C. S. (2017). An engineered minimal chromosomal passenger complex reveals a role for INCENP/Sli15 spindle association in chromosome biorientation. The Journal of cell biology, 216(4), 911–923. https://doi.org/10.1083/jcb.201609123

60. Fischböck-Halwachs, J., Singh, S., Potocnjak, M., Hagemann, G., Solis-Mezarino, V., Woike, S., Ghodgaonkar-Steger, M., Weissmann, F., Gallego, L. D., Rojas, J., Andreani, J., Köhler, A., & Herzog, F. (2019). The COMA complex interacts with Cse4 and positions Sli15/Ipl1 at the budding yeast inner kinetochore. eLife, 8. https://doi.org/10.7554/elife.42879

61. Foley, E. A., & Kapoor, T. M. (2013). Microtubule attachment and spindle assembly checkpoint signalling at the kinetochore. Nature reviews. Molecular cell biology, 14(1), 25–37. https://doi.org/10.1038/nrm3494

62. Gareau, J. R., & Lima, C. D. (2010). The SUMO pathway: emerging mechanisms that shape specificity, conjugation and recognition. Nature Reviews Molecular Cell Biology, 11(12), 861–871. https://doi.org/10.1038/nrm3011

63. Gassmann, R., Carvalho, A., Henzing, A. J., Ruchaud, S., Hudson, D. F., Honda, R., Nigg, E. A., Gerloff, D. L., & Earnshaw, W. C. (2004). Borealin: a novel chromosomal passenger required for stability of the bipolar mitotic spindle. The Journal of cell biology, 166(2), 179–191. https://doi.org/10.1083/jcb.200404001

64. Geiss-Friedlander, R., & Melchior, F. (2007). Concepts in sumoylation: a decade on. Nature Reviews. Molecular Cell Biology, 8(12), 947–956. https://doi.org/10.1038/nrm2293

65. Gladfelter, A., & Berman, J. (2009). Dancing genomes: fungal nuclear positioning. Nature Reviews. Microbiology, 7(12), 875–886. https://doi.org/10.1038/nrmicro2249

66. Gruneberg, U., Neef, R., Honda, R., Nigg, E. A., & Barr, F. A. (2004). Relocation of Aurora B from centromeres to the central spindle at the metaphase to anaphase transition requires MKlp2. The Journal of Cell Biology, 166(2), 167–172. https://doi.org/10.1083/jcb.200403084

67. Gu, Y., & Oliferenko, S. (2015). Comparative biology of cell division in the fission yeast clade. Current Opinion in Microbiology, 28, 18–25. https://doi.org/10.1016/j.mib.2015.07.011

68. Hadders, M. A., & Lens, S. M. (2022). Changing places: Chromosomal Passenger Complex relocation in early anaphase. Trends in Cell Biology, 32(2), 165–176. https://doi.org/10.1016/j.tcb.2021.09.008

69. Hassold, T., Hall, H., & Hunt, P. (2007). The origin of human aneuploidy: where we have been, where we are going. Human Molecular Genetics Online/Human Molecular Genetics, 16(R2), R203–R208. https://doi.org/10.1093/hmg/ddm243

70. Hay RT. SUMO: a history of modification. Mol Cell. 2005 Apr 1;18(1):1-12. doi: 10.1016/j.molcel.2005.03.012. PMID: 15808504.

71. Hegde, A. N. (2010). Ubiquitin-Dependent protein degradation. In Elsevier eBooks (pp. 699–752). https://doi.org/10.1016/b978-008045382-8.00697-3

72. Herrero, E., Stinus, S., Bellows, E., Berry, L. K., Wood, H., & Thorpe, P. H. (2020). Asymmetric transcription factor partitioning during yeast cell division requires the FACT chromatin remodeler and cell cycle progression. Genetics, 216(3), 701–716. https://doi.org/10.1534/genetics.120.303439

73. Howes, S. C., Geyer, E. A., LaFrance, B., Zhang, R., Kellogg, E. H., Westermann, S., Rice, L. M., & Nogales, E. (2017). Structural differences between yeast and mammalian microtubules revealed by cryo-EM. ˜the œJournal of Cell Biology/˜the œJournal of Cell Biology, 216(9), 2669–2677. https://doi.org/10.1083/jcb.201612195

74. Hsu, J., Sun, Z., Li, X., Reuben, M., Tatchell, K., Bishop, D. K., Grushcow, J. M., Brame, C. J., Caldwell, J. A., Hunt, D. F., Lin, R., Smith, M., & Allis, C. (2000). Mitotic Phosphorylation of Histone H3 Is Governed by Ipl1/aurora Kinase and Glc7/PP1 Phosphatase in Budding Yeast and Nematodes. Cell, 102(3), 279–291. https://doi.org/10.1016/s0092-8674(00)00034-9

75. Hümmer, S., & Mayer, T. U. (2009). CDK1 negatively regulates midzone localization of the mitotic kinesin MKLP2 and the chromosomal passenger complex. Current Biology, 19(7), 607–612. https://doi.org/10.1016/j.cub.2009.02.046

76. Ibarlucea-Benitez, I., Ferro, L. S., Drubin, D. G., & Barnes, G. (2018). Kinesins relocalize the chromosomal passenger complex to the midzone for spindle disassembly. The Journal of Cell Biology, 217(5), 1687–1700. https://doi.org/10.1083/jcb.201708114

77. Impens, F., Radoshevich, L., Cossart, P., & Ribet, D. (2014). Mapping of SUMO sites and analysis of SUMOylation changes induced by external stimuli. Proceedings of the National Academy of Sciences, 111(34), 12432–12437. https://doi.org/10.1073/pnas.1413825111

78. IPL1 | SGD. (n.d.). https://www.yeastgenome.org/locus/S000006130

79. JACOP. (n.d.). ImageJ Wiki. https://imagej.net/plugins/jacop

80. Jaiswal, P. K., Goel, A., & Mittal, R. D. (2015). Survivin: A molecular biomarker in cancer. The Indian journal of medical research, 141(4), 389–397. https://doi.org/10.4103/0971-5916.159250

81. Jalal, D., Chalissery, J., & Hassan, A. H. (2017). Genome maintenance in Saccharomyces cerevisiae: the role of SUMO and SUMO-targeted ubiquitin ligases. Nucleic Acids Research, gkw1369. https://doi.org/10.1093/nar/gkw1369

82. Jentsch, S., & Psakhye, I. (2013). Control of nuclear activities by Substrate-Selective and Protein-Group SUMOylation. Annual Review of Genetics, 47(1), 167–186. https://doi.org/10.1146/annurev-genet-111212-133453

83. Jeyaprakash, A. A., Basquin, C., Jayachandran, U., & Conti, E. (2011). Structural basis for the recognition of phosphorylated histone H3 by the Survivin subunit of the Chromosomal passenger Complex. Structure, 19(11), 1625–1634. https://doi.org/10.1016/j.str.2011.09.002

84. Jiménez, J., Queralt, E., Posas, F., & De Nadal, E. (2020). The regulation of Net1/Cdc14 by the Hog1 MAPK upon osmostress unravels a new mechanism regulating mitosis. Cell Cycle, 19(17), 2105–2118. https://doi.org/10.1080/15384101.2020.1804222

85. Jin, F., & Wang, Y. (2013). The signaling network that silences the spindle assembly checkpoint upon the establishment of chromosome bipolar attachment. Proceedings of the National Academy of Sciences, 110(52), 21036–21041. https://doi.org/10.1073/pnas.1307595111

86. Juanes, M. A., Twyman, H., Tunnacliffe, E., Guo, Z., Hoopen, R. T., & Segal, M. (2013). Spindle Pole Body History Intrinsically Links Pole Identity with Asymmetric Fate in Budding Yeast. Current Biology, 23(14), 1310–1319. https://doi.org/10.1016/j.cub.2013.05.057

87. Jwa, M., Kim, J. H., & Chan, C. S. (2008). Regulation of Sli15/INCENP, kinetochore, and Cdc14 phosphatase functions by the ribosome biogenesis protein Utp7. The Journal of cell biology, 182(6), 1099–1111. https://doi.org/10.1083/jcb.200802085

88. K, S. T., Joshi, G., Arya, P., Mahajan, V., Chaturvedi, A., & Mishra, R. K. (2021). SUMO and SUMOylation pathway at the forefront of host immune response. Frontiers in Cell and Developmental Biology, 9. https://doi.org/10.3389/fcell.2021.681057

89. Kalous, J., Jansová, D., & Šušor, A. (2020). Role of Cyclin-Dependent kinase 1 in translational regulation in the M-Phase. Cells, 9(7), 1568. https://doi.org/10.3390/cells9071568

90. Kawashima, S. A., Yamagishi, Y., Honda, T., Ishiguro, K., & Watanabe, Y. (2010). Phosphorylation of H2A by Bub1 prevents chromosomal instability through localizing shugoshin. Science (New York, N.Y.), 327(5962), 172–177. https://doi.org/10.1126/science.1180189

91. Keiten-Schmitz, J., Schunck, K., & Müller, S. (2020). SUMO chains rule on chromatin occupancy. Frontiers in Cell and Developmental Biology, 7. https://doi.org/10.3389/fcell.2019.00343

92. Kilmartin, J. V. (2014). Lessons from yeast: the spindle pole body and the centrosome. Philosophical Transactions - Royal Society. Biological Sciences, 369(1650), 20130456. https://doi.org/10.1098/rstb.2013.0456

93. Koca Caydasi Research Group - Ayşe Koca Çaydaşı. (2019, January 16). RESEARCH | Koca Caydasi Research Group - Ayşe Koca Çaydaşı. Koca Caydasi Research Group - Ayşe Koca Çaydaşı | Cell Cycle and Genome Stability Lab - Koca Caydasi Research Group. https://mysite.ku.edu.tr/aykoca/research/

94. Lallemand-Breitenbach, V., & De, H. (2010). PML nuclear bodies. Cold Spring Harbor Perspectives in Biology, 2(5), a000661. https://doi.org/10.1101/cshperspect.a000661

95. Lampson, M. A., & Cheeseman, I. M. (2011). Sensing centromere tension: Aurora B and the regulation of kinetochore function. Trends in cell biology, 21(3), 133–140. https://doi.org/10.1016/j.tcb.2010.10.007

96. Lascorz, J., Codina-Fabra, J., Reverter, D., & Torres-Rosell, J. (2022). SUMO-SIM interactions: From structure to biological functions. Seminars in Cell and Developmental Biology, 132, 193–202. https://doi.org/10.1016/j.semcdb.2021.11.007

97. Leisner, C., Kammerer, D., Denoth, A., Britschi, M., Barral, Y., & Liakopoulos, D. (2008). Regulation of mitotic spindle asymmetry by SUMO and the Spindle-Assembly Checkpoint in Yeast. Current Biology, 18(16), 1249–1255. https://doi.org/10.1016/j.cub.2008.07.091

98. Liu, D., Vader, G., Vromans, M. J., Lampson, M. A., & Lens, S. M. (2009). Sensing chromosome bi-orientation by spatial separation of aurora B kinase from kinetochore substrates. Science (New York, N.Y.), 323(5919), 1350–1353. https://doi.org/10.1126/science.1167000

99. Liu, S., Atkinson, E., Paulucci-Holthauzen, A., & Wang, B. (2023). A CK2 and SUMO-dependent, PML NB-involved regulatory mechanism controlling BLM ubiquitination and G-quadruplex resolution. Nature Communications, 14(1). https://doi.org/10.1038/s41467-023-41705-9

100. Luna-Maldonado, F., Andonegui-Elguera, M. A., Díaz-Chávez, J., & Herrera, L. A. (2021). Mitotic and DNA damage response proteins: maintaining the genome stability and working for the common good. Frontiers in Cell and Developmental Biology, 9. https://doi.org/10.3389/fcell.2021.700162

101. Magliozzi, J. O., & Moseley, J. B. (2021). Connecting cell polarity signals to the cytokinetic machinery in yeast and metazoan cells. Cell Cycle, 20(1), 1–10. https://doi.org/10.1080/15384101.2020.1864941

102. Makrantoni, V., Corbishley, S. J., Rachidi, N., Morrice, N. A., Robinson, D. A., & Stark, M. J. (2014). Phosphorylation of Sli15 by Ipl1 is important for proper CPC localization and chromosome stability in Saccharomyces cerevisiae. PloS one, 9(2), e89399. https://doi.org/10.1371/journal.pone.0089399

103. Marsoner, T., Yedavalli, P., Masnovo, C., Fink, S., Schmitzer, K., & Campbell, C. S. (2022). Aurora B activity is promoted by cooperation between discrete localization sites

in budding yeast. Molecular biology of the cell, 33(9), ar85. https://doi.org/10.1091/mbc.E21-11-0590

104. Matic, I., Schimmel, J., Hendriks, I. A., Van Santen, M. A., Van De Rijke, F., Van Dam, H., Gnad, F., Mann, M., & Vertegaal, A. C. O. (2010). Site-Specific identification of SUMO-2 targets in cells reveals an inverted SUMOylation motif and a hydrophobic cluster SUMOylation motif. Molecular Cell, 39(4), 641–652. https://doi.org/10.1016/j.molcel.2010.07.026

105. McKim, K. S. (2021). Highway to hell‐thy meiotic divisions: Chromosome passenger complex functions driven by microtubules. BioEssays, 44(1). https://doi.org/10.1002/bies.202100202

106. McLennan, R., Bailey, C. M., Schumacher, L. J., Teddy, J. M., Morrison, J. A., Kasemeier-Kulesa, J. C., Wolfe, L. A., Gogol, M. M., Baker, R. E., Maini, P. K., & Kulesa, P. M. (2017). DAN (NBL1) promotes collective neural crest migration by restraining uncontrolled invasion. The Journal of cell biology, 216(10), 3339–3354. https://doi.org/10.1083/jcb.201612169

107. McNally, F. J. (2013). Mechanisms of spindle positioning. The Journal of Cell Biology, 200(2), 131–140. https://doi.org/10.1083/jcb.201210007

108. McVey, S. L., Cosby, J. K., & Nannas, N. J. (2021). Aurora B tension sensing mechanisms in the kinetochore ensure accurate chromosome segregation. International Journal of Molecular Sciences, 22(16), 8818. https://doi.org/10.3390/ijms22168818

109. MERCK. Polymerase chain reaction. (2024). https://www.sigmaaldrich.com/GR/en/technical-documents/technical-article/genomics/pcr/polymerase-chain-reaction

110. Montpetit, B., Hazbun, T. R., Fields, S., & Hieter, P. (2006). Sumoylation of the budding yeast kinetochore protein Ndc10 is required for Ndc10 spindle localization and regulation of anaphase spindle elongation. The Journal of Cell Biology, 174(5), 653–663. https://doi.org/10.1083/jcb.200605019

111. Mossessova, E., & Lima, C. D. (2000). ULP1-SUMO crystal structure and genetic analysis reveal conserved interactions and a regulatory element essential for cell growth in yeast. Molecular Cell, 5(5), 865–876. https://doi.org/10.1016/s1097-2765(00)80326-3

112. Mullis, K. B., & Faloona, F. A. (1987). [21] Specific synthesis of DNA in vitro via a polymerase-catalyzed chain reaction. Methods in Enzymology on CD-ROM/Methods in Enzymology, 335–350. https://doi.org/10.1016/0076-6879(87)55023-6

113. Munk, S., Sigurðsson, J. O., Xiao, Z., Batth, T. S., Franciosa, G., Von Stechow, L., Lopez-Contreras, A. J., Vertegaal, A. C. O., & Olsen, J. V. (2017). Proteomics Reveals Global Regulation of Protein SUMOylation by ATM and ATR Kinases during Replication Stress. Cell Reports, 21(2), 546–558. https://doi.org/10.1016/j.celrep.2017.09.059

114. Murayama, Y., Samora, C. P., Kurokawa, Y., Iwasaki, H., & Uhlmann, F. (2018). Establishment of DNA-DNA Interactions by the Cohesin Ring. Cell, 172(3), 465–477.e15. https://doi.org/10.1016/j.cell.2017.12.021

115. Musacchio, A., & Desai, A. (2017). A Molecular view of kinetochore assembly and function. Biology, 6(4), 5. https://doi.org/10.3390/biology6010005

116. Nakajima, Y., Tyers, R. G., Wong, C. C., Yates, J. R., 3rd, Drubin, D. G., & Barnes, G. (2009). Nbl1p: a Borealin/Dasra/CSC-1-like protein essential for Aurora/Ipl1 complex function and integrity in Saccharomyces cerevisiae. Molecular biology of the cell, 20(6), 1772–1784. https://doi.org/10.1091/mbc.e08-10-1011

117. National Human Genome Research Institute. (n.d.). 1879: Mitosis observed. Genome.gov. https://www.genome.gov/25520234/online-education-kit-1879-mitosis-observed

118. NBL1 | SGD. (n.d.). https://www.yeastgenome.org/locus/S000029704

119. New England Biolabs. (n.d.). Q5® High-Fidelity DNA Polymerase | NEB. https://www.neb.com/en/products/m0491-q5-high-fidelity-dna-polymerase

120. Nicklas, R. B., & Koch, C. A. (1969). CHROMOSOME MICROMANIPULATION. The Journal of Cell Biology, 43(1), 40–50. https://doi.org/10.1083/jcb.43.1.40

121. Nie, M., Vashisht, A. A., Wohlschlegel, J. A., & Boddy, M. N. (2015). High confidence fission yeast SUMO conjugates identified by tandem denaturing affinity purification. Scientific Reports, 5(1).

122. Nilsson, J., Yekezare, M., Minshull, J., & Pines, J. (2008). The APC/C maintains the spindle assembly checkpoint by targeting Cdc20 for destruction. Nature Cell Biology, 10(12), 1411–1420. https://doi.org/10.1038/ncb1799

123. Numeracy, Maths and Statistics - Academic Skills kit. (n.d.). https://www.ncl.ac.uk/webtemplate/ask-assets/external/maths-resources/statistics/regression-and-correlation/strength-of-correlation.html

124. Oeser, M. L., Amen, T., Nadel, C. M., Bradley, A. I., Reed, B. J., Jones, R. D., Gopalan, J., Kaganovich, D., & Gardner, R. G. (2016). Dynamic Sumoylation of a Conserved Transcription Corepressor Prevents Persistent Inclusion Formation during Hyperosmotic Stress. PLoS Genetics, 12(1), e1005809. https://doi.org/10.1371/journal.pgen.1005809

125. Ohkuni, K., Pasupala, N., Peek, J., Holloway, G. L., Sclar, G. D., Levy-Myers, R., Baker, R. E., Basrai, M. A., & Kerscher, O. (2018). SUMO-Targeted ubiquitin ligases (STUBLs) reduce the toxicity and abnormal transcriptional activity associated with a mutant, Aggregation-Prone fragment of huntingtin. Frontiers in Genetics, 9. https://doi.org/10.3389/fgene.2018.00379

126. Papini, D., Levasseur, M. D., & Higgins, J. M. (2021). The Aurora B gradient sustains kinetochore stability in anaphase. Cell Reports, 37(6), 109818. https://doi.org/10.1016/j.celrep.2021.109818

127. Pasupala, N., Easwaran, S., Hannan, A., Shore, D., & Mishra, K. (2012). The SUMO E3 Ligase Siz2 Exerts a Locus-Dependent Effect on Gene Silencing in Saccharomyces cerevisiae. Eukaryotic Cell, 11(4), 452–462. https://doi.org/10.1128/ec.05243-11

128. Peplowska, K., Wallek, A. U., & Storchova, Z. (2014). Sgo1 regulates both condensin and Ipl1/Aurora B to promote chromosome biorientation. PLoS genetics, 10(6), e1004411. https://doi.org/10.1371/journal.pgen.1004411

129. Pereira, G., & Schiebel, E. (2003). Separase regulates INCENP-Aurora B anaphase spindle function through Cdc14. Science (New York, N.Y.), 302(5653), 2120–2124. https://doi.org/10.1126/science.1091936

130. Petsalaki, E., Akoumianaki, T., Black, E. J., Gillespie, D. A., & Zachos, G. (2011). Phosphorylation at serine 331 is required for Aurora B activation. The Journal of cell biology, 195(3), 449–466. https://doi.org/10.1083/jcb.201104023

131. Pinsky, B. A., Kung, C., Shokat, K. M., & Biggins, S. (2005). The Ipl1-Aurora protein kinase activates the spindle checkpoint by creating unattached kinetochores. Nature Cell Biology, 8(1), 78–83. https://doi.org/10.1038/ncb1341

132. Qiao, R., Weissmann, F., Yamaguchi, M., Brown, N. G., VanderLinden, R., Imre, R., Jarvis, M. A., Brunner, M. R., Davidson, I. F., Litos, G., Haselbach, D., Mechtler, K., Stark, H., Schulman, B. A., & Peters, J. (2016). Mechanism of APC/C CDC20 activation by mitotic phosphorylation. Proceedings of the National Academy of Sciences of the United States of America, 113(19). https://doi.org/10.1073/pnas.1604929113

133. Sandall, S., Severin, F., McLeod, I. X., Yates, J. R., 3rd, Oegema, K., Hyman, A., & Desai, A. (2006). A Bir1-Sli15 complex connects centromeres to microtubules and is required to sense kinetochore tension. Cell, 127(6), 1179–1191. https://doi.org/10.1016/j.cell.2006.09.049

134. Sane, A., Sridhar, S., Sanyal, K., & Ghosh, S. K. (2021). Shugoshin ensures maintenance of the spindle assembly checkpoint response and efficient spindle disassembly. Molecular Microbiology, 116(4), 1079–1098. https://doi.org/10.1111/mmi.14796

135. Schwienhorst, I., Johnson, E. S., & Dohmen, R. J. (2000). SUMO conjugation and deconjugation. MGG Molecular & General Genetics, 263(5), 771–786. https://doi.org/10.1007/s004380000254

136. Sherwin, D., & Wang, Y. (2019). The opposing functions of protein kinases and phosphatases in chromosome bipolar attachment. International Journal of Molecular Sciences, 20(24), 6182. https://doi.org/10.3390/ijms20246182

137. Shimogawa, M. M., Widlund, P. O., Riffle, M., Ess, M., & Davis, T. N. (2009). BIR1 is required for the tension checkpoint. Molecular Biology of the Cell, 20(3), 915–923. https://doi.org/10.1091/mbc.e08-07-0723

138. SLI15 | SGD. (n.d.). https://www.yeastgenome.org/locus/S000000360

139. Sriramachandran, A. M., & Dohmen, R. J. (2014). SUMO-targeted ubiquitin ligases. Biochimica Et Biophysica Acta (BBA) - Molecular Cell Research, 1843(1), 75–85. https://doi.org/10.1016/j.bbamcr.2013.08.022

140. Stevermann, L., & Liakopoulos, D. (2012). Molecular mechanisms in spindle positioning: structures and new concepts. Current Opinion in Cell Biology, 24(6), 816–824. https://doi.org/10.1016/j.ceb.2012.10.005

141. Takeda, D. Y., & Dutta, A. (2005). DNA replication and progression through S phase. Oncogene, 24(17), 2827–2843. https://doi.org/10.1038/sj.onc.1208616

142. Talamillo, A., Barroso-Gomila, O., Giordano, I., Ajuria, L., Grillo, M., Mayor, U., & Barrio, R. (2020). The role of SUMOylation during development. Biochemical Society Transactions, 48(2), 463–478. https://doi.org/10.1042/bst20190390

143. Tanaka, K., Mukae, N., Dewar, H., Van Breugel, M., James, E. K., Prescott, A. R., Antony, C., & Tanaka, T. U. (2005). Molecular mechanisms of kinetochore capture by spindle microtubules. Nature, 434(7036), 987–994. https://doi.org/10.1038/nature03483

144. Tanaka, T. U., Rachidi, N., Janke, C., Pereira, G., Galova, M., Schiebel, E., Stark, M. J., & Nasmyth, K. (2002). Evidence that the Ipl1-Sli15 (Aurora Kinase-INCENP) Complex Promotes Chromosome Bi-orientation by Altering Kinetochore-Spindle Pole Connections. Cell, 108(3), 317–329. https://doi.org/10.1016/s0092-8674(02)00633-5

145. Thu, Y. M., Van Riper, S. K., Higgins, L., Zhang, T., Becker, J. R., Markowski, T. W., Nguyen, H. D., Griffin, T. J., & Bielinsky, A. K. (2016). SLX5/SLX8 promotes

replication stress tolerance by facilitating mitotic progression. Cell Reports, 15(6), 1254–1265. https://doi.org/10.1016/j.celrep.2016.04.017

146. Trivedi, P., & Stukenberg, P. T. (2020). A condensed view of the Chromosome passenger complex. Trends in Cell Biology, 30(9), 676–687. https://doi.org/10.1016/j.tcb.2020.06.005

147. Uehara, R., Tsukada, Y., Kamasaki, T., Poser, I., Yoda, K., Gerlich, D. W., & Goshima, G. (2013). Aurora B and Kif2A control microtubule length for assembly of a functional central spindle during anaphase. The Journal of Cell Biology, 202(4), 623–636. https://doi.org/10.1083/jcb.201302123

148. Umbreit, N. T., Gestaut, D. R., Tien, J. F., Vollmar, B. S., Gonen, T., Asbury, C. L., & Davis, T. N. (2012). The Ndc80 kinetochore complex directly modulates microtubule dynamics. Proceedings of the National Academy of Sciences of the United States of America, 109(40), 16113–16118. https://doi.org/10.1073/pnas.1209615109

149. University of Leicester. (2020, October 26). The cell cycle, mitosis and meiosis for higher education: Virtual Genetics Education Centre. University of Leicester. https://le.ac.uk/vgec/topics/cell-cycle/the-cell-cycle-higher-education

150. Vallardi, G., Cordeiro, M. H., & Saurin, A. T. (2017). A Kinase-Phosphatase Network that Regulates Kinetochore-Microtubule Attachments and the SAC. Progress in Molecular and Subcellular Biology, 457–484. https://doi.org/10.1007/978-3-319-58592-5_19

151. Van Der Horst, A., & Lens, S. M. (2013). Cell division: control of the chromosomal passenger complex in time and space. Chromosoma, 123(1–2), 25–42. https://doi.org/10.1007/s00412-013-0437-6

152. van der Horst, A., Vromans, M. J., Bouwman, K., van der Waal, M. S., Hadders, M. A., & Lens, S. M. (2015). Inter-domain Cooperation in INCENP Promotes Aurora B Relocation from Centromeres to Microtubules. Cell reports, 12(3), 380–387. https://doi.org/10.1016/j.celrep.2015.06.038

153. Vigneron, S., Prieto, S., Bernis, C., Labbé, J., Castro, A., & Lorca, T. (2004). Kinetochore Localization of spindle checkpoint proteins: Who controls whom? Molecular Biology of the Cell, 15(10), 4584–4596. https://doi.org/10.1091/mbc.e04-01-0051

154. Wang, Y., & Dasso, M. (2009). SUMOylation and deSUMOylation at a glance. Journal of Cell Science, 122(23), 4249–4252. https://doi.org/10.1242/jcs.050542

155. Watson, J. D. (2014). Molecular biology of the gene (2016th ed.). Benjamin-Cummings Publishing Company

156. What is Cell Cycle? What are Phases of it?- CUSABIO. (n.d.). CUSABIO. https://www.cusabio.com/Cell-Biology/Cell-Cycle.html

157. What is Histone SUMOylation?- CUSABIO. (n.d.). https://www.cusabio.com/histones/histone-sumoylation.html

158. Wilkinson, K. A., & Henley, J. M. (2010). Mechanisms, regulation and consequences of protein SUMOylation. Biochemical Journal, 428(2), 133–145. https://doi.org/10.1042/bj20100158

159. Winey, M., & O'Toole, E. T. (2001). The spindle cycle in budding yeast. Nature Cell Biology, 3(1), E23–E27. https://doi.org/10.1038/35050663

160. Yamagishi, Y., Honda, T., Tanno, Y., & Watanabe, Y. (2010). Two Histone marks establish the inner centromere and chromosome Bi-Orientation. Science, 330(6001), 239–243. https://doi.org/10.1126/science.1194498

161. Yamamoto, K., Tran, T. N. M., Takegawa, K., Kaneko, Y., & Maekawa, H. (2017). Regulation of mating type switching by the mating type genes and RME1 in Ogataea polymorpha. Scientific Reports, 7(1). https://doi.org/10.1038/s41598-017-16284-7

162. Yang, S., Galanis, A., Witty, J., & Sharrocks, A. D. (2006). An extended consensus motif enhances the specificity of substrate modification by SUMO. The EMBO Journal, 25(21), 5083–5093. https://doi.org/10.1038/sj.emboj.7601383

163. Yau, T., Sander, W., Eidson, C., & Courey, A. J. (2021). SUMO Interacting Motifs: Structure and function. Cells, 10(11), 2825. https://doi.org/10.3390/cells10112825

164. Zhang, G., & Neubert, T. A. (2009). Use of stable isotope labeling by amino acids in cell culture (SILAC) for phosphotyrosine protein identification and quantitation. Methods in molecular biology (Clifton, N.J.), 527, 79–xi. https://doi.org/10.1007/978-1-60327-834-8_7

165. Zimniak, T., Stengl, K., Mechtler, K., & Westermann, S. (2009). Phosphoregulation of the budding yeast EB1 homologue Bim1p by Aurora/Ipl1p. The Journal of Cell Biology, 186(3), 379–391. https://doi.org/10.1083/jcb.200901036